MISMATCH REPAIR ACTS AS A BARRIER TO HOMEOLOGOUS RECOMBINATION IN *SACCHAROMYCES CEREVISIAE*

A Dissertation Presented

By

Erica Marie Selva

Submitted to the faculty of the University of Massachusetts Graduate School of Biomedical Sciences in partial fulfillment of the requirements for the degree of:

Doctor of Philosophy in Biochemistry and Molecular Biology

July, 1996

MISMATCH REPAIR ACTS AS A BARRIER TO HOMEOLOGOUS RECOMBINATION IN *SACCHAROMYCES CEREVISIAE*

A Dissertation Presented

By

Erica Marie Selva

Approved as to style and content by:

Reid Gilmore, Ph.D., Chair of Committee

Kendall Knight, Ph.D., Member of Committee

Martha Fedor, Ph.D., Mmeber of Committee

Duane Jenness, Ph.D., Member of Committee

Dean Dawson, Ph.D., Member of Committee

Robert S. Lahue, Ph.D., Thesis Adviser

Thomas B. Miller, Ph.D., Dean of
Graduate School of Biomedical Sciences

Department of Biochemistry and Molecular Biology

July, 1996

Dedicated to

David for his love, support and believing in me

even when I did not believe in myself

and

my family for an upbringing that encouraged

me to follow my dreams and whose

constant support helped me achieve this goal.

ACKNOWLEDGMENTS

I gratefully thank Bob Lahue for being all the things that a mentor should be: a knowledgeable and talented scientist, a patient and caring teacher and, when he needed to be, an understanding friend.

Thanks to the members of the Lahue lab, past and present, for helpful scientific discussion, creating a fun and friendly place to come to work each day and most of all, for playing excellent music on the CD player. My thanks to "Breck O" Parker, Patricia Hess, Juan Jose Miret, Luis Pessoa-Brendao, Samantha Rudginsky, Maria Milla and Anna Barcelo.

I would like to acknowledge the Gilmore lab for putting up with me over the years, especially the last week when I monopolized your computer. Special thanks to Reid Gilmore, Peter Rapiejko and Susana Silberstein for their friendship and support.

I am grateful to the wonderful friends I have made at the University especially: Jose Teixeira for challenging, supporting and understanding me, Caroline Clairmont for her warm and continued friendship, Denise Silva for her kindness and help, whenever I asked for it, and Alan Maderazo for his friendship and scientific contribution to this work.

I fondly remember Dr. Efraim Racker, Cornell University, who gave me my start in biochemistry.

ABSTRACT

Homeologous recombination refers to genetic exchanges between DNA partners containing similar but not identical DNA sequences. Heteroduplex intermediates in such exchanges are expected to contain multiple DNA mismatches at positions of sequence divergence and hence are potential targets for mismatch correction. Thus recombination of this type is of particular interest in understanding the role of DNA mismatch correction on recombination fidelity. Previous studies that examined this question in prokaryotic systems suggested that mismatch repair acts as a barrier to recombination between diverged sequences. The central hypothesis of this thesis is that mismatch correction acts as a barrier to homeologous recombination in yeast. The objectives of these studies was to elucidate the role of mismatch correction in homeologous recombination as a means of dissecting its mechanism in eukaryotic organisms.

To examine homeologous genetic events in yeast, I developed an *in vivo* assay system to evaluate recombination between diverged DNA sequences. A homeologous gene pair consisting of *Saccharomyces cerevisiae SPT15* and its *Schizosaccharomyces pombe* homolog were present as a direct repeat on chromosome V, with the exogenous *S. pombe* sequences inserted either upstream or downstream of the endogenous *S. cerevisiae* gene. Each gene carried a different inactivating mutation, rendering this starting strain Spt15$^-$. Recombinants that regenerated *SPT15* function were identified by genetic selection and the rates of recombination in different backgrounds were compared.

The homeologous mitotic recombination assay was utilized to test the role of *S. cerevisiae* mismatch repair genes *PMS1*, *MSH2* and *MSH3* on recombination fidelity. In strains wild type for mismatch repair, homeologous recombination was reduced 150-180 fold relative to homologous controls, indicating that multiply mispaired sequences act in *cis* as part of an inhibitory mechanism. In the upstream orientation of the homeologous gene pair, *msh2* or *msh3* mutations resulted in 17-fold and 9.6-fold elevations in recombination and the *msh2 msh3* double mutant exhibited an 43-fold increase, implying that each *MSH* gene can function independently in *trans* to prevent homeologous recombination. Homologous recombination was not significantly affected by the *msh* mutations. In the other orientation, only *msh2* strains were elevated (12-fold) for homeologous recombination. A mutation in *MSH3* did not affect the rate of recombination in this orientation. Surprisingly, a *pms1* deletion mutant did not exhibit elevated homeologous recombination in either case.

Next, I investigated whether mismatch correction acts as a specific or general obstacle to homeologous recombination by blocking one or many exchange pathways. To answer this question, I performed structural analysis on numerous recombinant products from each strain to determine the percentage of products that fell into a given class (crossovers or gene conversions). Each percentage was then multiplied by the overall rate to arrive at a rate of recombination for individual events. Typically 90-100% of homologous and homeologous recombinant products could be accounted for, either as crossovers or gene conversions. Recombination for all classes of products was inhibited when divergent sequences were present, indicating that homeology blocks

formation of both crossovers and gene conversions. Sequence analysis of a limited number of homeologous recombinants indicated that transfer of DNA occurred in continuous stretches and that endpoints fell within regions of 3-11 base pairs of perfect homology. Mutations in the mismatch repair genes *MSH2* or *MSH3* that elevate the overall rate of homeologous recombination produced similar rate increases in formation of each recombinant class. This suggests that mismatch correction proteins block multiple types of homeologous recombination events. Taken together, these results support the hypothesis that homeologous and homologous recombination occur by the same (or similar) pathways, with mismatch repair superimposed as an extra level of control over the fidelity of the process.

I also investigated whether this homeologous recombination system would be useful in a genetic screen to identify novel genes or new alleles of genes known to increase exchanges between diverged DNA sequences. Hyper-homeologous recombination mutants were isolated following ethylmethane sulfonate mutagenesis of yeast that harbored the *spt15* homeologous duplication. Preliminary characterization of these mutants demonstrated that some of these isolates yielded phenotypes that were consistent with mutations in mismatch repair genes verifying the utility of this method to identify such mutants. To improve the use of this system for a mutant screen, I developed a second generation homeologous duplication using *URA3*. These new starter strains are expected to be important for efficient isolation and characterization of hyper-homeologous recombination mutants.

TABLE OF CONTENTS

Dedication iii

Acknowledgments iv

Abstract v

Table of Contents viii

List of Figures xi

List of Tables xiii

List of Abbreviations xiv

CHAPTER I: Introduction 1

Mismatch repair 1

Mismatch repair and gene conversion 10

Mismatch repair and homeologous recombination 14

CHAPTER II: Experimental Methods 24

Media and Chemicals 24

E. coli manipulations 29

S. cerevisiae manipulations 29

Phenotypic complementation of FW1259 34

Construction of *spt15* homeologous duplication 35

Isolation of disruption and deletion alleles of DNA repair genes 37

Recombination analysis 38

Reversion analysis 39

Intervening marker loss 39

Genomic DNA preparation and Southern analysis of *SPT15* recombinants 40
Calculation of rates for individual recombinant classes 42
Sequence analysis of PCR products 43
Ethylmethane sulfonate mutagenesis (EMS) and hyper-homeologous recombination screening 44
Plasmid construction for the *ura3* homeologous duplication 46
Development of strains for selection and characterization of hyper-homeologous recombination mutants 48
CHAPTER III: Mismatch Correction Acts As a Barrier To Homeologous Recombination *Saccharomyces cerevisiae* 51
Experimental rationale 51
Description of tester strain 56
Orientation 2 homeologous recombination 63
Orientation 2A homeologous recombination 70
Orientation 1 homeologous recombination 73
CHAPTER IV: Homologous and Homeologous Recombinants in Wild Type and Mismatch Repair Deficient *Saccharomyces cerevisiae* 78
Summary 78
Structural analysis of Orientation 2 recombination products 79
Structural analysis of the Orientation 1 recombination products 86
Sequence analysis of selected recombinant products 94
Structural analysis of recombinants in pms1 strains 98

RAD52 effects on homologous and homeologous recombination 101

CHAPTER V: Isolation of Hyper-homeologous Recombination Mutants 104

Summary 104

Mutagenesis and selection of hyper-homeologous recombination mutants with *spt15* duplication 104

Testing and development of *URA3* as a new homeologous gene 110

Development of starter stains for mutagenesis and screening for hyper-homeologous recombination mutants 119

CHAPTER VI: Discussion 125

Mismatch correction acts as a barrier to homeologous recombination in *Saccharomyces cerevisiae* 125

Homologous and homeologous recombinants in wild type and mismatch repair deficient *Saccharomyces cerevisiae* 133

Isolation of hyper-homeologous recombination mutants 142

CHAPTER VII: References 149

LIST OF FIGURES

Figure 1. Mechanism of mismatch correction in *E. coli.* 2

Figure 2. The role of mismatch correction in gene conversion and post meiotic segregation..... 11

Figure 3. The effect of mismatch repair on homeologous recombination 18

Figure 4. DNA sequence comparison of the homeologous region and complementation of *spt15-21*. 52

Figure 5. Chromosomal structure of the Orientation 2 *SPT15* duplication and predicted recombinant products..... 57

Figure 6. Chromosomal structure of the Orientation 2A *spt15* homeologous duplication. 59

Figure 7. Chromosome structure of the Orientation 1 *SPT15* duplication and predicted recombination products. 61

Figure 8. Comparison of the relative increase in Orientation 2 recombination in yeast defective for mismatch correction. 66

Figure 9. Chromosomal structure of the Orientation 2 homeologous duplication and recombinant products. 80

Figure 10. Chromosomal structure of Orientation 1 homeologous duplication and recombinant products. 87

Figure 11. Identification of crossover end points by sequence analysis of functional *SPT15* hybrid genes..... 96

Figure 12. Schematic map of *URA3.H3* and the nucleotide sequence of oligonucleotides that were used to construct homeologous *URA3*. 112

Figure 13. Sequence comparison of *URA3.H3* with homeologous *URA3* genes. 115

Figure 14. Chromosomal structure of the *ura3* homeologous and *spt15* homologous direct repeat duplications. 122

LIST OF TABLES

Table 1. Yeast Mismatch Repair Genes 6

Table 2. Oligonucleotides 25

Table 3. Strains and Genotypes 30

Table 4. Recombination Rates and Intervening Marker Loss Orientation 2 65

Table 5. Homeologous Recombination Rates and Intervening Marker Loss Orientation 2A 72

Table 6. Recombination Rates and Intervening Marker Loss Orientation 1 74

Table 7. Distribution of Orientation 2 Recombination Products 83

Table 8. Distribution of Orientation 1 Recombination Products 91

Table 9. Distribution of Recombinants from *pms1* Strains 99

Table 10. Effect of *rad52* on Homologous and Homeologous Recombination 102

Table 11. Summary of BL206 Mutagenesis and Screening 107

LIST OF ABBREVIATIONS

Arg, Arginine
ATP, Adenosine Triphosphate
Can, Canavanine
CTP, Cytidine Triphosphate
DHFR, Dihydrofolate Reductase
DNA, Deoxyribonucleic Acid
EDTA, Ethylenediaminetetraacetic Acid
EMS, Ethylmethane Sulfonate
5-FOA, 5-Flourootic acid
His, Histidine
HNPCC, Hereditary Nonpolyposis Colorectal Cancers
LiOAc, Lithium Acetate
Lys, Lysine
MLH, *mutL* Homolog
MMS, Methylmethane Sulfonate
MSH, *mutS* Homolog
PCR, Polymerase Chain Reaction
PMS, Post Meiotic Segregation
SC, Synthetic Complete Media
SDS, Sodium Dodecyl Sulfate
SPT, Supressor of Ty
SSA, Single-Strand Annealing
SSC, Sodium Citrate Buffer
TBP, Tris Borate EDTA Buffer
TGF-β, Transforming Growth Factor-β
tk, Thymidine Kinase
TPE, Tris Phosphate EDTA Buffer
Trp, Tryptophan
Ura, Uracil
YPD, Complete Media (Yeast Extract, Peptone, Dextrose)

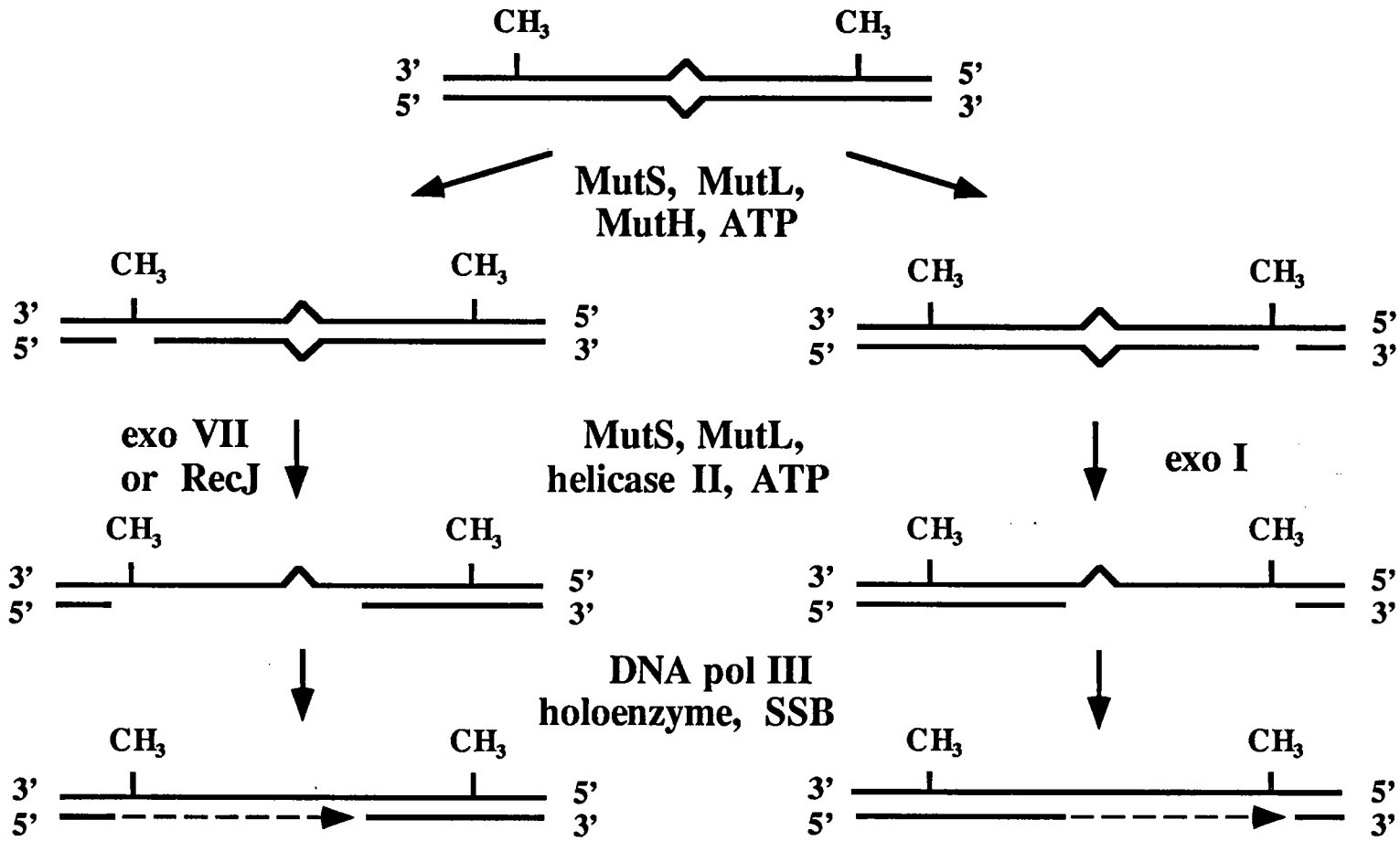
CHAPTER I
INTRODUCTION

Mismatch repair

The existence of a DNA mismatch repair system was demonstrated more than 20 years ago in bacteria (Nevers and Spatz, 1975; Tiraby and Fox, 1973). Mismatch correction displays a broad substrate specificity that acts to correct post replicative biosynthetic errors, mismatches caused by the deamination of 5-methylcytosine and heteroduplexes that arise as a result of allelic differences between recombination partners. The importance of this pathway for maintaining the integrity of the genetic complement was inferred from experiments in which its absence resulted in a significant elevation in the spontaneous mutation rate (Nevers and Spatz, 1975). The biological significance of mismatch correction is further illustrated by its strong evolutionary conservation from bacteria to humans. The ramifications of inactivating the mismatch repair system in humans has recently been realized as an important factor in cancer (reviewed in Modrich and Lahue, 1996).

DNA mismatch correction has been extensively studied in *Escherichia coli*, and as a result its molecular mechanism is well understood (Fig. 1). During replication misincorporation or strand slippage events that escape the editing function associated with DNA polymerases are subject to correction. The *E. coli* mismatch repair system utilizes the state of methylation as a means to discriminate the strand containing the correct base from that containing the

Figure 1. Mechanism of mismatch correction in *E. coli.* (from Modrich and Lahue, 1996). The figure is described in the text.


CH3
CH3
3'
5'
5'
3'
MutS, MutL,
MutH, ATP
exo VII
or RecJ
MutS, MutL,
helicase II, ATP
exo I
DNA pol III
holoenzyme, SSB

incorrect base. Dam Methylase modifies the adenine of d(GATC) sites in a post replicative process that follows mismatch correction (Pukkila et al., 1983). Thus, newly synthesized DNA transiently lacks methylation, targeting its repair. The first step in the repair process is recognition and binding of MutS, presumably as a homodimer (Su and Modrich, 1986), to the mismatch. MutS binds all single base mismatches with varying affinities, except C-C mismatches which are weakly bound and poorly repaired (Su et al., 1988) and small insertions ranging in size from 1 to 3 nucleotides (Parker and Marinus, 1992). There is a strong correlation between the affinity of MutS binding and the efficiency of the repair reaction (Parker and Marinus, 1992; Su et al., 1988) . MutL, likely functioning as a homodimer, joins to the MutS-DNA complex in a reaction that requires ATP, but not ATP hydrolysis (Grilley et al., 1989). The ternary complex activates the MutH endonuclease to generate a nick on the unmethylated strand at d(GATC) sites. The nick serves as an entry point for nucleases and helicase that excise nucleotides on the nicked strand. The MutSLH complex preferentially utilizes the hemimethylated d(GATC) sequences closest to the lesion and as a result the excision step can initiate from either side of the mismatch (Cooper et al., 1993). When the strand break is generated on the 5' side of the lesion the 5'-->3' exonucleolytic activity of either Exo VII or RecJ are required to remove nucleotides from the nick to a position past the mismatch in a reaction that depends on the addition of DNA helicase II to the complex. The ExoI 3'-->5' exonuclease excises the nucleotides when the strand breaks originates on the 3' side of the mismatch (Cooper et al., 1993; Grilley et al., 1993). The last step in the repair process is gap repair performed by DNA polymerase III holoenzyme followed by ligation (Lahue et al., 1989).

The evolutionary conservation of the mismatch repair system is exemplified by the structural and functional homologies it shares in organisms ranging from bacteria to mammals. To date, six genes from *Saccharomyces cerevisiae* (Hollingsworth et al., 1995; Marsischky et al., 1996; New et al., 1993; Reenan and Kolodner, 1992; Ross-MacDonald and Roeder, 1994)and three genes from humans (Drummond et al., 1995; Fishel et al., 1993; Leach et al., 1993; Liu et al., 1994; Palombo et al., 1995) have been identified that share sequence homology to *mutS*. A list of the yeast MutS homologs or *MSH* genes with their functions are presented in Table 1. *yMSH1* and *yMSH2* were isolated by a PCR based approach designed to identify genes with homology to *mutS* (Reenan and Kolodner, 1992). Disruption of *yMSH1* resulted in a respiratory defect, suggesting it has a mitochondrial function (Reenan and Kolodner, 1992). Biochemical analysis of purified Msh1 demonstrated heteroduplex specific binding that is enhanced by ATP (Chi and Kolodner, 1994; Chi and Kolodner, 1994). Taken together these results suggest that Msh1 is part of a mismatch correction system that repairs the mitochondrial genome. The absence of *yMSH2* resulted in a mutator phenotype (high rate spontaneous mutation rate) and elevated post meiotic segregation (see below) consistent with a role in mismatch correction (Reenan and Kolodner, 1992). Furthermore, nuclear extracts prepared from *msh2* mutant yeast were deficient in heteroduplex DNA binding compared to wild type extracts (Miret et al., 1993). Human cells (Fishel et al., 1993; Leach et al., 1993) and transgenic mice (de Wind et al., 1995) deleted for *MSH2* also show phenotypes consistent with a deficiency in mismatch match repair. Recently, yMsh3, identified by homology to its mammalian counterpart (New et al., 1993),

Table 1

Yeast Mismatch Repair Genes

Yeast Gene	Mutant Phenotype	Function
MSH1	respiratory defect	mitochondrial mismatch repair
MSH2	mitotic mutator dinucleotide repeat instability increased homeologous recombination increased post meiotic segregation	repairs single base mismatches and small insertion as a heterodimer with Msh3 or Msh6
MSH3	weak mitotic mutator dinucleotide repeat instability increased homeologous recombination	repairs small insertion as a heterodimer with Msh2
MSH4	decreased spore viability increased non-disjunction decreased crossovers	meiotic crossover
MSH5	decreased spore viability increased non-disjunction decreased crossovers	meiotic crossover
MSH6	mitotic mutator	repairs single base mismatches and small insertion as a heterodimer with Msh2
PMS1	mitotic mutator dinucleotide repeat instability increased post meiotic segregation	forms heterodimer with Mlh1
MLH1	mitotic mutator dinucleotide repeat instability increased post meiotic segregation	forms heterodimer with Pms1
MLH2	none known	unknown
MLH3	unknown	unknown

and yMsh6, cloned in the genome sequencing project, have been shown to form a heterodimer with yMsh2 (Johnson et al., 1996; Marsischky et al., 1996). The heterodimer either yMsh2/yMsh3 or yMsh2/yMsh6 dictates the specificity of mismatch binding (Johnson et al., 1996; Marsischky et al., 1996). A role for *yMSH2* and *yMSH3* in recombination between divergent DNA sequences and their genetic interaction have also been demonstrated by experiments performed in this thesis and by others (Datta et al., 1996). Human Msh2 and Msh6 were purified as a functional heterodimer that specifically binds G-T mismatch and 1, 2 and 3 base insertions (Drummond et al., 1995; Palombo et al., 1995). The function of hMsh3 (Rep3), isolated by its chromosomal proximity to *DHFR* (Linton et al., 1989; Liu et al., 1994), has not been determined to date although it may be similar to its yeast counterpart. Both *yMSH4* and *yMSH5* were isolated based upon their meiotic function (Hollingsworth et al., 1995; Ross-MacDonald and Roeder, 1994). Although neither *msh4* nor *msh5* mutations lead to defects in mismatch repair per se, both genes function in the same pathway to facilitate reciprocal crossovers during meiosis (Hollingsworth et al., 1995; Ross-MacDonald and Roeder, 1994), suggesting they may play a role in chromosome pairing interactions.

The structural and functional conservation of mismatch repair also extends to eukaryotic homologs of *mutL*. Table 1 shows that yeast have four MutL homologs (Kramer et al., 1989; Prolla et al., 1994; Williamson et al., 1985), while three human homologs have been identified (Bronner et al., 1994; Nicolaides et al., 1994; Papadopoulos et al., 1994; Risinger et al., 1995). Perhaps the best characterized of all eukaryotic mismatch repair proteins is the MutL

homolog, *yPMS1*, which was isolated and named based upon its post meiotic segregation phenotype (discussed below, (Williamson et al., 1985). Mutations in *yPMS1* produce a mutator phenotype (Williamson et al., 1985) and an inability to repair heteroduplex plasmid substrates (Kramer et al., 1989). Similarly extracts prepared from human cells deficient for *PMS2*, the gene most closely related *yPMS1* (Nicolaides et al., 1994), lacked mismatch repair activity. *hPMS2* deficient cells also had other defects characteristic of *ypms1* (Risinger et al., 1995). Deletion of *PMS2* in mice confers a mismatch deficient phenotype and produces abnormalities in meiotic chromosome synapsis, which suggests the *PMS2* gene product also plays a role in recombination during meiosis (Baker et al., 1995). Two additional genes *yMLH1* and *yMLH2* (for MutL homolog) were identified based on their homologies to MutL (Prolla et al., 1994). A function for *MLH2* has not been determined, but *mlh1* mutations in yeast and humans produce phenotypes that are consistent with a function in mismatch correction (Nicolaides et al., 1994; Prolla et al., 1994; Risinger et al., 1995). A biochemical interaction between yMlh1 and yPms1 was demonstrated using affinity chromatography, suggesting that the functional form of these genes *in vivo* is a heterodimer (Prolla et al., 1994). This conclusion is further supported by the fact that *mlh1 pms1* double mutants have the same phenotype as either single mutation (Prolla et al., 1994). Another yeast *MLH* gene was identified, here referred to as *MLH3*, by the yeast genome sequencing project. However, experiments have yet to be reported that address its function in mismatch repair. While there is a great deal known about the structure and function of the various MutS and MutL homologs from *S. cerevisiae* and mammals, very little is understood about other components of eukaryotic mismatch repair. Two

exceptions are *S. pombe exoI* (Szankasi and Smith, 1995) and *S. cerevisiae RTH1* (Johnson et al., 1995), which both have been implicated as 5' to 3' exonucleases in mismatch repair. Given the complexity of *mutS* and *mutL* homologs in eukaryotic mismatch repair it seems likely that the relationship between other components will be equally complex.

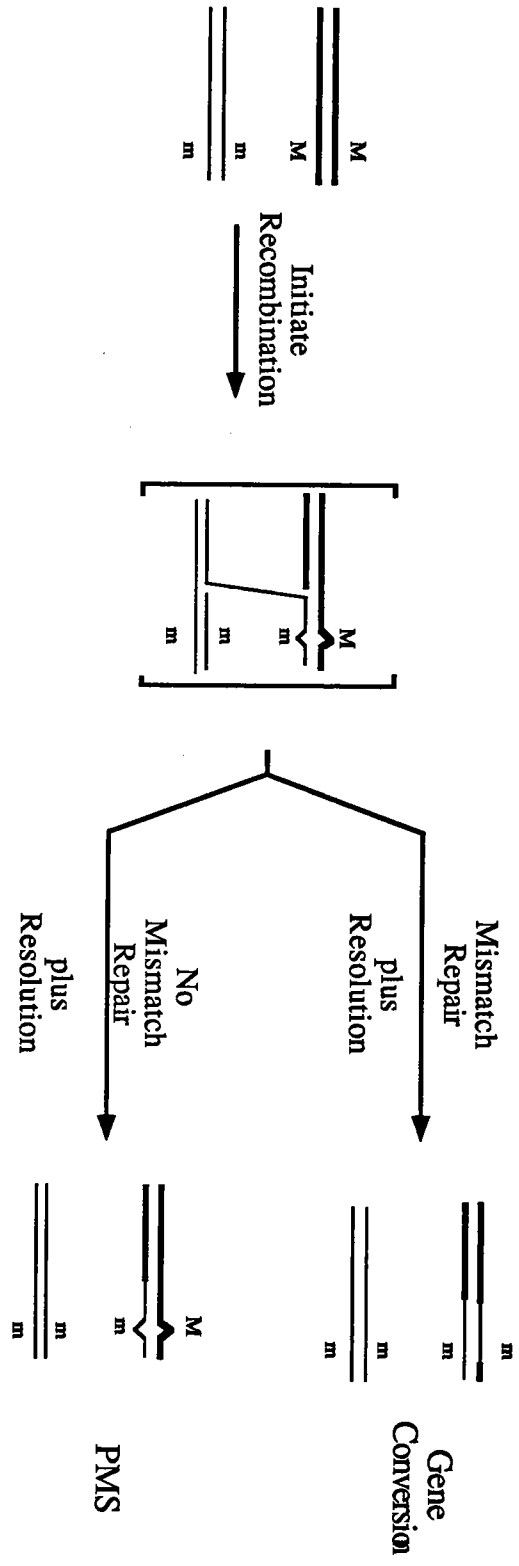
The expansion and contraction of dinucleotide repeats was recently identified as another phenotype indicative of the absence of functional mismatch repair (Strand et al., 1993). Changes in dinucleotide tract length are likely to occur by a mechanism that involves replication slippage generating insertion/deletions in multiples of two nucleotides (Strand et al., 1993). Indeed, yeast that have mutations in *msh2*, *pms1*, *mlh1* or *msh3* exhibit increases in dinucleotide tract instability of 40- to 1000-fold (Strand et al., 1995; Strand et al., 1993) on plasmids and 80-fold on the chromosome (Strand et al., 1993) relative to wild type (Table 1). This finding lead to a breakthrough in understanding the mechanisms that govern the progressive genetic destabilization that results in certain forms of human cancers. Human tissue derived from sporadic and hereditary nonpolyposis colorectal cancers (HNPCC) shows an instability in the size of their microsatellite DNA, which are composed of simple mono-, di- and trinucleotide repeat sequences (Aaltonen et al., 1993; Ionov et al., 1993; Thibodeau et al., 1993). The genetic loci linked to HNPCC microsatellite destabilization were all identified as homologs of *mutS* or *mutL* (Drummond et al., 1995; Fishel et al., 1993; Leach et al., 1993; Liu et al., 1994; Palombo et al., 1995). Furthermore, deletion of *MSH2* and *PMS2* in transgenic mice cause microsatellite destabilization and an increased incidence of lymphomas (de Wind

et al., 1995) and sarcomas (Baker et al., 1995). These mutations have subsequently been linked to some other forms of human cancer (Modrich and Lahue, 1996). Two additional observations strengthen the likelihood that loss of mismatch repair activity is the cause of rather than an effect of genetic destabilization leading to cancer. First, mismatch repair deficient non-cancerous cell lines have been identified, suggesting that loss of mismatch repair activity precedes cell transformation (Parsons et al., 1995). Second, frameshift mutations within repetitive DNA sequences of the Type II TGF-β receptor found in mismatch repair deficient cancer cells can explain the uncontrolled cellular growth phenotype of these cancers (Markowitz et al., 1995)

Mismatch repair and gene conversion

Meiotic recombination between homologous chromosomes most frequently proceeds by a reciprocal mechanism where markers segregate 2:2. When describing segregation properties, another nomenclature is frequently used that specifically denotes each of the eight DNA strands. Hence Mendelian segregation is inferred as 4:4. One to 10% of all meiotic events from unselected yeast tetrads yield gene conversions, defined as aberrant events where markers segregate 6:2 or 2:6. It has long been hypothesized that DNA mismatch repair activity is responsible for these non-reciprocal exchanges (Holliday, 1964; Meselson and Radding, 1975). One model of recombination proposes that strand invasion will result in heteroduplex (mismatched) DNA at sites of allelic variations (Fig 2). Repair of the heteroduplex by mismatch correction on the recipient strand, using the invading strand as template, results in gene

Figure **2.** The role of mismatch correction in gene conversion and post meiotic segregation. After initiation of recombination between two alleles of a gene M (thick lines) and m (thin lines), a heteroduplex is formed at the position of sequence difference. Top, mismatch correction repairs the mismatch in favor of m to produce gene conversion. Bottom, the mismatch escapes repair and the M/m heteroduplex persists. Post meiotic segregation occurs upon the first mitotic division.


M
M
m
m
Initiate
Recombination
M
m
m
m
Mismatch
Repair
plus
Resolution
No
Mismatch
Repair
plus
Resolution
m
m
m
m
M
m
m
m
Gene
Conversion
PMS

conversion after resolution. Conversely, repair in favor of the recipient strand would restore the mismatch to its original sequence. An alternative mechanism for meiotic gene conversion is the gap repair model (Szostak et al., 1983). This model suggests that double stranded gaps, formed from expanded double strand breaks, are repaired by strand invasion from the unbroken chromosome followed by repair synthesis using the invading strand as template. Gene conversion can be explained by gap repair without the involvement of a heteroduplex. The original model also allows for heteroduplex formation and repair at the edge of gaps. Recent modifications to the gap repair model suggest that double strand breaks might be resected by single strand degradation exposing extensive single strand regions for heteroduplex formation (Cao et al., 1990; Haber, 1992; Petes et al., 1991; Sun et al., 1989). Thus formation and correction of mispaired intermediates are important features of gene conversion in both prominent models of recombination.

The best evidence for involvement of mismatch repair in gene conversion comes from studies of other aberrant segregation events. If heteroduplex DNA persists through meiosis, the two strands will segregate at the first mitotic division and each half of the resulting colony receives information from a different allele. This leads to a 5:3 or 3:5 aberrant segregation pattern, referred to as post meiotic segregation (PMS, Fig. 2) and is visualized in unselected yeast tetrads as a sectored colony. Those mismatches that are poor substrates for mismatch repair, such as C-C (Bishop et al., 1987; Detloff et al., 1991; Kramer et al., 1989; McDonald and Rothstein, 1994) and hairpin loops (Nag and Petes, 1991; Nag et al., 1989), show a high frequency of PMS, suggesting that these

mismatches escape detection by the mismatch repair machinery. Furthermore, yeast deficient in mismatch repair, mutations in *mlh1*, *pms1* or *msh2*, display an increase in the recovery of PMS segregants with a corresponding drop in gene conversion (Kramer et al., 1989; Prolla et al., 1994; Reenan and Kolodner, 1992; Williamson et al., 1985). These results provide strong evidence that mismatch correction is responsible for the recognition and repair of heteroduplex DNA in recombination intermediates to produce gene conversion, since its absence results in reduced mismatch repair and high PMS. Further evidence that heteroduplex structures exist in recombination intermediates and an active mismatch correction system is responsible for their repair come from physical analysis of the DNA. Recombination intermediates have been detected by Southern analysis (Goyon and Lichten, 1993) and PCR (Haber et al., 1993). The presence of heteroduplex DNA in the intermediate, that was dependent on C-C mismatch or a *pms1* mutation, was demonstrated by differential restriction enzyme cutting of each strand or sequence analysis of PCR products, respectively. Heteroduplex molecules that survive through resolution also were recovered from meiotic products containing poorly repaired mismatches like C-C (Lichten et al., 1990).

Mismatch repair and homeologous recombination

Homeologous recombination refers to genetic exchanges between similar, but not identical (diverged), DNA sequences. This distinguishes it from gene conversion, where exchange partners differ by only one or a few nucleotides. Recombination between homeologous DNA sequences presents opportunities for

genetic diversity as well as dangers to genetic integrity. Positive aspects of homeologous recombination include the potential to generate new genes during evolution and to serve as a source of genetic material to support recombinational repair (Resnick et al., 1992). Non-reciprocal genetic transfer (gene conversion) between variable chain genes and divergent pseudogenes is essential in chicken (Reynaud et al., 1985; Reynaud et al., 1989; Thompson and Neiman, 1987) and important in mouse (Wheeler et al., 1990) for achieving immunoglobulin diversity. Ectopic exchanges between divergent non-allelic genes in yeast can restore function to mutant genes (Bailis and Rothstein, 1990; Harris et al., 1993). On the other hand inappropriate exchanges could compromise genetic stability with serious consequences for cell viability and survival of the organism. A number of human genetic disorders associated with chromosomal deletions, inversions and translocations could potentially arise via homeologous genetic exchanges or gene conversions (Krawczak and Cooper, 1991; Meuth, 1990). Unequal or abnormal crossover within the interferon gene cluster has been proposed as one explanation for deletions on chromosome 9 that lead to glioma formation (Olopade et al., 1992). In *S. cerevisiae* recombination between divergent delta elements yielded genomic deletions and inversions (Rothstein et al., 1987). These examples illustrate the delicate balance that must exist to promote beneficial homeologous exchanges while inhibiting potentially deleterious chromosomal rearrangements.

Homeologous exchanges can occur because recombination strand transfers can proceed through regions of imperfect homology (DasGupta and Radding, 1982; Iype et al., 1994; Muller et al., 1993). *In vitro* RecA catalyzed

strand exchange was inhibited by substrates that diverge by more than 30% (DasGupta and Radding, 1982), but RuvA and RuvB facilitate bypass of internal heterologies (Iype et al., 1994). These *in vitro* results suggest that strand exchange can tolerate considerable sequence divergence. However, there is a wealth of *in vivo* evidence that indicates sequence divergence acts to block genetic exchanges. Shen and Huang (Shen and Huang, 1986) demonstrated that recombination efficiency in *E. coli* progressively decreases with increasing sequence divergence. In mouse cells, intrachromosomal recombination is extremely sensitive to sequence divergence. Genetic exchanges between duplicated thymidine kinase (*tk*) genes sharing 81% sequence identity occur 1000-fold less frequently than a homologous duplication (Waldman and Liskay, 1987) and introduction of as few as two base pairs in a 232 base stretch reduced mitotic recombination by 20-fold (Waldman and Liskay, 1988). Similarly 0.6% sequence divergence reduced targeted integration in mouse ES cells by 15- to 50-fold. Thus in *E. coli* and mouse, homeology poses a significant barrier to homologous recombination.

Recombination in yeast is less sensitive to sequence divergence, yet it is a considerable obstacle to recombination. Ectopic chromosomal genetic exchanges between 17% diverged *SAM1* and *SAM2* (Bailis and Rothstein, 1990) and 15% diverged *PMA1* and *PMA2* (Harris et al., 1993) were reduced 20- and 75-fold, respectively, compared to homologous substrates. Recombination products recovered from these exchanges exhibited a continuous transfer of information (Bailis and Rothstein, 1990) ending in junctions as small as 3 to 26 nucleotides of sequence identity with maintenance of both sequence alignment and accuracy

(Harris et al., 1993). Intermolecular gene conversions from a plasmid to a chromosomal copy of *HIS4* that diverged by 14% was 5 to 10-fold lower than homologous substrates (Wu and Marinus, 1994). Cytochrome P450 homeology (27%) also posed a similar block to extrachromosomal recombination (10- to 25-fold lower) (Alani et al., 1994; Mezard et al., 1992). Furthermore, yeast have the ability to distinguish between different levels of sequence divergence. For example, crossovers between β-tubulin genes that are 9% divergent were inhibited 40-fold relative to homologous controls, whereas 23% divergence between *spt15* genes decreased crossovers by 2000-fold (Datta et al., 1996). Thus increases in the degree of homeology result in corresponding decreases in the rate of recombination.

The nature of inhibition of homeologous recombination was inferred from the idea that recombination heteroduplexes arising from exchanges between diverged sequences should contain multiple mismatches and could act as a target for mismatch repair proteins (Fig. 3) (Radman, 1988). Several studies have addressed the specific prediction that DNA mismatch correction acts to suppress homeologous exchanges (anti-recombination activity). Sequence divergence (20%) inhibits interspecies conjugational crosses between *E. coli* and *S. typhimurium* by five orders of magnitude relative to intraspecies crosses (Rayssiguier et al., 1989). This block to recombination was partly due to the action of mismatch correction since mutations in *mutS, mutL, mutH* and *mutU* (*uvrD*) increased interspecies recombination 50- to 1000-fold (Rayssiguier et al., 1989). Similarly mutations in *mutS* and *mutL* stimulated recombination between duplicated heteroalleles (Petit et al., 1991), further supporting the idea that one

Figure 3. The effect of mismatch repair on homeologous recombination (adapted from Radman, 1988). Divergent recombination partners are shown as thick or thin lines. Upon initiation strands are transferred and branch migration produces a mismatched intermediate. Resolution yields a mismatched chromosome which can segregate at the next mitotic division. Mismatch repair blocks this process (possibly at the branch migration step) by recognition of the mismatches. The exact mechanism of the block is unknown. (Please note: this diagram is for illustrative purposes only. No implications as to the mechanism of recombination are intended.)

Initiate
Branch Migrate
Resolve
Mismatch Repair Block ?

function of DNA mismatch correction is to prevent homeologous genetic exchanges in bacteria. Constitutive induction of the *E. coli* SOS response in this system revealed an additive increase in homeologous recombination in *mutS* and *mutL* deficient backgrounds (Petit et al., 1991), suggesting that high recA levels can drive homeologous exchanges. Subsequent experiments demonstrated that the homeologous exchanges approached homologous levels with the cumulative effects of SOS induction and the absence of mismatch repair (Matic et al., 1995). Analysis of recombinant products from conjugational crosses showed that, in most cases, the transfer of genetic material was continuous and the nature of products was not significantly affected by the presence or absence of *mutS*, *mutL* or *mutH* (Matic et al., 1994). MutS and MutL have also been shown to inhibit RecA mediated recombination *in vitro* between substrates that diverge by only 3% (Worth et al., 1994). Homologous controls were unaffected by the presence of MutS or MutL, thus mispaired DNA is required for the block. Analysis of these recombination products suggested that the block occurs at the branch migration step (Fig. 3, (Worth et al., 1994).

Several studies have provided evidence that mismatch correction also serves to maintain the fidelity of genetic exchanges in eukaryotic organisms. Mitotic gene conversions between endogenous *SAM1* and *SAM2* increased 4.5-fold when the *mutL* homolog *PMS1* (Kramer et al., 1989) was disrupted, but a similar increase was also observed for homologous exchanges (Bailis and Rothstein, 1990). The absence of *PMS1* increased crossovers between 9% diverged β-tubulin genes (Datta et al., 1996). Elevated crossover rates were observed for both 9% and 23% diverged substrates (Datta et al., 1996) in strains

bearing disruptions of the *mutS* homologs *MSH2* (Reenan and Kolodner, 1992) or *MSH3* (New et al., 1993). Recently, mismatch correction was implicated in sequence divergence dependent species isolation in eukaryotic organisms. Crosses between *S. cerevisiae* and *Saccharomyces paradoxus*, estimated to diverge by 11 to 20%, rarely yielded viable spores and in the few spores recovered from the interspecies cross the recombination frequency was low (Hunter et al., 1996). However, spore viability was improved by 6.1- and 8.7-fold and crossing-over increased to 9 to 27% and 20 to 69% of homologous levels in *pms1* and *msh2* homozygous deletion strains, respectively (Hunter et al., 1996). An anti-recombination function has also been attributed to the mouse *MSH2* gene (de Wind et al., 1995). Mutations in yeast *MSH1* result in respiratory growth defects, consistent with loss of mitochondrial function, as well as major rearrangements within mitochondrial DNA (Reenan and Kolodner, 1992). One suggestion (Chi and Kolodner, 1994; Selva et al., 1995) to explain these rearrangements is that loss of *MSH1* function results in increased homeologous recombination in the mitochondria, although this idea has not yet been tested.

In this work, an *in vivo* assay system was developed to directly test the hypothesis that mismatch correction acts to maintain the fidelity of genetic exchanges by inhibiting recombination between diverged DNA sequences. The recombination rate was measured between a direct repeat of inactive heteroalleles of *SPT15* from *S. cerevisiae* and its homolog from *S. pombe* which are 25% divergent at the nucleotide level. Exchanges between homeologous substrates were 150- to 180-fold lower than homologous controls. The homeologous recombination block was due, at least in part, to mismatch

correction, since disruption of *MSH2* and in some cases *MSH3* increased the rate of exchanges 10- to 17-fold between *SPT15* heteroalleles. These results indicate that the activities of Msh2 and Msh3 in homeologous exchanges are either independent or act in overlapping, competing pathways since the *msh2 msh3* double mutant yielded a greater than additive increase (43-fold) in the homeologous recombination rate compared to either mutation alone.

These initial observations were then extended to include a structural analysis of homologous and homeologous exchange products recovered from wild type and mismatch repair deficient yeast. The structure of many homeologous recombinants were evaluated to determine the rates of formation of popouts (single-strand annealing, intra- or intermolecular crossover), gene conversions and G2 unequal crossovers. Homeology was found to be an obstacle to all types of exchanges events. Mismatch repair mutations that increased the overall homeologous recombination rate released the barrier for each class of homeologous exchange. My results are consistent with the idea that homeologous recombination occurs by the same (or similar) mechanisms used for homologous exchanges, with mismatch repair superimposed as an extra control over the fidelity of the process.

I also tested whether the homeologous *spt15* duplication could be used as a genetic screen to identify mutations that produce a hyper-homeologous recombination phenotype. A preliminary experiment was performed with mutagenized cells that harbored the *spt15* homeologous duplication; of 17,000 mutagenized cells evaluated, 0.3% yielded a hyper-homeologous recombination

phenotype. Approximately 15% of these isolates also showed a mutator phenotype, consistent with the notion that these mutation might be in genes involved in mismatch correction. Because the *spt15-21* genetic background has additional phenotypes that make characterization of mutants difficult, a second homeologous gene was constructed with *URA3*. This *ura3* homeologous duplication is expected to facilitate the isolation and characterization of hyper-homeologous recombination mutants.

CHAPTER II

EXPERIMENTAL METHODS

Media and Chemicals

E. coli strains were grown on LB liquid or 1.5% LB-agar supplemented with 75 μg/ml ampicillin. Yeast strains were grown on either complete media, YPD, or synthetic complete media, SC (Sherman et al., 1979). Synthetic complete (SC) media contained 0.67% nitrogen base, 2% dextrose, 0.2% drop out mix, which had all amino acids and nutrients except those necessary for selective growth, and 2% agar for solid media. All media was obtained from Difco. Restriction endonucleases and DNA modifying enzymes were from New England Biolabs, except Taq polymerase, which was from Promega. Radioactive isotopes γ-^{32}P-ATP (6000 Ci/mmol), α-^{35}S-dATP (1370 Ci/mmol) and α-^{32}P-dCTP (3000 Ci/mmol) were from New England Nuclear. All other chemical reagents were from Sigma. All oligonucleotides used in this study were synthesized on an Applied Biosystems 392 DNA synthesizer and are listed in Table 2. Oligonucleotides greater than 40 nucleotides (nt) in length were routinely run on denaturing acrylamide gels, eluted from gel slices and purified on Waters C18 Sep-pac columns. Sep-pac acetonitrile eluates were dried down and resuspended in TE (10 mM Tris, pH 8.0 and 1 mM EDTA) (Knight and Sauer, 1988).

Table 2

Oligonucleotides

Name	Sequence[a]	Use	Coordinates[b]
oBL3	TTT ACC TGA GGC GAA A	*Bsu36*I mutagenic primer	*TBP* 332 to 315 complement
oBL21	GTG ACT TTG GGG TGC AGG TT	*SPT15* 5' PCR primer	*SPT15* 220 to 239
oBL23	CTT CCC TTT GCT TTG CAC CA	*SPT15* 3' PCR primer	*SPT15* 644 to 623 complement
oBL31	ATG TCG GGA TTC CCT TTG CT	*SPT15* 5' PCR primer	*SPT15* -395 to -376
oBL32	CCT CAC GGA CTT TCG CAC CA	*TBP* 3' PCR primer	*TBP* 636 to 617 complement

Table 2 continued

Name	Sequence[a]	Use	Coordinates[b]
oBL57	GAG TTC GCC AGT GAC TTG GG	*SPT15* 3' PCR primer	*SPT15* 1164 to 1145 complement
oBL60	CCC CAA GCG TTT TGC TGC TG	*SPT15* 5' sequencing primer	*SPT15* 285 to 304
oBL64	GAG GAC CAT TAA TAA TTG AG	*SPT15* 3' sequencing primer	*SPT15* 794 to 775 complement
oBL70	TTT TTC TAA CTT CAC TTA GC	Identifies *spt15-21* intrageneic supressors	*SPT15* 718 to 699 complement
oBL71	TTT TAA TAT CAT GCA CGA AA	*URA3 Hind*III mutagenic PCR primer	*URA3* 62 to 81

Table 2 continued

Name	Sequence[a]	Use	Coordinates[b]
oBL73	CAG TAT TCT TAA CCC AAC TG	*URA3* sequencing primer	*URA3* -55 to -36
oBL96	GCC TGC TTC AAA CCG CTA AC	*URA3* sequencing primer	*URA3* 407 to 388 complement
oBL100	GGG TTG CTG TCC GTG CGA TTT CAA GAC TGC TCA TTT CGC ACG ATG TCT GAC ACA TGC AGC TCC CG	5' primer *hpr1Δ::TRP1*	*HRP1* -168 to -124 *TRP1* -437 to -418
oBL101	GGG ACA CTA TGC ATG AAT TTG TTA TCA GTT TAA AAT TTC TAT TAA TGC CGA TTT CGG CCT ATT GG	5' primer *hpr1Δ::TRP1*	*HRP1* 2312 to 2268 *TRP1* 859 to 840 complement

Table 2 continued

Name	Sequence[a]	Use	Coordinates[b]
oBL104	TCA AAC CGC TAA CAA TAC CTG GG	*URA3* PCR primer	*URA3* 400 to 378 complement
oBL105	GAA TGC TAA CCC TTC TAG ACG	Identifies *spt15-21* /*spt15-21* point mutation replacement	*SPT15* 510 to 530 complement

[a] Underlined nucleotides indicate important function.
[b] The oligonucleotide locations are relative to the first nucleotide of the translation initiation codon.

E. coli manipulations

TG-1 (*K12, Δ (lac-pro), supE, thi, hsdΔ5/F'traD36, proA⁺B⁺, lacI^q, lacZ Δ M15*) or DH5α (*F'/endA1, hsdR16($r_k^-m_k^-$) supE44, thi-1, recA1, gyrA (Nal^R) relA1, Δ(lacIZYA-argF)U169, deoR (ϕ80dlacΔ(lacZ)M15)*) were used for plasmid manipulations described. All molecular biology manipulations were carried out by standard methods (Ausubel et al., 1994). Transformation were performed by the method of Hanahan (Hanahan, 1983) and all plasmids used in this study confer ampicillin resistance.

S. cerevisiae manipulations

All yeast strains used in this study are listed in Table 3. FW1259 (Eisenmann et al., 1989), FY567 and FY294 (Eisenmann et al., 1992) were obtained from Fred Winston, Harvard University. Most strains that harbored *spt15* homologous duplications were prepared in the Crouse Laboratory, Emory University. FW1259 derivatives with *spt15* chromosomal duplication were maintained on SC lacking histidine (SC- His). Crosses were performed by standard techniques (Ausubel et al., 1994). All yeast transformations were performed by the Lithium Acetate (LiOAc) method as previously described (Schiestl and Gietz, 1989) omitting the initial LiOAc preincubation in TE/LiOAc (Gietz et al., 1992).

Table 3.

Strains and Genotypes

Strain	Genotype
FW1259	*MATα, his4-917δ, lys2-173R2, ura3-52, trp1Δ1, spt15-21*
FY567	*MATa, his4-917δ, lys2-173R2, ura3-52, leu2Δ1, spt15-21*
FY294	*MATa, his4-917δ, lys2-173R2, ura3-52, trp1Δ63, leuΔ1, spt3202*
3235.18	*MATα, ade5, his4$_{am}$, lys2$_{oc}$, trp1$_{am}$, trp1$_{oc}$, SUP3$_{oc}^{ts}$, cry1^{R}, cyh2^{R}*
FW1259 Derivatives[a]	
BL124	*Δleu2*
BL101	*Δpms1*
BL102	*msh2::Tn10LUK*
BL103	*msh3::TRP1*
BL130	*msh2::Tn10LUK, msh3::TRP1*
BL205	*Δleu2 Δade8*
Orientation 1 *spt15* Homeologous Duplication[a]	
BL105	*spt15-21::pYIS2*
BL105B	*Δleu2, spt15-21::pYIS5*
BL108	*Δpms1, spt15-21::pYIS2*
BL108B	*Δpms1, spt15-21::pYIS5*
BL111	*msh2::Tn10LUK, spt15-21::pYIS5*
BL114	*msh3::TRP1, spt15-21::pYIS2*
BL117	*spt15-21::pYIS10*

Table 3 continued

Strain	Genotype
Orientation 2 *spt15* Homeologous Duplication[a]	
BL117B	*Δleu2, spt15-21::pYIS8*
BL138	*Δleu2, msh2::Tn10LUK, msh3::LEU2, spt15-21::pYIS5*
Orientation 2 *spt15* Homeologous Duplication[a]	
BL119	*Δpms1, spt15-21::pYIS10*
BL119B	*Δpms1, spt15-21::pYIS8*
BL121	*msh2::Tn10LUK, spt15-21::pYIS8*
BL121B	*Δleu2, msh2::Tn10LUK, spt15-21::pYIS8*
BL123	*msh3::TRP1, spt15-21::pYIS10*
BL123B	*Δleu2, msh3::LEU2, spt15-21::pYIS8*
BL140	*Δleu2, msh2::Tn10LUK, msh3::LEU2, spt15-21::pYIS8*
Orientation 2A *spt15* Homeologous Duplication[a]	
BL116	*spt15-21::pYIS9*
BL118	*Δpms1, spt15-21::pYIS9*
BL120	*msh2::Tn10LUK, spt15-21::pYIS7*
BL122	*msh3::TRP1, spt15-21::pYIS9*
BL139	*Δleu2, msh2::Tn10LUK, msh3::LEU2, spt15-21::pYIS7*
BL206	*Δleu2, Δade8, spt15-21::pYIS9*
Orientation 1 *spt15* Homologous Duplication[a]	
BL144	*spt15-21::p306RB*
BL145	*Δpms1, spt15-21::p306RB*

Table 3 continued

Strain	Genotype
Orientation 1 *spt15* Homologous Duplication[a]	
BL146	*msh2::Tn10LUK, spt15-21::p304RB*
BL147	*msh3::TRP1, spt15-21::p306RB*
BL174	*Δleu2, msh2::Tn10LUK, msh3::LEU2, spt15-21::p304RB*
Orientation 2 *spt15* Homologous Duplication[a]	
BL152	*spt15-21::p306.2A*
BL153	*Δpms1, spt15-21::p306.2A*
BL154	*msh2::Tn10LUK, spt15-21::p304.2A*
BL155	*msh3::TRP1, spt15-21::p306.2A*
BL176	*Δleu2, msh2::Tn10LUK, msh3::LEU2, spt15-21::p304.2A*
FW1259 *rad52* Derivatives[a]	
BL178	*rad52::LEU2, spt15-21::pYIS2*
BL180	*rad52::LEU2, spt15-21::pYIS10*
BL181	*rad52::LEU2, spt15-21::p306RB*
BL183	*rad52::LEU2, spt15-21::p306·2A*
FW1259 *ura3* Homeologous Duplication[a]	
BL208	*URA3, Δleu2, Δade8,*
BL210	*ura3ΔP/H3, Δleu2, Δade8,*
BL212	*ura3ΔP/H3, Δleu2, Δade8, spt15-21::p305SK*

Table 3 continued

Strain	Genotype
FY567 *ura3* Homeologous Duplication[b]	
BL207	*cyh2*^{R}
BL209	*URA3, cyh2*^{R}
BL211	*ura3ΔP/H3, cyh2*^{R}

[a] All strains were derived from FW1259. Only differences in genotypes are listed.
[b] All strains were derived from FY567. Only differences in genotypes are listed.

Phenotypic complementation of FW1259

Complementation of *spt15-21* by clones of *SPT15*, *TBP* and several *SPT15/TBP* hybrids allowed functional analysis of these derivatives. A clone of *Saccharomyces cerevisiae SPT15* was obtained from Fred Winston, Harvard University. A 2377-bp *Eco*RI/*Bam*HI fragment was cloned into the corresponding sites of pRS316 (Eisenmann et al., 1989; Sikorski and Hieter, 1989) and will be referred to as pYCS2 in this study. The *Schizosaccharomyces pombe* homologue of *SPT15*, *TBP*, acquired from L. Guarente, MIT, as a 1338-bp *Not*I fragment in Bluescript SK+ (Fikes et al., 1990) was cloned into the *Not*I site of pRS316 to produce pYCS1. *S. pombe TBP* was placed under constitutive transcriptional control of the *S. cerevisiae PGK* promoter. The *PGK* promoter, isolated as a 670-bp *Xho*I/*Bam*HI fragment from pPGK (Kang et al., 1990), was cloned 5' of *TBP* into corresponding sites in pYCS1 to yield pYCS3. A *Bsu*36I site was introduced into *TBP* at nucleotide 322 of the coding sequence to produce pYCS4 by oligonucleotide-directed mutagenesis. The mutagenic oligonucleotide oBL3 (Table 2) was used with an Amersham oligonucleotide-directed mutagenesis kit version 2.0 according to the manufacturer's instructions. Chimeric hybrids of the *SPT15* genes were isolated by exchanging 3' *Bsu*36I and *Sac*I fragments from pYCS2 and pYCS4 to produce pYCS5 and pYCS6. pYCS5 had P_{PGK} 5', *TBP* 5' coding DNA and *SPT15* 3' coding and flanking DNA sequences; pYCS6 had *SPT15* 5' flanking and coding sequence and *TBP* 3' coding sequences and flanking sequences (Figure 4B). A 704-bp deletion of pYCS6 from *Sna*BI to *Bsu*36I that removed all of *S. cerevisiae SPT15* except 882-bp of the 5' most flanking sequence was performed by blunt-ended ligation to create pYCS9.

Complementation of *spt15-21* was tested by transformation of FW1259 with individual plasmids followed by genetic tests of appropriate markers. pYCS2, pYCS4, pYCS5, pYCS6, pYCS9 and pRS316 were used to transform FW1259 and transformants were selected on SC-Ura. The phenotype of transformants was determined by growing patches of 6 independent isolates from each transformation on SC for 2 days at 30° and then replica plating the patches onto SC individually lacking lysine, histidine, uracil or tryptophan. Growth of the patches was scored after a 24 h incubation at 30°. The plasmid responsible for a given phenotype was unambiguously identified by isolating a crude glass bead phenol:chloroform plasmid extract from yeast, transforming *E. coli* with the extract, and performing restriction analysis on the isolated plasmid (Ausubel et al., 1994).

Construction of *spt15* homeologous duplication

The purpose of these experiments was to create several variant strains containing homeologous duplications of *spt15* and *tbp* or homologous duplications of *spt15*. The chromosomal structure of the integrated *spt15* duplication plasmids are presented in Figures 5A, 6 and 7A. The Orientation 1 homeologous *SPT15* gene was constructed by cloning a 330-bp *Bsu*36I to *Hind*III fragment of *TBP* from pYCS4 into the identical sites of *S. cerevisiae SPT15* in pYCS2 (Fig. 7). The hybrid gene was inactivated by deleting 704-bp of promoter and coding sequence of *SPT15* from *Sna*BI to *Bsu*36I (*Δ704tbp*). The resulting, deleted, hybrid gene was cloned into integrating vectors pRS306 (*URA3*) or pRS304 (*TRP1*) to produce pYIS2 and pYIS5, respectively. The inactive hybrid

gene was integrated into FW1259 upstream of *spt15-21* by transforming with *Pfl*MI linearized pYIS2 or pYIS5. The homologous Orientation 1 duplications were constructed in an identical manner except all sequences were derived from *S. cerevisiae SPT15* yielding p306RB (*URA3*) and p304RB (*TRP1*). The exogenous copy of *SPT15* was inactivated by the 704-bp deletion between *Sna*BI and *Bsu*36I.

Orientation 2 integration plasmids allowed downstream integration of *Δ704tbp* (Fig. 5A). Orientation 2 homeologous constructions pYIS10 (*URA3*) or pYIS8 (*TRP1*) were essentially identical to pYIS2 and pYIS5 except the 5' *Eco*RI site was deleted by restriction site ablation and an additional 1.0-kb of 3' flanking sequence of *SPT15* was included for purposes of integration. The inactive hybrid gene was integrated into FW1259 downstream of *spt15-21* by digesting pYIS10 or pYIS8 with *Eco*RI. Homologous Orientation 2 constructs p306·2A and p304·2A were identical to their homeologous counterparts pYIS10 and pYIS8 except all sequences were derived from *S. cerevisiae SPT15*. As described above, the exogenous copy of *SPT15* was inactivated by the 704-bp deletion.

Variants lacking 5' flanking sequence were also generated. Orientation 2A homeologous constructs, pYIS9 (*URA3*) or pYIS7 (*TRP1*), were identical to Orientation 2 except these plasmid completely lack 5' *SPT15* homology (*Δ5'tbp*). Integration of these plasmids downstream from *spt15-21* was performed by *Eco*RI digestion and transformation. A homologous Orientation 2A construct, p305SK, was also prepared but this derivative was cloned into a *LEU2* marked intergration vector, pRS305, and was integrated in to the chromosome by *Hind*III digestion. All homologous *spt15* duplication plasmids except p305SK were

prepared in the Crouse Laboratory, Emory University. The structure of all *SPT15* chromosomal duplications were verified by Southern analysis using at least two different restriction enzymes, described below.

Isolation of disruption and deletion alleles of DNA repair genes

This study included isolation of isogenic derivatives of FW1259 harboring mutations in selected mismatch repair and recombination genes. Two step deletion (Scherer and Davis, 1979) of the *PMS1* was performed to produce a 1-kb internal deletion of *PMS1* from *Eco*RI to *Cla*I (Kramer et al., 1989). One step disruption of *MSH2* (Rothstein, 1983) was performed by transforming *Spe*I digested pmsh2::Tn10 LUK obtained from R. Kolodner, Dana Farber Cancer Center (Reenan and Kolodner, 1992) *MSH3* disruption plasmids were prepared by replacing *HIS3* from *Nhe*I to *Sac*I of pmsh3Δ1::HIS3 (New et al., 1993) by blunt-ended ligation of an 850-bp *Eco*RI/*Bgl*II *TRP1* fragment or a 2-kb *Hpa*I/*Apa*LI *LEU2* fragment, yielding pmsh3::TRP1 or pmsh3::LEU2, respectively. *MSH3* one step disruptions were carried out in FW1259 by transforming either *Bam*HI/*Eco*RI digested pmsh3::TRP1 or *Bam*HI/*Aat*II digested pmsh3::LEU2. Deletion of *LEU2* in FW1259 to produce BL124 was generated by the two step method to produce a 690-bp internal deletion of *LEU2* between *Eco*NI sites. All disruption and deletions were verified by Southern analysis and mutator phenotype where appropriate. *RAD52* was disrupted by transforming *Bam*HI digested pSM20 (provided by Lorraine Symington, Columbia University) and selecting for growth on SC-Leucine. *RAD52*

disruptions were confirmed by sensitivity to 0.017% methylmethane sulfonate (MMS) and Southern analysis.

Recombination analysis

Analysis of homeologous and homologous recombination rates was performed by fluctuation analysis. Strains were streaked for single colonies on media lacking histidine as well as other appropriate nutrients (for example, media also lacking tryptophan when *TRP1* was present as the intervening marker between duplicated Spt15 sequences). Ten to 12 single colonies from each strain were used to inoculate individual 4 ml cultures of YPD. The initial inoculum was diluted 10^2 and 0.1 ml of the dilution was plated on YPD to determine initial number of cells in the culture, which was used to calculate the number of doublings the culture has undergone. Cultures were grown non-selectively to a density of 3×10^7 cells/ml at 30° and 60 rpm in a drum roller for 18 to 24 h. An aliquot of each culture was then diluted 10^4 and 0.1 ml of the dilution was plated onto YPD, in duplicate, to determine the final number of cells in the cultures. A 3 ml volume of each culture was transferred to a sterile tube, cells were pelleted by brief centrifugation and the pellets were washed in the same volume of H_2O. Repelleted cells were resuspended in 1/10 volume H_2O and 0.1 ml of the suspension, or an appropriate dilution, was plated onto SC lacking lysine (SC-Lys), in duplicate, to determine the number of lysine prototrophic cells in the culture. Colonies on all media were counted after 36 to 48 h of growth at 30°. The median frequency of lysine prototrophy was used to

determine the rate of chromosomal rearrangement of the *SPT15* duplications in a given strain by the method of Lea and Coulson (Lea and Coulson, 1948).

Reversion analysis

The rate of reversion of the *spt15-21* point mutation was determined in the Crouse laboratory by the method of Lea and Coulson as described for the recombination analysis (Lea and Coulson, 1948). Briefly, strains that lacked duplication at the *SPT15* locus and were wild type for mismatch repair or had disruption in *PMS1*, *MSH2* and *MSH3* (FW1259, BL101, BL102 and BL103, respectively) were grown non-selectively and plated to identify lysine prototrophs. The reversion rate in FW1259 was 1.1×10^{-8} events/generation. The reversion rates determined for mismatch repair mutants BL101, BL102, and BL103 were slightly higher at 5×10^{-8}, 1.2×10^{-7} and 1.8×10^{-8} events/generation, respectively.

Intervening marker loss

Genetic analysis of *SPT15* recombinants included examination of the presence or absence of the intervening plasmid marker. Ten to 50 single colonies from the recombination experiments were patched onto SC-Lys and grown 2 days at 30° followed by replica plating onto media lacking either uracil or tryptophan. Alternatively, the entire plate of lysine prototrophic cells were replica plated directly. Replica plates were incubated 24 h at 30° and the number of cells that were lysine prototrophs and uracil or tryptophan prototrophs were

counted. The percent marker loss was determined for each individual culture as the number of Ura^- or Trp^- colonies divided by the total number of Lys^+ colonies tested. Marker loss for a strain was then calculated by averaging the percent marker loss from all independent cultures (33 to 49 homeologous and 12 to 24 homologous).

Genomic DNA preparation and Southern analysis of *SPT15* recombinants

Physical analysis of *SPT15* recombinant products was performed to identify the molecular changes that had occurred in these isolates. Independently isolated recombinants, identified as lysine prototrophs, were restreaked on media lacking lysine, lysine and tryptophan, or lysine and uracil as appropriate and grown at 30°. Single colonies from restreaks were used to inoculate 5 ml cultures of the same selective media. Cultures were grown at 30° for 2 days at 65 rpm in a roller. Pelleted cells were used to prepare genomic DNA using the glass beads disruption method (Ausubel et al., 1994). Genomic DNA was resuspended in 50 µl of TE and 10 µl of each sample was digested with *EcoR*I, *Bgl*I or *Xho*I.

Digested genomic DNA was run on 1% agarose gels (Biorad) buffered with 80 mM Tris-phosphate, pH 8.0 and 2 mM EDTA (TPE). DNA in the gels was subsequently denatured in 0.5 M NaOH/1.5 M NaCl, neutralized in 1 M Tris pH 8.0/1.5 M NaCl, then transferred to Biotrans nylon membranes (ICN) by capillary action in 10X SSC (1.5 M NaCl/0.15 M sodium citrate, pH 7.0). DNA was cross-linked to membranes at 80° under vacuum for 1 h. Membranes were

pre-hybridized in 50% formamide/10% Denhardt's/5X SSPE/1% SDS and 0.1 mg/ml denatured calf thymus DNA at 42° for 1 h. Hybridization was performed at 42° for 18 h after the addition of either a ^{32}P-labeled 470-bp *Hind*III/*Bam*HI *SPT15* common 3′ fragment or a ^{32}P-labeled 330-bp *Bsu*36I/*Hind*III *TBP* specific fragment (Figures 9 and 10). Probes were prepared by the random primer method with α-^{32}P-dCTP (Feinberg and Vogelstein, 1983) and used at 1 to 5 x 10^6 cpm/ml. Blots were washed 3 times at 65° in 0.2X SSC and 1% SDS. Genomic DNA from strains containing the homologous duplications were digested with *Bgl*I to yield fragments of 5.8-kb (*spt15-21*) and 2.8-kb (*Δ704spt*) for Orientation 1 and 4.5-kb (*spt15-21*) and 5.1-kb (*Δ704spt*) for Orientation 2 when hybridized with the *SPT15* probe. Insertion of the promoter resulted in *Bgl*I fragments of 3.4-kb and 5.8-kb from Orientations 1 and 2, respectively.

Identification of nucleotide changes confined to short stretches of DNA were performed by Southern hybridization with 5′ end labeled oligonucleotide probes. oBL39 is complementary to the coding sequence of *S. pombe TBP* and corresponds to the region of the *spt15-21* G --> A point mutation. Replacement of the *spt15-21* point mutation to the wild type G in homologous duplications was determined by hybridization with oBL105. Presence of a known intragenic suppressor of *spt15-21* (Eisenmann et al., 1992) was analyzed by hybridization with oBL70. This oligonucleotide is complementary to *SPT15* coding except for an A --> C point mutation at position 709 conferring the suppressor phenotype. Oligonucleotides were 5′ end-labeled using polynucleotide kinase and γ-^{32}P-ATP (Ausubel et al., 1994). Blots were prehybridized at 25° in 6X SSC, 5X Denhardt's, 0.5% SDS, 0.05% sodium pyrophosphate, and 0.1 mg/ml denatured calf thymus

DNA. Hybridization was performed at 42° for 18h in the same buffer with 1X Denhardt's and oBL39, oBL102 or oBL70 (~2 x 10^4 cpm/ml). Blots were washed in 6X SSC and 0.05% sodium pyrophosphate for 30 min each. The temperature was progressively elevated to increase stringency. Blots hybridized with oBL39 and oBL102 were washed at 52°, 55° and 58° each, while blots hybridized with oBL70 were washed at 48°, 50° and 52°. The stringency of the final wash was designed to maintain binding of only perfectly base paired oligonucleotides.

Calculation of rates for individual recombinant classes

Overall recombination rates from strains that harbored *spt15* duplications were determined as the median frequency (Lea and Coulson, 1948) of lysine prototrophy after non-selective growth. Recombinants were initially classified as either popouts or non-popouts by replica plating onto media lacking tryptophan or uracil. These data were then used to calculate the percent popout (marker loss) as previously described (Selva et al., 1995). Non-popouts, *i.e.* those retaining the intervening marker, were further characterized by Southern blotting. These data were used to calculate the percentages of promoter insertion, point mutation replacements and (for Orientation 1) G2 unequal crossovers. Each percentage was multiplied by the overall recombination rate to yield the rate of recombination for a given class of events.

Sequence analysis of PCR products

The genomic DNA preparations described above were used in PCR reactions to generate products for sequence analysis. These experiments were performed by Alan Maderazo, University of Massachusetts Medical School. PCR was performed in 50 µl reactions with 5% glycerol, 2.5 mM $MgCl_2$, 50 mM KCl, 10 mM Tris pH 9.0, 0.1% Triton X-100, 200µM dNTP's, 0.5 µM oligonucleotide primers and 1 to 2 µl of genomic DNA (~100- 200 ng). Reactions were cycled 30 times (95°/1.5 min, 55°/2 min and 72°/2 min) after the addition of 1 U Taq polymerase. The 5′ primers were either oBL21 or oBL31 located in the *SPT15* coding and promoter regions, respectively. Complementary 3′ primers were either oBL23 present in *SPT15*, oBL32 located in the *TBP* coding region in the sequence position corresponding to *SPT15* oBL23 or oBL57 present in the common 3′ flanking region. PCR primers were removed from the PCR products using Magic PCR preps (Promega) according to the manufacturer's instructions.

The double stranded PCR products were sequenced by the Sanger method using ^{35}S-dATP (Sanger et al., 1977) and a modified annealing step. Purified PCR product (~1 pmole) in 9 µl of 0.1X TE, pH 8.0 was heated to 95° for 2 min, snap frozen in a dry ice/ethanol bath for 1 min and 1 pmole of sequencing primers was added. Samples were pulsed in a microfuge to thaw and mix (Ausubel et al., 1994). Sequencing primers included the terminal oligonucleotides described above for the PCR reactions or primers internal to the PCR products oBL60 of *SPT15* and oBL64 located in the *SPT15* common 3′ flanking region. Sequencing reactions were resolved on 8% polyacrylamide gels.

Ethylmethane sulfonate mutagenesis (EMS) and hyper-homeologous recombination screening

Mutagenesis experiments were performed to assess the utility of the *spt15* duplication for the identification of mutants that exhibit a hyper-homeologous recombination phenotype. The strain used for mutagenesis and selection, BL206 (Table 2), harbors an Orientation 2A homeologous duplication for the identification of mutations that produce a hyper-homeologous recombination phenotype and an additional *ade8* marker necessary for future characterization of mutants. BL206 was derived from BL124 by 2-step deletion of *ADE8* that removes nt -249 to 471 of *ADE8*, which includes 73% of the coding region (BL205) followed by integration of pYIS9, described above. A saturated culture of BL206 ($A_{590} \simeq 2$) grown in SC-His-Ura to prevent premature recombination of the homeologous duplication was mutagenized. The culture was washed in an equal volume 0.1 M sodium phosphate buffer, pH 7.0 and 1 ml of the culture was diluted in 1 ml of the same buffer ($A_{590} \simeq 1$). A 50 µl aliquot of 100% ethylmethane sulfonate (EMS) was added and cells were treated for 2 h at 22°. Following the incubation, cells were pelleted and the mutagen was neutralized by the addition of 5 ml 5% sodium thiosulfate. A 0.1 ml aliquot of cells was added to 9.9 ml sodium thiosulfate and 0.1 and 0.2 ml aliquot of the suspension was plated on YPD immediately prior to and following the addition of EMS to determine cell survival (30%). The mutagenized culture was washed twice more in SC-His-Ura and resuspended in a final volume of 4 ml SC-His-Ura. Twenty individual pools were prepared by diluting 0.1 ml of the mutagenized culture in

4 ml SC-His-Ura. Pools were a grown at 22° for 4 days ($A_{590} \simeq 0.5$), transferred to the same volume of YPD and stored at 4° for future screening.

Cells from the mutagenesis were screened in three rounds for hyper-homeologous recombination and mutator phenotypes. Cells from a single pool were grown non-selectively on 150 mm dishes of YPD, approximately 250 to 500 cells/plate on 20 plates (5000 to 10,000 cells/pool). Plates were incubated for 3 days at 30° until colonies were large (~3 to 4 mm diameter containing ~5 x 10^7cells/colony). YPD plates were then replica plated to SC-Lys and SC-His and selective plates grown 2 days at 30°. In this primary screen, hyper-homeologous recombination was scored as those colonies that yielded one or more papillae in a colony on SC-Lys. Positives from the primary screen were patched from the SC-His replica plate to an SC-His master plate to maintain a stock of mutants in an unrecombined state. The secondary screen was performed by patching cells from the master plate to YPD plates (~2 mm x 10 mm patches). YPD patches was grown for 2 days at 30° then replica plated to SC-Lys and SC-His. Replica plates were grown for 2 days at 30° and the hyper-homeologous recombination phenotype was scored as a patch with 2 or more papillae on SC-Lys. Larger YPD patches (~10 mm x 10 mm) from the SC-His master plate were used for the tertiary screen. Secondary positives were patched on YPD and then grown and replica plated as described for the secondary screen. Tertiary positives were identified as those patches that yielded 5 or more papillae on SC-Lys. The mutator phenotype on SC-Arg+Can were also evaluated in the secondary and tertiary screens, as some mismatch repair mutations that produce a hyper-homeologous recombination phenotype in this assay are also mutators. Tertiary

positives were restreaked to SC-His from the master plate and the hyper-homeologous recombination phenotype from 3 single colonies was re-evaluated. Two of these were stored at -70° in 15% glycerol for future characterization.

Plasmid construction for the *ura3* homeologous duplication

The purpose of these constructions was to develop an alternative to the *SPT15/TBP* homeologous gene pair. *URA3* was used for this purpose by creating a new *URA3* sequence that did not alter the amino acid sequence, but contained nucleotide divergence. It was useful to first create a *Hind*III site at position 56 of *URA3*, which was accomplished by PCR using a mutagenic primer. Vent polymerase amplification of pRS306 was performed as described above for Taq polymerase, except 2 mM $MgSO_4$ was used in place of 2.5 mM $MgCl_2$ with 10 mM KCl and 20 mM Tris. The primers, oBL71 of *URA3* with an A-->T 5' point mutation and oBL72, allowed amplification of the entire plasmid. The 4.4-kb linear amplified fragment was phosphorylated with T4 polynucleotide kinase, gel purified, ligated and transformed into *E. coli*. Plasmid were screened for the presence of a *Hind*III site generated by the point mutation and two positives were sequenced using oBL72 and oBL73. A 292-bp *Nde*I/*Nco*I fragment that flanked the *Hind*III site was cloned into pRS306 and pRS316 to yield pRS306-H3 and pYCS19 which have a *Hind*III site at position 58 of *URA3*. A 73-bp deletion of *URA3* from *Pst*I (-18) to *Hind*III yielded pYIS15. Figure 12A shows a schematic diagram of *URA3-H3*.

Next, centromeric plasmid were constructed to evaluate the consequence of specific mutations on *URA3* expression. A plasmid marked with both *ADE8* and *URA3*, pYCS15, was prepared by blunt-ended ligation of a 1.8-kb *Hind*III/*Bst*HI *ADE8* fragment into the *Hind*III and *Spe*I sites of the pRS316 polylinker. The 292-bp *Nde*I/*Nco*I fragment from pRS306-H3 and the 219-bp *Nde*I/*Nco*I fragment from pYIS15 were cloned into there corresponding sites of pYCS15 to yield, pYCS16 and pYCS18, respectively. pYCS17 was generated by ablation of the *Nco*I site in pYCS16. The Ura phenotype of these plasmids was evaluated by transforming pYCS16, 17 and 18 into BL205, selecting for Ade^+ transformants and evaluating the growth phenotype of Ade^+ transformants on SC-Ura.

Integration vectors were prepared to generate a defined deletion of *URA3* on the chromosome and the vector for introduction of the homologous and homeologous *URA3* duplications. An integration plasmid marked with both *URA3* and *LEU2*, pYIS12, was prepared by blunt-ended ligation of a 2-kb *Hpa*I/*Apa*LI *LEU2* fragment into the polylinker of pRS306-H3. A 73-bp *Pst*I/*Hind*III deletion of *URA3* in pYIS12 resulted in pYIS18, a *URA3* 2-step deletion plasmid. The homologous *URA3* duplication plasmid, pYIS16, was prepared by ligating a 3.3-kb *Hind*III/*Bam*HI *ADE8* fragment into pRS306 corresponding polylinker sites and deleting the *Nco*I site.

The homeologous *URA3* duplication plasmid was prepared in several steps. First, degenerate oligonucleotides oHomeo1 through 4 were synthesized and gel purified (Fig. 12). oHomeo3 and 4 were then annealed, extended with

dNTPs and the large Klenow fragment of *E. coli* DNA polymerase I and digested with *Nco*I and *Bsm*I. This fragment was then subcloned into the corresponding sites of pYCS19 and used to transform *E. coli*. All the colonies from a single plate were collected and used to prepare a pool of plasmid DNA, pHomeo-3'pool. Next, oHomeo1 and 2 were annealed, extended with dNTPs and the large fragment of*E. coli* DNA polymerase I, *Hind*III/*Nco*I digested and cloned into the corresponding sites of pHomeo-3'pool. *E. coli* was transformed with this construct and plasmid DNA was prepared from an entire plate of transformants to generate, pHomeo-pool. The plasmid pool was used to transform yeast (BL124) and selected for Ura$^+$ colonies. Ten Ura$^+$ colonies were used to prepare plasmid DNA for *E. coli* transformation (Ausubel et al., 1994). Two homeologous plasmids, pHomeoURA3-1 and -2, were sequenced in the University of Massachusetts Medical School Nucleic Acids Facility using an ABI automated DNA sequencer and oBL73 and oBL96 primers. Finally, the homeologous *ura3* duplication plasmids, pYIS17-1 and -2, were prepared by cloning a 2-kb *Nde*I/*Sac*I fragment from pHomeoURA3-1 and -2 into the corresponding sites of pYIS16 and deleting the *Nco*I site.

Development of strains for selection and characterization of hyper-homeologous recombination mutants

The goal of these experiments were to develop two strains. The first strain, designed for mutageneis and selection of hyper-homeologous recombination mutants, has both a *ura3* homeologous duplication and an *spt15* homologous duplication and a marker for crosses. A second isogenic tester

strain designed for characterization of the mutants, possesses the same *ura3* homeologous duplication, a marker for crosses and cycloheximide reisitance for random spore isolation. The genotype of all the strains described in this section are listed in Table 3. Development of these strains required many steps. Initially, a cycloheximide resistant derivative of FY567, BL207, was recovered by non-selective growth in YPD followed by selection on YPD with 10 μg/ml cycloheximide. The presence of a $cyh2^R$ mutation was confirmed by crossing BL207 with a $cyh2^R$ strain, 3235.18 (provided by D. Jenness, University Massachusetts Medical School). Next, BL205 and BL207 were transformed with the 1.1-kb *Hind*III fragment of *URA3* and selected for Ura$^+$ transformants to yield BL208 and BL209, respectively. Restoration of *URA3* in BL208 and BL209 was confirmed by Southern analysis.

The next step was to construct a defined 73-bp *Pst*I/*Hind*III chromosomal deletion of *URA3* in BL210 and BL211. The deletion was performed by the 2-step method in BL208 and BL209, respectively using *Nde*I linearized pYIS18. Deletions were confirmed by colony PCR using oBL103 and oBL104. Briefly, a small aliquot of cells from the colony of interest was resuspended in 100 μl H_2O and boiled 5 min. Next, 10 μl of the boiled cell suspension was added to 10 μl of 2X reaction buffer, described above, and cycled 40 times. Reaction products were resolved on 2% agarose TPE gels.

An Orientation 2A homologous *spt15* duplication was introduced into BL110 by transforming with *Hind*III digested p305SK and selecting for Leu$^+$ transformants to yield BL212. The chromosomal structure was confirmed by

Southern analysis. The final strain for mutagenesis and selection, BL213, is in the process of being prepared by transformation of BL212 with *Nde*I digested pYIS17-1 to introduce the *ura3* homeologous duplication. The final isogenic tester strain will be generated from BL211 by integration of *Nde*I digested pYIS17-1 and the introduction an additional nutritional marker for crossing to the mutagenesis strain.

The utility of the *ura3* homeologous duplication and BL213 to identify mutations that produce a hyper-homeologous recombination phenotype will be tested by introducing *MSH2* and *HPR1* (Aguilera and Klein, 1990) mutations into BL213. An *msh2Δ::TRP1* disruption in BL213 will be obtained by transformation of *Aat*II/*Pvu*II digested pEAI99 (provided by Eric Alani, Cornell University) and selection for Trp^+ transformants. A *TPR1* marked deletion for *HPR1* (Aguilera and Klein, 1990) will also be generated in BL213. The *hpr1Δ::TRP1* deletion fragment was obtained by PCR amplification of pRS304 using oBL100 and oBL101 to yield a product. These oligonucleotides possess both 45-bp of 5' and 3' *HPR1* flanking sequence for chromosomal integration and 20-bp of 5' and 3' *TRP1* flanking sequence for amplification (Hummerich and Lehrach, 1995). Homeologous and homologous recombination in BL213 and its *msh2* and *hpr1* derivatives will be tested after non-selective growth in YPD by papillation on SC-Ura and SC-Lys.

CHAPTER III

MISMATCH CORRECTION ACTS AS A BARRIER TO HOMEOLOGOUS RECOMBINATION *SACCHAROMYCES CEREVISIAE*

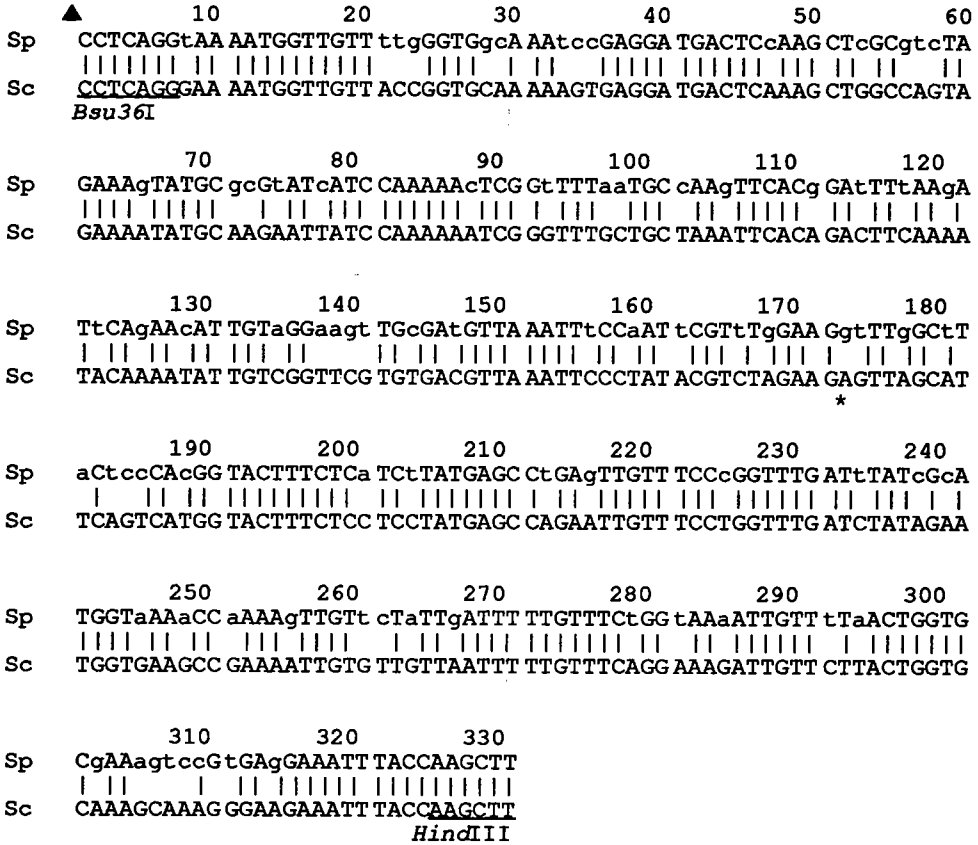
Experimental rationale

A mitotic recombination assay was developed to test the hypothesis that mismatch repair influences recombination fidelity in *S. cerevisiae.* The premise underlying this assay is that recombination between homeologous genes involves a mispaired heteroduplex that would be a target for mismatch repair function. Heteroduplexes that escape mismatch repair would undergo resolution, resulting in recombinant products containing hybrid sequence information. To score recombination events, we used a homeologous gene pair in which each gene harbors a different inactivating mutation. The mutations are situated such that production of a functional hybrid gene, either by crossover or gene conversion, involves association of the homeologous sequences and hence a mispaired heteroduplex. The effect of mismatch repair is assessed by comparing the rates of recombinant events in isogenic strains that are wild type or mutant in specific mismatch repair genes.

The gene pair chosen for this study was *S. cerevisiae SPT15* and its *S. pombe TBP* homologue encoding TATA binding protein (TBP). This gene pair shares 73% identity in their 3' coding region, which encodes the essential carboxyl repeat domains of TBP (Poon et al., 1991). Figure 4A shows the alignment of the 330-bp homeologous region from *SPT15* and *TBP* that was used in this study.

Figure 4. DNA sequence comparison of the homeologous region and complementation of *spt15-21*. (A) Sequence alignment of a 330-bp region of homeology from *Bsu*36I to *Hind*III shared between *SPT15* and *TBP*. The bottom sequence corresponds to *S. cerevisiae SPT15* (Sc) from nucleotide 349 to 679 of the coding region (Eisenmann et al., 1989). The upper aligned sequence (Sp) is from the corresponding homeologous region of the *S. pombe TBP* gene from nucleotide 320 to 650 (Fikes et al., 1990). Vertical hashes denote sequence identity, while lower case letters in the upper *S. pombe* DNA sequence indicate sequence variations. The asterisk points out the G-->A *spt15-21* point mutation. The triangle represents the 704-bp deletion from *TBP*. (B) Complementation of *spt15-21* by expression of various forms of *SPT15* in FW1259. The centromeric plasmids pRS316, pYCS2, pYCS4, pYCS9, pYCS5 and pYCS6 (described in Materials and Methods) were transformed into FW1259 (*spt15-21*) and transformants were selected on SC-Ura. The phenotype of the transformants was subsequently determined by replica plating patched colonies onto SC-Lys and SC-His. Open bars represent sequences derived from *SPT15* and hatched bars indicate sequences from *TBP*. The triangle represents a 704-bp promoter deletion from *Sna*BI to *Bsu*36I.

A



B

Plasmid in FW1259	Growth On SC -Lysine	GrowthOnSC-Histidine
VECTOR	−	+
P_{SPT15}	+	−
P_{PGK}	+	−
$P_{\Delta SPT15}$	−	+
P_{SPT15}	+	−
P_{PGK}	+	−

The homeologous region is 75% identical with a maximum of 15 matched and 5 mismatched continuous nucleotides in a stretch. Hence these sequences satisfy the requirement for homeology.

A second feature of *SPT15* and *TBP* that make them particularly useful in a homeologous recombination assay is that their wild type function has an easily selectable phenotype in the genetic background of FW1259 (Eisenmann et al., 1989). The presence of *spt15-21*, a chromosomal point mutation, causes FW1259 to be lysine auxotrophic (Lys^-) and histidine prototrophic (His^+). This phenotype in FW1259 is due to the presence of δ-elements from the Ty retrotransposon in the 5' proximal region of *LYS2* and *HIS4*. In *SPT15* strains with the δ-element insertions, transcriptional initiation from the *HIS4* promoter produced a non-functional transcript, causing histidine auxotrophy, while a functional *LYS2* transcript produced lysine prototrophy. However, the reverse phenotype was observed when cells harbored a suppressor of the Ty insertion, *spt15-21*; these cells were histidine prototrophs and lysine auxotrophs. Both *SPT15* (Eisenmann et al., 1989) and *TBP* (Fikes et al., 1990) were cloned by complementation of the FW1259 lysine auxotrophy, so that when these genes were expressed in high copy FW1259 cells became Lys^+ and His^-. Our attempt to complement the FW1259 phenotype with single-copy genes yielded the same results (Figure 4B). When a vector alone was used to transform FW1259, the cells remained Lys^- and His^+. However the strain was Lys^+ and His^- when *SPT15* or *TBP* (under the control of *S. cerevisiae PGK* promoter) was present on a single copy plasmid. Therefore this gene pair satisfies two important criteria that make it useful in a homeologous recombination assay. First, each gene in single copy complements

spt15-21 and second, the Spt phenotype can be readily monitored via the *LYS2* and *HIS4* markers.

Another important feature of the gene pair is the existence of inactivating mutations in each partner. The mutations should be spatially separated to allow crossovers between mutant alleles as one possible recombination event. The *spt15-21* mutation provides inactivation of *SPT15*. In *TBP* a deletion was made *in vitro* of a 704-bp region encompassing the promoter and 5' coding region up to *Bsu*36I (position 320; Figure 4A). As expected the *Δ704tbp* was not able to complement *spt15-21* (Figure 4B). Therefore, FW1259 can become lysine prototrophic by homeologous recombination between *spt15-21* and *Δ704tbp* to produce a chimeric gene with sequences from both genes.

A final test of this gene pair was to demonstrate that a hybrid gene derived from portions of *SPT15* and *TBP* could complement the Spt15$^-$ phenotype. This point lends credence to the idea that recombinant products arising through homeologous recombination between *spt15-21* and *Δ704tbp* would yield a functional protein. We made fusions between the two genes at a common restriction site, *Bsu*36I, that lies within the structural gene, resulting in exchange of the 3' ends of the genes. These chimeric forms were expressed in FW1259 on a centromeric plasmid. Figure 4B shows that both the *SPT15-TBP* and *TBP-SPT15* fusions complemented *spt15-21*, as expected since these genes share 93% amino acid identity in this region (Fikes et al., 1990). This result suggests that recombinant products between *spt15-21* and *Δ704tbp* can be readily detected in FW1259 as Lys$^+$ cells.

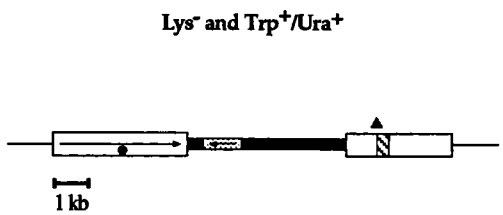
Description of tester strain

The *Δ704tbp* gene was integrated as a direct repeat in chromosome V adjacent to *spt15-21* to place the genes in a conformation that would facilitate genetic exchange. Figures 5A, 6 and 7A show the chromosomal structure of the integrants. In Orientation 1 (Figure 7A) *Δ704tbp* is integrated upstream of *spt15-21*. The integrated copy of *Δ704tbp* maintains 5' and 3' flanking DNA sequence from *SPT15* to provide regions of perfect homology to serve as initiation sites for recombination and for purposes of integration. The gene pair is separated by 4.5 kb of plasmid sequences including either *TRP1* or *URA3* as a selectable marker. Orientation 2 (Figure 5A) is essentially the same situation but with *Δ704tbp* integrated downstream of *spt15-21*. (Orientation 2 also contains an extra 1-kb of flanking sequence on the 3' end that was necessary for purposes of integration.) The Orientation 2A duplication (Figure 6) is identical to Orientation 2, buts lacks the 5′ region of *SPT15* sequence identity. Strains containing the duplication in either orientation maintain an Spt$^-$ phenotype (Lys$^-$ and His$^+$). Strains that contained the homeologous duplications were always propagated on media lacking histidine to select against premature rearrangements of the duplicated genes.

Null mutations in *MSH2*, *MSH3* or *PMS1* were introduced into strains bearing the *spt15* duplication to determine the effect of these mutations on homeologous genetic exchanges. Disruption mutations in the *mutS* homologues *MSH2* (Reenan and Kolodner, 1992) and *MSH3* (New et al., 1993) were generated to assess their potential similarity to *mutS* in recombination fidelity as these

Figure 5. Chromosomal structure of the Orientation 2 *SPT15* duplication and predicted recombinant products. (A) The Orientation 2 duplication has the exogenous *Δ704tbp* gene integrated on chromosome V downstream from endogenous *spt15-21*. Open bars denote DNA sequences derived from *SPT15*. The hatched bar represents the 330 nucleotide homeologous region from *Bsu*36I to *Hind*III (Figure 4) of *TBP*. Intervening plasmid sequences (not drawn to scale) are shown in black, except for the plasmid marker, either *URA3* or *TRP1*, which is stippled. Arrows indicate the direction of gene transcription. The black dot represents the *spt15-21* point mutation and the triangle denotes 704-bp deletion of promoter and 5' coding sequence inactivating the integrated homeologous gene. The phenotype of FW1259 that harbors this duplication is Lys^- and His^+. (B) Depicts the Lys^+ products that could be obtained from recombination of the Orientation 2 duplication. Panel 1. Intergenic crossover by a single step loop out or deletion by SSA can occur to produce a functional hybrid *SPT15* on the chromosome. Either type of event can occur with or without an associated gene conversion. Panel 2. G2 unequal crossover will produce the same functional product, in which the intervening marker has been lost. Panel 3. Gene conversions to restore *SPT15* function can be achieved either by insertion of the promoter deletion in *tbp* by sequences from *spt15-21* or by replacement of the *spt15-21* point mutation with sequences from *tbp*. Conversions could arise either by intrachromosomal events (as shown) or by interchromosomal events.

A

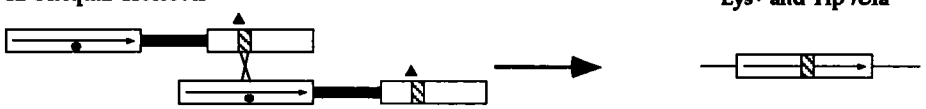


B

1. Crossover or SSA (+/- Gene Conversion)



2. G2 Unequal Crossover



3. Gene Conversion or Post-mitotic Segregation

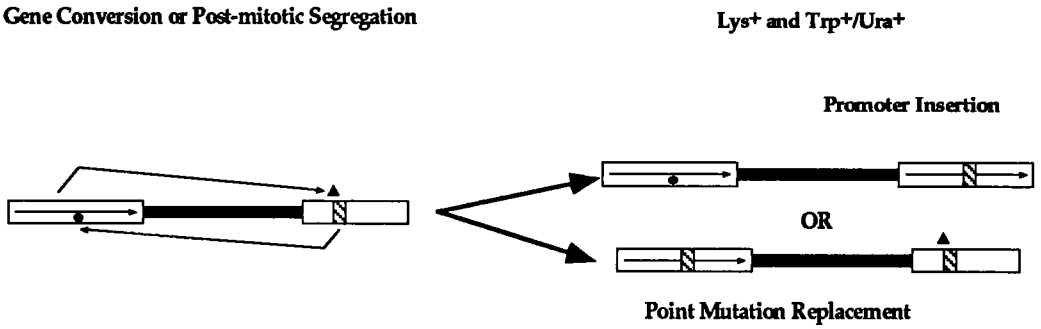


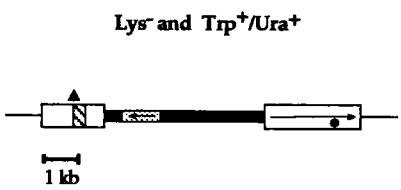
Figure 6. Chromosomal structure of the Orientation 2A *spt15* homeologous duplication. In Orientation 2A an exogenous *Δtbp* heteroallele is integrated downstream from *spt15-21* on chromosome V. This copy of *tbp* completely lacks a region of 5′ sequence identity (*Δ5′tbp*). The triangle represents the 5′ deletion and all other designations are the same as Fig. 5.

Lys$^-$ and Trp$^+$/Ura$^+$



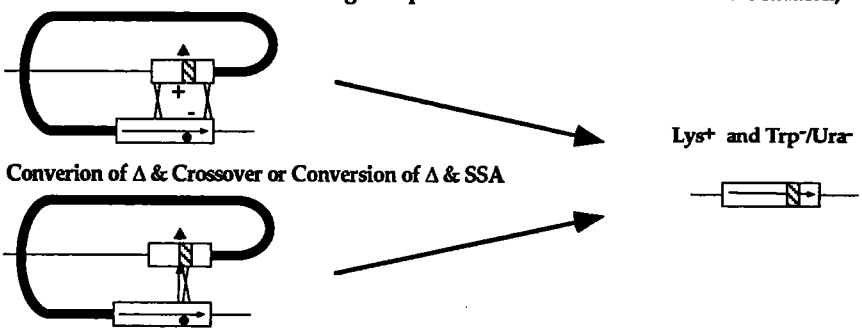
Figure 7. Chromosome structure of the Orientation 1 *SPT15* duplication and predicted recombination products. (A) The Orientation 1 duplication lacking 1-kb of 3' flanking sequence is integrated upstream of endogenous *spt15-21*. All designations are the same as described in Figure 5. (B) Depiction of possible Lys^+ rearrangement products after non-selective growth. The symbolic meaning of the filled in bars has been maintained from A, but the intervening marker gene has been omitted for simplicity. Panel 1. Single strand-annealing plus gene conversion or crossover plus gene conversion would be predicted to yield a single-copy, functional recombinant product, with concomitant loss of the intervening marker. The phenotype of these cells would be Lys^+ and Trp^-/Ura^-. Panel 2. G2 unequal cross-over between misaligned sister chromatids would produce a triplication of the *spt15* sequences to produce a single functionally WT hybrid gene flanked on either side by the original mutants. Intervening marker genes in these products are retained. Panel 3. Gene conversion could produce Lys^+ cells that have retained intervening plasmid sequences (Trp^+/Ura^+) either by restoration of the promoter deletion or point mutation, as described in the legend of Figure 5.

A

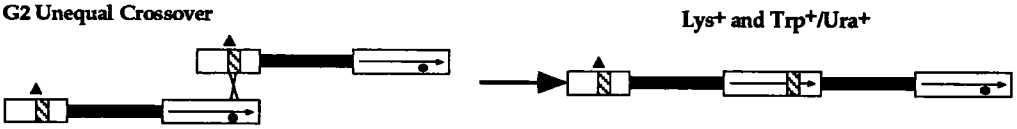


B

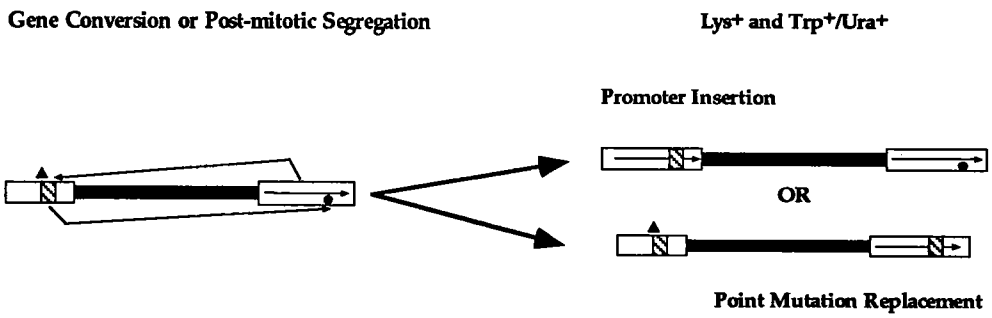
1. Crossover or SSA with Switching of Repair Tract between Δ and the Point Mutation,



2. G2 Unequal Crossover



3. Gene Conversion or Post-mitotic Segregation



genes were both cloned by virtue of their homology to *mutS*. *MSH2* has clearly been identified as a *mutS* equivalent in yeast (Alani et al., 1994; Miret et al., 1993; Reenan and Kolodner, 1992). However, only a modest mismatch repair phenotype has been detected for *MSH3* (Alani et al., 1994; New et al., 1993). A one kb deletion of *PMS1*, an *E. coli mutL* homologue, was also utilized. *PMS1* was originally identified based on its post meiotic segregation phenotype (Williamson et al., 1985) and is necessary for the repair of single base mismatches in plasmid substrates (Kramer et al., 1989). If our hypothesis is correct, one or more of these mutations will relax the block to homeologous genetic exchanges and crossovers between the *spt15* heteroalleles or gene conversions to correct either allele should increase relative to cells that are wild type for mismatch repair.

Orientation 2 homeologous recombination

Experiments done with the Orientation 2 homeologous duplication (Figure 5A) were considered first due to the clearer results obtained in this orientation. Cells containing either the homeologous or homologous chromosomal duplication and null mutation in mismatch repair genes were grown non-selectively until cultures reached late log phase (~ 3 x10^7 cells/ml). Appropriate dilutions of these cultures were then plated on media lacking lysine to determine how many cells in the culture underwent recombination to produce a functionally wild type (Lys$^+$) copy of *SPT15*. The rates of homeologous recombination were calculated as the median frequency of lysine prototrophs (Lea and Coulson, 1948). Results obtained from strains that had mutations in

mismatch repair genes were compared to cells that were wild type for mismatch repair.

The results obtained from the experiments described above are detailed in Table 4 and portrayed graphically in Figure 8. Comparison of the rates obtained for homeologous and homologous recombination in cells wild type for mismatch repair reveals that sequence divergence blocks recombination. The rate of homeologous recombination in BL117 (5.3×10^{-7}) is 150-fold lower than homologous recombination in BL152 (7.9×10^{-5}). This result is consistent with several other studies showing a decrease in recombination between diverged sequences (Alani et al., 1994; Harris et al., 1993; Mezard et al., 1992; Resnick et al., 1992). The decrease in homeologous recombination relative to identically matched DNA sequences suggests that multiple mismatches in a recombination intermediate serves as a target to block completion of the process and thus result in a reduced rate of recombinant product formation. Hence, divergence between two sequences act in *cis* as one factor in preventing recombination between these sequences.

Mutations in certain mismatch repair genes yielded significant enhancement of homeologous recombination rates (Table 4). An *msh2* strain (BL121) yielded a homeologous recombination rate which was 17-fold higher than the isogenic *MSH2* strain (BL117). The rate of homeologous recombination was also increased almost 10-fold in *msh3* cells (BL123). These results demonstrate that mutations in *MSH2* or *MSH3* partially relax the block to homeologous recombination, supporting the hypothesis that mismatch repair acts as a barrier to genetic exchanges between diverged DNA sequences. This

Table 4

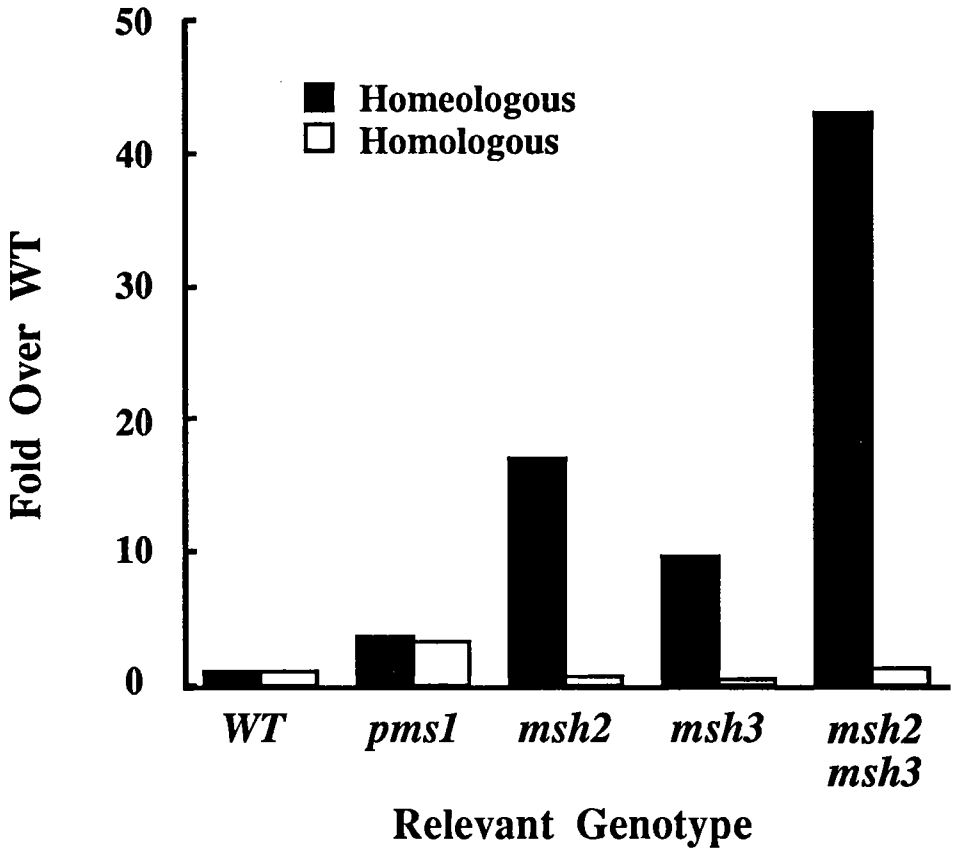
Recombination Rate and Intervening Marker Loss Orientation 2

	Strain	Genotype	Rate x10^8 (events/cell division)± SD[a]	Fold Over WT	% Marker Loss[b]
Homeologous	BL117	WT	53 ± 8	1.0	70
	BL119	*pms1*	190 ± 6	3.6	50
	BL121	*msh2*	900 ± 36	17	56
	BL123	*msh3*	510 ± 24	9.6	58
	BL140	*msh2msh3*	2300 ± 430	43	55
Homologous	BL152	WT	7900 ± 330	1.0	80
	BL153	*pms1*	25000 ± 180	3.2	58
	BL154	*msh2*	5400 ± 460	0.7	36
	BL155	*msh3*	4300 ± 680	0.5	37
	BL176	*msh2msh3*	11000 ± 400	1.3	42

[a] Recombination rates were calculated as the median frequency of lysine prototrophs by the method of Lea and Coulson (Lea and Coulson 1949). Rates were determined as an average of 3 independent experiments. Each experiment was done with 6 to 21 individual cultures.

[b] Marker loss was calculated as an average of the proportion of cells that have lost the intervening marker from independent cultures.

Figure 8. Comparison of the relative increase in Orientation 2 recombination in yeast defective for mismatch correction. Recombination rates were calculated as described in Materials and Methods. The fold over wild type was determined by dividing a mutant recombination rate by the wild-type recombination rate that had the same duplication. Results are reported for both the homeologous (filled bars) and homologous (open bars) Orientation 2 duplication.


50
40
30
20
10
0
Fold Over WT
Homeologous
Homologous
WT
pms1
msh2
msh3
msh2
msh3
Relevant Genotype

conclusion is further supported by the fact that these mismatch repair mutations had limited effect on the rate of homologous recombination (BL154, BL155; Table 2, Fig. 8). Little or no increase over wild type was observed for homologous recombination gene pairs. This suggests that the increased rate of homeologous recombination in *msh2* and *msh3* cells is specifically due to presence of mismatches and is not a general effect on recombination. Surprisingly, a *pms1* deletion mutant had only a small effect on the rate of genetic exchange between these heteroalleles (BL119; Table 4, Fig.5), a finding that also occurred with the homologous duplication (BL153).

In a strain harboring the *msh2 msh3* double mutant (BL140) the rate of homeologous recombination was elevated 43-fold, a result that is greater than either single mutation alone (Figure 8). The implications of this result are two fold. First, *MSH2* and *MSH3* apparently act independently to block homeologous recombination. This point as well as alternative interpretations are considered more thoroughly in the Discussion. Second, the rate of homeologous recombination in the *msh2 msh3* double mutant BL140 is approximately 30% the rate of homologous recombination in the wild type strain BL152 (2.3×10^{-5} versus 7.9×10^{-5}). This suggests that *MSH2* and *MSH3* participate in an important mechanism that prevents exchanges between diverged sequences.

Recombination of Orientation 2 duplications to produce lysine prototrophic cells might be predicted to occur by a number of different mechanisms depicted in Figure 5B. Panel 1 shows the product that would be obtained if an intrachromosomal crossover ("popout") event or single-strand

annealing (SSA) (Fishman-Lobell et al., 1992; Lin et al., 1984; Schiestl and Prakash, 1988) occurred to produce lysine prototrophy. Either event can occur with or without an associated gene conversion. Cells utilizing these mechanisms of chromosome rearrangement to become Spt15$^+$ should have a single hybrid copy of the gene present in the chromosome with concomitant loss of intervening plasmid and marker sequences. Therefore these cells will be Lys$^+$ and Trp$^-$/Ura$^-$. Unequal crossover between sister chromatids, panel 2, would also be expected to produce the same product with a single hybrid copy on the chromosome and simultaneous loss of the intervening marker to produce cells that are Lys$^+$ and Trp$^-$/Ura$^-$. Southern analysis (Chapter 4) verified the predicted structure of these products. In Orientation 2, events occurring by intrachromatid recombination, SSA or G2 unequal crossover yield identical products and hence are indistinguishable. However, the fact that a single hybrid copy of *SPT15* can be obtained by distinct mechanisms would suggest this product should be a large percentage of the total lysine prototrophic products. Alternatively, lysine prototrophic cells could be obtained by gene conversion events, panel 3, whereby *spt15-21* provides sequence information to *Δ704tbp* to restore the promoter or *Δ704tbp* sequence information is used to replace the *spt15-21* point mutation. Note that true gene conversions cannot be distinguished from post-mitotic segregation in this assay since either type of event will yield substitution of sequence information. In fact, we would expect that the frequency of gene conversions would be decreased in mismatch repair mutants (Alani et al., 1994; Kramer et al., 1989; New et al., 1993; Reenan and Kolodner, 1992; Williamson et al., 1985). However this limitation does not affect the interpretation of results

presented here because in either instance a multiply mismatched intermediate is presumed to escape the block to homeologous recombination.

The frequency of plasmid marker loss was used as an approximate method for analyzing the recombination pathway that produced Spt15$^+$ cells. Lysine prototrophic cells generated in the rate experiments were tested for the presence or absence of the intervening plasmid markers, either *TRP1* or *URA3*. The last column in Table 4 shows the percent loss of intervening plasmid sequences. Marker loss in all the Orientation 2 strains was high (36 to 80%), which was expected since several types of events could independently yield the same product (Fig. 5B). A change in the spectrum of marker loss in hyper-recombinant strains might indicate a specific pathway was being used to achieve the higher recombination rate in these strains. However, there was no substantial difference in the percent marker loss between the hyper-recombinant stains (BL121, BL123 and BL140) and nonhyper-recombinant strains (BL117 and BL119). Marker loss in wild type strains for both homeologous and homologous Orientation 2 duplications was slightly elevated over mismatch repair deficient strains, but the statistical significance of this increase, if any, remains unclear.

Orientation 2A homeologous recombination

The validity of Orientation 2 results were supported by a second set of experiments that used a modified structure, called Orientation 2A, that lacked all sequence identity 5' of the region of homeology (Fig. 6). The recombination assay was performed as described for Orientation 2. Results with this variant yielded

essentially identical effects for *msh2*, *msh3* and *pms1* strains to those described for Orientation 2, although homologous controls were not performed. The structural change in Orientation 2A did not have a substantial effect on homeologous exchanges, since the absolute rate of recombination for wild type and mismatch repair mutants were comparable in Orientation 2 and 2A (Table 4 and Table 5). Table 5 shows *msh2* and *msh3* (BL120 and BL122) backgrounds increased the rate of Orientation 2A homeologous exchanges 14- and 3.9-fold, respectively relative to wild type. The exchange rate in the *msh2 msh3* double mutant, BL138, was greater than additive of either single mutation alone (78-fold). A result that further supports the idea that *MSH2* and *MSH3* independently block recombination between diverged DNA sequences. Again, the absence of *PMS1* did not change the Orientation 2A homeologous recombination rate. Thus, the effects of these mismatch repair mutations were consistent with two independent homeologous duplications.

Lysine prototrophs in Orientation 2A are predicted to be generated by the same crossover, SSA and gene conversion mechanisms described for Orientation 2 (Fig. 5B). The only consequence of removal of the 5' homology region is that gene conversion events to insert a promoter into *Δ704tbp* are disfavored. Absence of 5' sequence identity prevents both recombination initiation from this site and branch migration through it, thus disfavoring formation of this product. The somewhat higher recovery of wild type popouts in Orientation 2A (85%, Table 5) relative to Orientation 2 (70%, Table 4) might reflect a bias in favor of popouts due to an inability to restore Spt15$^+$ function by promoter insertion.

Table 5

Homeologous Recombination Rate and Intervening Marker Loss

Orientation 2A

Strain	Genotype	Rate x10^8 (events/cell division)$\pm$ SD[a]	Fold Over WT	% Marker Loss[b]
BL116	WT	85 $\pm$ 5	1.0	85
BL118	*pms1*	130 $\pm$ 4	1.5	82
BL120	*msh2*	1200 $\pm$ 34	14	47
BL122	*msh3*	330 $\pm$ 39	3.9	67
BL139	*msh2msh3*	6600 $\pm$ 25	78	63

[a] Recombination rates were calculated as the median frequency of lysine prototrophs by the method of Lea and Coulson (Lea and Coulson 1949). Rates were determined as an average of 2 independent experiments. Each experiment was done with 4 to 12 individual cultures.

[b] Marker loss was calculated as an average of the proportion of cells that have lost the intervening marker from independent cultures.

Orientation 1 homeologous recombination

In Orientation 1 *Δ704tbp* is integrated upstream of *spt15-21* (Fig. 7A). Experiments with Orientation 1 *spt15* duplications were performed as described for Orientation 2. Results of the Orientation 1 experiments (Table 6), although less specific due to increased homologous recombination rates, reveal that three features of homeologous recombination in Orientation 1 were very similar to the results observed for Orientation 2. First, the rate of homeologous recombination in a mismatch repair wild type strain, BL105, was 180-fold lower than the homologous recombination rate of BL144 (5×10^{-8} versus 9×10^{-6}). Thus in both orientations sequence divergence contributes to the recombination block. Second, the block was at least partially caused by the action of mismatch repair. In an Orientation 1 *msh2* strain (BL111) the rate of homeologous recombination was 12 fold higher than the mismatch repair wild type strain (BL105; Table 6). This result further supports the hypothesis that Msh2 contributes to a barrier to homeologous recombination and thus serves to maintain the fidelity of genetic exchanges. Third, deletion of *PMS1* had no significant effect on homeologous recombination of Orientation 1 duplications (2.4×10^{-8} compared to WT; 5×10^{-8}), consistent with the results in Orientation 2.

Several differences were noticed about recombination events in Orientation 1. The absolute recombination rates were reduced in Orientation 1 compared with Orientation 2. For example, the wild type strains BL105 and BL144 yielded approximately 10-fold lower rates than their Orientation 2 counterparts BL117 and BL152 (Tables 3 and 5). This point is considered more

Table 6

Recombination Rate and Intervening Marker Loss Orientation 1

	Strain	Genotype	Rate x10^8 (events/cell division)[a]	Fold Over WT	% Marker Loss[b]
Homeologous	BL105	WT	5 ± 14	1.0	22
	BL108	*pms1*	2.4 ± 1	0.5	15
	BL111	*msh2*	60 ± 3	12	27
	BL114	*msh3*	6 ± 19	1.2	2.0
	BL138	*msh2msh3*	55 ± 7	11	15
Homologous	BL144	WT	900 ± 37	1.0	6.2
	BL145	*pms1*	8700 ± 34	10	10
	BL146	*msh2*	6200 ± 170	7.0	47
	BL147	*msh3*	1600 ± 27	1.8	1.0
	BL174	*msh2msh3*	2600 ± 21	2.8	9.0

[a] Recombination rates were calculated as the median frequency of lysine prototrophs by the method of Lea and Coulson (Lea and Coulson 1949). Rates were determined from 12 to 20 independent cultures.

[b] Marker loss was calculated as an average of the proportion of cells that have lost the intervening marker from independent cultures.

completely in the Discussion section. However it should be noted that the relative changes in rates within the Orientation 1 data set and the Orientation 2 data set largely parallel one another. Thus we believe that our basic conclusions are not significantly affected by the difference in absolute rates.

Another difference is that the *msh3* mutant (BL114) was not significantly increased relative to wild type (BL105). Furthermore, the *msh2 msh3* double mutant (BL138) displayed a similar increase in homeologous recombination to the *msh2* single mutant (BL111). Thus by two criteria loss of Msh3 does not affect the overall rate of recombination in Orientation 1. Possible reasons for this observation are presented in the Discussion. Table 6 also shows that the rate of homologous recombination in Orientation 1 was elevated in *msh2* (BL146) and *pms1* (BL145) strains. A particularly surprising result was the 10-fold higher rate of BL145 recombination, since the rate of recombination in all other *pms1* strains (BL108, BL119 and BL153) were virtually identical to their isogenic wild type strains (BL105, BL117 and BL152). Similar findings were observed by Bailis and Rothstein (Bailis and Rothstein, 1990) in a study where *pms1* was found to increase homeologous recombination rates and parallel experiments revealed a similar stimulation in homologous recombination. The 7-fold elevation in homologous recombination rate of the *msh2* strain BL146 was also puzzling, since the double *msh2 msh3* mutant (BL174) did not display as dramatic an increase (2.8-fold over WT). The increase in BL145 and BL146 recombination rates might be due to anomalies in the isolates chosen for the experiments, but this seems unlikely since 2 or 3 independent isolates were used. Although we do not fully understand these findings, any homologous recombination effects must be

partially due to the Orientation 1 chromosomal structure, since *pms1* and *msh2* did not significantly increase the rate of Orientation 2 homologous recombination (Table 4 and Fig. 8).

The upstream integration of *Δ704tbp* in Orientation 1 would be predicted to yield a different spectrum of recombination products than Orientation 2. Figure 7B depicts two consequences of this structural difference. First, as shown in panel 1, a hybrid Spt15$^+$ chromosomal copy that lacks the intervening plasmid marker (Lys$^+$ and Trp$^-$/Ura$^-$) could be generated by a mechanism involving single-strand annealing and conversion or by crossover and conversion. A single intrachromosomal event, either single strand annealing or crossover, would not show up as Lys$^+$ in our assay unless accompanied by a conversion. The second consequence of the Orientation 1 structure is that G2 unequal crossover would yield a different product than predicted for the same event in Orientation 2. Crossing-over between misaligned sister chromatids (Panel 2) should generate a triplication of *SPT15* heteroalleles, with a functional hybrid gene flanked upstream by *Δ704tbp* and downstream by *spt15-21* and two copies of intervening plasmid sequences, to produce Lys$^+$ and Trp$^+$/Ura$^+$ cells. Lysine prototrophic products that retain the intervening marker (Lys$^+$ and Trp$^+$/Ura$^+$) can also be obtained by gene conversion (or post-mitotic segregation) events to correct either *Δ704tbp* or the *spt15-21* point mutation, as described for Orientation 2. Hence, the net result of genetic exchanges in Orientation 1 should produce a large proportion of Trp$^+$/Ura$^+$ cells among the *SPT15* recombinants.

Marker loss results for Orientation 1 duplications are listed in the last column of Table 6. As predicted the overall percentage of Lys^+ cells that have lost their intervening marker in Orientation 1 (1 to 47%) was generally lower than that observed for Orientation 2 (36 to 80%). The most notable effect from this analysis is that percent marker loss from *msh3* strains with both homeologous and homologous duplications was considerably lower (2 and 1%, respectively) than all other Orientation 1 strains tested (ranging from 9 to 47%). It is possible that the inability of *msh3* Orientation 1 strains to yield crossover-like products might in part account for the absence of homeologous recombination stimulation (see Discussion). A more detailed analysis of the products might reveal if other pathways are also reduced in the *msh3* background, which could account for an even higher percentage of the overall products. The *msh2* mutation also seems to have a general effect on Orientation 1 marker loss, since it is higher than isogenic wild type strains for the homologous duplications (47 versus 6.2%) and to a lesser extent for the homeologous duplication (27 versus 22%). This change in the spectrum of *msh2* cells may reflect a preference in events occurring specifically in the absence of Msh2 function. Interestingly, the increase in marker loss detected in *msh2* cells (BL111, BL114) was not observed in the double *msh2 msh3* mutant (BL138, BL174). Perhaps the presence of *msh2* acts in some way to counteract the *msh3* effect.

CHAPTER IV

HOMOLOGOUS AND HOMEOLOGOUS RECOMBINANTS IN WILD TYPE AND MISMATCH REPAIR DEFICIENT *SACCHAROMYCES CEREVISIAE*

Summary

In the previous chapter wild type and mismatch repair deficient strains that harbor *spt15* duplications were used to determine the overall rates of recombination (Selva et al., 1995). These experiments demonstrated that mutations in the mismatch repair genes *msh2* and, in some cases, *msh3* elevate the rate of recombination between diverged *spt15* genes. In order to further understand the mechanism of homeologous recombination, structural analysis was performed on numerous recombinant products from wild type and mismatch repair deficient strains to determine the percentage of products that fell into a given class. Each percentage was then multiplied by the overall rate to arrive at a rate of recombination for individual events. The recovery of a functional gene from *spt15-21* and *Δ704tbp* could arise by a number of different mechanism, which include intrachromosomal crossovers (popout), interchromosomal crossover (G2 unequal crossover), SSA or gene conversions that either replace the point mutation in *spt15-21* or insert a new promoter into *Δ704tbp*. The absence of mismatch repair function could exert its effect to elevate the overall rate of homeologous recombination by a mechanism that increases any one or all of these pathways of genetic exchange. The results of these experiments demonstrated mutations in the mismatch repair genes *MSH2* and *MSH3* that elevate the overall rate of homeologous recombination produced

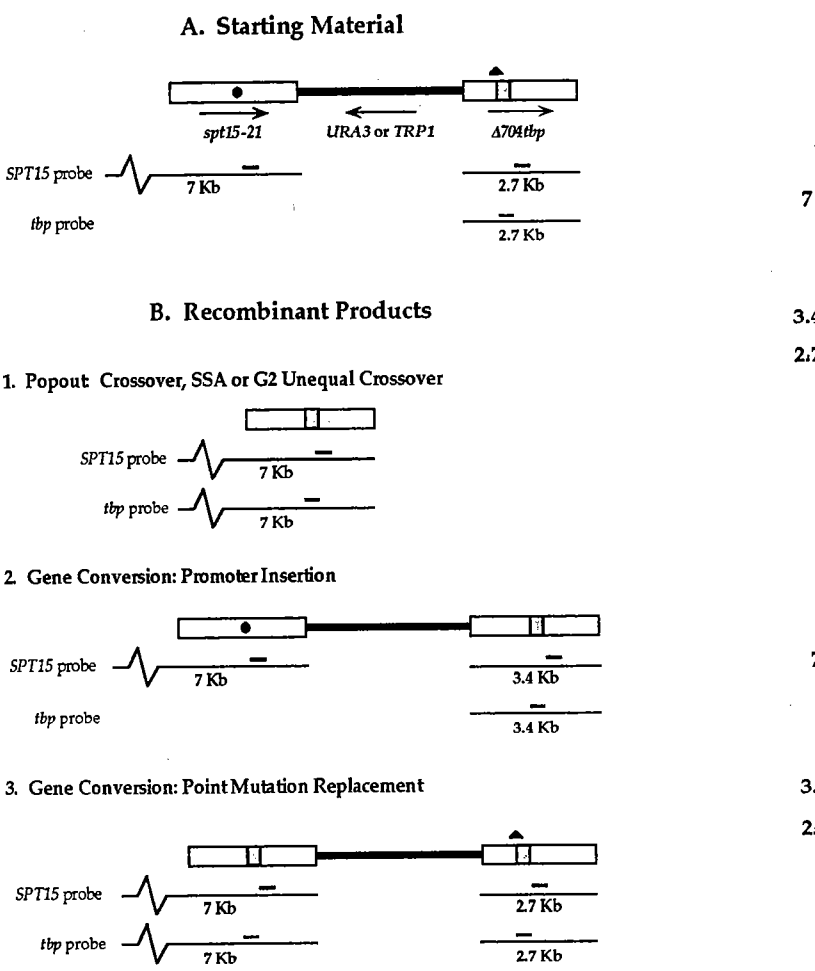
similar rate increases in the formation of each recombinant class. This suggests that mismatch correction proteins block multiple types of homeologous recombination events.

Structural analysis of Orientation 2 recombination products

Southern analysis allowed us to deduce the molecular rearrangements between the homeologous gene pair (Fig. 9). DNA isolated from the starting strain yielded two bands when cleaved with *Xho*I, blotted and probed with DNA from the 3′ region shared by both heteroalleles (*SPT15*). The 7-kb band is indicative of endogenous *spt15-21* and the 2.7-kb band represents *Δ704tbp* (compare lanes F and S in top panel, Fig. 9C). Blots hybridized with a second probe from the *S. pombe* homeology region (*tbp* probe) yielded only the 2.7-kb *Δ704tbp* band (compare lanes F and S in Fig. 9C, lower panel).

Recombinant molecules are expected to yield the structures shown in Figure 9B. The first panel illustrates the predicted "popout" structure of Lys^+ and Ura^-/Trp^- recombinant progeny. Popouts generated by intrachromosomal crossover, G2 unequal crossovers between sister chromatids or single strand annealing (SSA), result in a loss of intervening plasmid DNA (Fig. 9B, panel 1). Also indicated is the 7-kb *XhoI* product that would be expected to hybridize to the common *SPT15* probe and the *tbp* probe, since a single functional chimeric gene would contain sequences originating from both heteroalleles. Hybridization of the 7-kb popout product to both probes (Fig. 9C, lane 1) verifies this prediction. Restoration of a functionally wild type copy of *SPT15* (Lys^+) can

Figure 9. Chromosomal structure of the Orientation 2 homeologous duplication and recombinant products. The Orientation 2 duplication has the exogenous *Δ704tbp* gene integrated downstream from endogenous *spt15-21*. Inactivating mutations are shown as a black dot for the *spt15-21* G-->A point mutation and a black triangle for the *Δ704tbp* deletion. The gray box shows the 330-bp *S. pombe* region of homeology, while the white boxes signify regions of homology derived from *SPT15*. The black arrows show the direction of transcription and the gray arrow indicates the orientation of the non-transcribed *Δ704tbp*. Below are the expected fragments from Southern blots of *Xho*I digested genomic DNA when blots were hybridized with either a common probe for both heteroalleles or a probe specific for *S. pombe TBP*. (B) Diagram of the predicted chromosomal structure of products generated by recombination of the Orientation 2 homeologous duplication. Below each diagram is the expected Southern product when genomic samples were digested with *Xho*I and blots were probed as described above. Panel 1 shows the popout product by intrachromosomal crossover, G2 unequal crossover or SSA. Panel 2 illustrates the product generated by a conversion event at the promoter region in *Δ704tbp* to restore function. Gene conversion to replace the point mutation is shown in panel 3. (C) Representative Southern blots of *Xho*I digested genomic DNA from FW1259 prior to introduction of the duplication (lane F), the unrecombined starting strain (lane S), popout (lane 1), promoter insertion (lane 2), and gene conversion to replace the point mutation (lane 3). The top panel shows hybridization with the common 3′ *SPT15* probe. The bottom panel shows hybridization with the *S. pombe* specific probe. Numbers and arrows indicate the molecular weight of the bands (in kb). These bands identify the following: the 7-kb band endogenous *spt15-21*, the 2.7-kb band *Δ704tbp* and the 3.4-kb band *Δ704tbp* with a restored promoter.


A. Starting Material
spt15-21
URA3 or TRP1
Δ704tbp
SPT15 probe
7 Kb
2.7 Kb
tbp probe
2.7 Kb
B. Recombinant Products
1. Popout Crossover, SSA or G2 Unequal Crossover
SPT15 probe
7 Kb
tbp probe
7 Kb
2. Gene Conversion: Promoter Insertion
SPT15 probe
7 Kb
3.4 Kb
tbp probe
3.4 Kb
3. Gene Conversion: Point Mutation Replacement
SPT15 probe
7 Kb
2.7 Kb
tbp probe
7 Kb
2.7 Kb
C. Southern Analysis
Products
F S 1 2 3
7
3.4
2.7
SPT15 Probe
Products
F S 1 2 3
7
3.4
2.7
tbp Probe

also be achieved by gene conversion or post mitotic segregation events in which the intervening marker remains intact (Ura$^+$ or Trp$^+$). Gene conversion products occurred either by inserting DNA to restore promoter function to *Δ704tbp* (Fig. 9B, panel 2) or by replacement of the *spt15-21* point mutation (Fig. 9B, panel 3). Introduction of a promoter to *Δ704tbp*, as illustrated in panel 2, increased the size of the *Xho*I *Δ704tbp* band from 2.7-kb to 3.4-kb, while *spt15-21* was unchanged (Fig. 9C, lane 2 top and bottom). Conversion events that replace the *spt15-21* point mutation (panel 3) should have the same overall chromosomal structure as the starting duplication except that some genetic material would have to be donated from *Δ704tbp*. Southern analysis substantiates this prediction, since the 7-kb band that represents *spt15-21* now hybridizes to both the *SPT* and *tbp* probe (Fig. 9C, lane 3). Thus the different types of recombination events can be distinguished by the number of bands, the size of the lower band and by probe-specific hybridization. Recombinant products arising from homologous control sequences were analyzed in an analogous manner.

Table 7 shows the results of marker tests and Southerns from numerous independent Lys$^+$ recombinants arising from the Orientation 2 homologous and homeologous duplication. Strains were either wild type for mismatch repair or had null mutations in *msh2*, *msh3* or *msh2 msh3*. Our previous results (Selva et al., 1995) demonstrated that *msh2*, *msh3* and *msh2 msh3* increase the overall rates of homeologous genetic exchanges of the Orientation 2 duplication, with little or no effect on the rate of homologous recombination. The results in Table 7 provide a breakdown of the rates of formation of popouts, promoter insertions and point mutation replacements. Individual rates were determined by

Table 7

Distribution of Orientation 2 Recombination Products

			Rate x 10^8 (events/cell division)[b]			
	Strain	Genotype	Popout[c]	Promoter Insertion[d]	Point Mutation Replacement[d]	Other[d, e]
Homologous	BL152	WT [a]	6100	370	1400	< 79
	BL154	*msh2*	2600 (0.4)	440 (1.2)	2400 (1.7)	< 250
	BL155	*msh3*	1800 (0.3)	470 (1.3)	2000 (1.4)	< 43
	BL176	*msh2 msh3*	4700 (0.8)	580 (1.6)	5600 (4.0)	150
Homeologous	BL117	WT [a]	36	7.1	8.0	2.4
	BL121	*msh2*	490 (14)	55 (7.8)	350 (44)	< 9.0
	BL123	*msh3*	300 (8.5)	55 (7.8)	150 (19)	< 5.1
	BL140	*msh2 msh3*	1300 (37)	140 (20)	720 (90)	100

[a] The overall rate of recombination was 7.9×10^{-5} (homologous) and 5.3×10^{-7} (homeologous) events/cell division (Selva *et al.* 1995).

[b] Numbers in parentheses represent the fold increase over wild type.

[c] Calculated from 29 to 55 independent Lys^+ Ura^-/Trp^- cultures, as described in Materials and Methods.

[d] Calculated from 37 to 49 independent Lys^+ Ura^+/Trp^+ recombinants, as described in Materials and Methods.

[e] In some cases no products of this class were recovered. Numbers accompanied by a less than symbol indicate a lower detection limit of 1%.

multiplying the overall recombination rate for a given strain by the percentage of each recombinant class, as determined by Southern. Those products that could not be categorized by Southern are listed as Other, a class that is considered more thoroughly below. Rate analysis is particularly helpful in assessing effects of sequence divergence and mismatch repair functions because it allows direct comparison of the formation of all types of recombinant products.

Among homologous recombinants in Orientation 2, popouts were recovered at the highest rate in the wild type background (Table 7). This result is presumably due to the fact that popouts can arise in this orientation by several mechanisms, including intrachromosomal crossover, G2 unequal crossovers and SSA (Fig. 9). Point mutation replacements occurred next most readily, followed by promoter insertions. These events are predicted to occur by gene conversion or post-mitotic segregation (Fig. 9). The mismatch repair mutations *msh2*, *msh3* and *msh2 msh3* had only modest effects on the rates of product formation; rate values, relative to the wild type strain (numbers in parentheses), were all within 4-fold. All recombinants in these strains could be accounted for by the three predicted classes of events, as shown by the lack of products (less that 1%) that fell into the Other category. These findings are in agreement with previous studies of recombination between gene duplications in yeast (Jackson and Fink, 1981; Klein, 1988; Thomas and Rothstein, 1989).

Homeologous recombination events in the wild type background were greatly reduced relative to homologous controls (Table 7). For example, strain BL117 gave a rate of popout formation of 36×10^{-8}/cell division, corresponding

to a decrease of 170-fold relative to BL152. Similar decreases of 50-fold and 180-fold were observed for the rates of promoter insertions and point mutation replacements, respectively. Each of these changes is similar in magnitude to the overall rate decrease for homeologous recombination of 150-fold (Selva et al., 1995). These data suggest that homeology interferes with all types of recombination events. We also note that greater than 95% of homeologous recombinants are accounted for by predicted products. Taken together, these results support the idea that homologous and homeologous recombination occur by the same or similar mechanisms.

All categories of homeologous recombinant products occur at increased rates in *msh2*, *msh3* and *msh2 msh3* strains relative to wild type (Table 7). Rate increases in these mutant backgrounds ranged from 7.8- to 90-fold for the various classes of recombinants. In each strain, the accelerated rate for each type of recombinant closely reflected the overall increase in rate. For example, the overall *msh2 msh3* homeologous recombination rate was 42-fold higher than wild type (Selva et al., 1995) and the rate of each individual class was 37-, 20- and 90-fold higher than wild type (Table 7). Thus the rate increases for individual recombinant classes are within about twofold of the overall rate increase. Similar comparisons can be made for both *msh2* and *msh3* single mutants, which yield 17- and 9.6-fold increases in the overall rate, respectively (Selva et al., 1995). We conclude that *MSH2* and *MSH3* function to block all types of homeologous recombination events, since all events are elevated in their absence. Furthermore, *MSH2* and *MSH3* appear to act independently to block each homeologous recombination event, since the rate of each category in the *msh2*

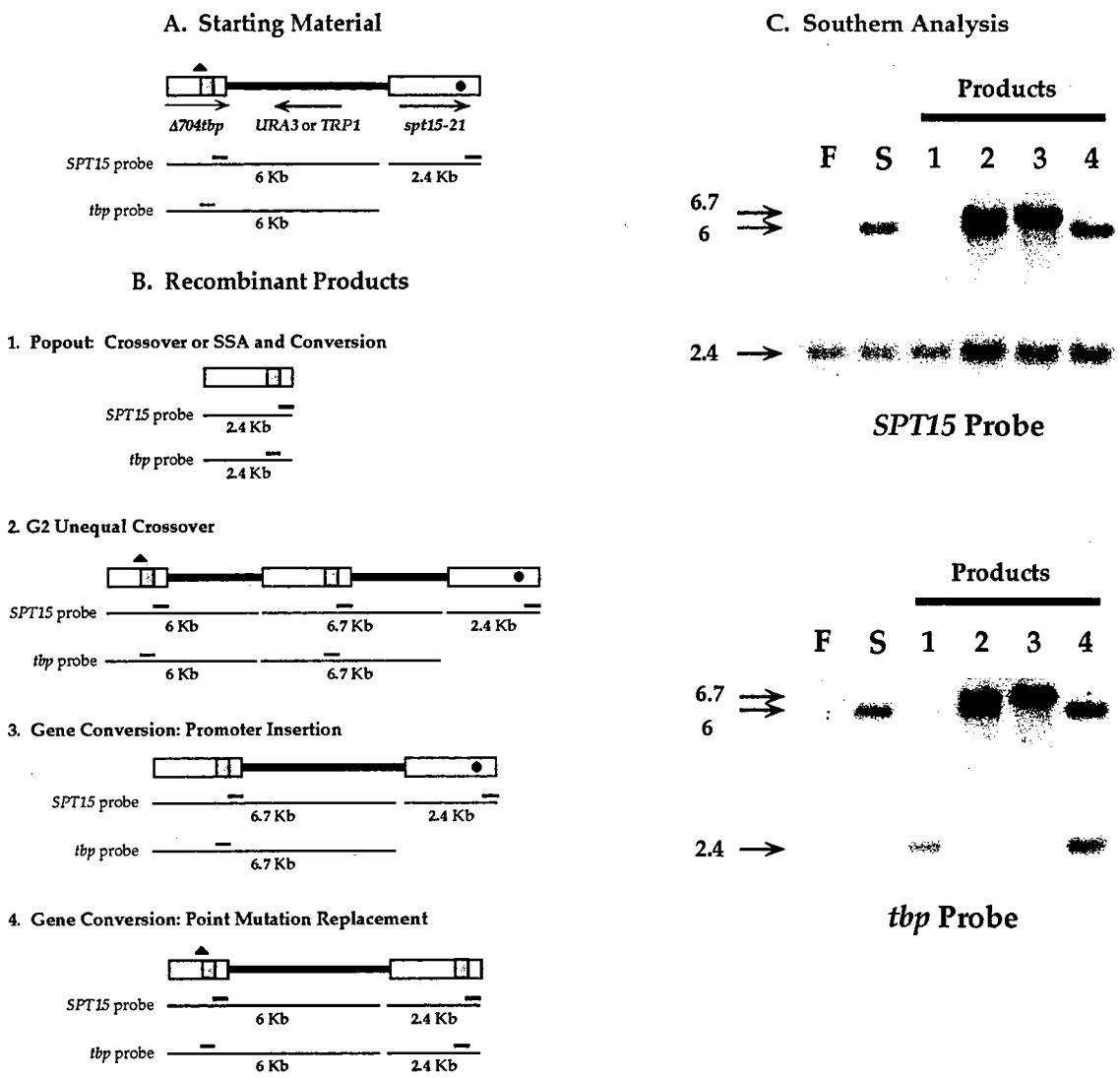
msh3 double mutant is approximately additive of *msh2* and *msh3* alone. Although all types of recombinant events are elevated in *msh2*, *msh3* and *msh2 msh3* backgrounds, these mutations did somewhat change the spectrum of product recovery. The fold increases of point mutation replacement (44-, 19- and 90-fold) are consistently higher than the overall fold increases in rate (17-, 9.6- and 43-fold; (Selva et al., 1995), whereas the increases in promoter insertions are consistently lower (7.8-, 7.8- and 20-fold). A possible explanation for this effect is provided in the Discussion section.

In summary, the results from Orientation 2 demonstrate that homologous and homeologous genetic exchanges can be accounted for by crossover, SSA or gene conversions. Homeology was a significant block in formation of all types of products. In *msh2*, *msh3* and *msh2 msh3* backgrounds, elevated rates of homeologous recombination for each class of product occurred, consistent with the idea that *MSH2* and *MSH3* interfere with multiple types of recombination events that proceed through a mismatched intermediate.

Structural analysis of the Orientation 1 recombination products

As a further test of the effects of homeology and mismatch repair on recombination, product formation was evaluated for Orientation 1 in which *Δ704tbp* was integrated upstream of *spt15-21*. Figure 10A illustrates that the chromosomal structure of Orientation 1 is similar to Orientation 2, except that Orientation 1 contains about 1.0-kb less 3' flanking DNA. The predicted fragments obtained following *Eco*RI digestion are also indicated. Southern blots

Figure 10. Chromosomal structure of Orientation 1 homeologous duplication and recombinant products. (A) Starting chromosomal structure with *Δ704tbp* integrated upstream from endogenous *spt15-21* on chromosome V. Symbolic designation in the diagram are the same as described in Figure 9. Also shown is the expected *Eco*RI digestion pattern from the unrecombined starting strain upon hybridization with the common *SPT15* probe or the *S. pombe* specific probe. (B) Diagrams of the predicted recombinant products, with expected bands from Southern analysis. Panel 1 represents popout products generated by intrachromosomal crossover with conversion or SSA and conversion. The triplication product obtained from G2 unequal crossover is shown in panel 2. Gene conversion products yielding either insertion of a promoter (Panel 3) or replacement of the point mutation (Panel 4) are illustrated. (C) Southern blots of *Eco*RI digested genomic DNA from FW1259 (lane F), the Orientation 1 starting strain duplication (lane S), popout (lane 1), triplication (lane 2), promoter restoration (lane 3) and point mutation correction (lane 4) when probed with *SPT15* (top) or *tbp* (bottom). Numbers and arrows indicate the molecular weight of the bands in kb. These bands identify the following; the 2.4-kb band endogenous *spt15-21*, the 6-kb band *Δ704tbp* and the 6.7-kb band *Δ704tbp* with a restored promoter.


A. Starting Material
Δ704tbp
URA3 or TRP1
spt15-21
SPT15 probe
6 Kb
2.4 Kb
tbp probe
6 Kb
B. Recombinant Products
1. Popout: Crossover or SSA and Conversion
SPT15 probe
2.4 Kb
tbp probe
2.4 Kb
2. G2 Unequal Crossover
SPT15 probe
6 Kb
6.7 Kb
2.4 Kb
tbp probe
6 Kb
6.7 Kb
3. Gene Conversion: Promoter Insertion
SPT15 probe
6.7 Kb
2.4 Kb
tbp probe
6.7 Kb
4. Gene Conversion: Point Mutation Replacement
SPT15 probe
6 Kb
2.4 Kb
tbp probe
6 Kb
2.4 Kb
C. Southern Analysis
Products
F S 1 2 3 4
6.7
6
2.4
SPT15 Probe
Products
F S 1 2 3 4
6.7
6
2.4
tbp Probe

of *Eco*RI digested genomic DNA prior to (lane F) and following (lane S) introduction of the Orientation 1 duplication are shown in Figure 2C. The 2.4-kb band present in both lanes F and S represents *spt15-21* and the 6-kb band identifies *Δ704tbp* when blots were hybridized with the common *SPT15* probe (Top panel).

The Orientation 1 chromosomal structure presents a unique facet of recombination which has two important distinctions from Orientation 2. First, formation of popouts requires that gene conversion accompany either intrachromosomal crossover or SSA (Fig. 10B, Panel 1). Due to the alignment of the *spt15-21* point mutation and the *tbp* promoter deletion, intrachromosomal crossover or SSA without gene conversion would yield a mutant form of the *spt15* gene on the chromosome which would not be recovered as a lysine prototroph (Selva et al., 1995). Figure 10B (panel 1) shows the predicted 2.4-kb *Eco*RI fragment from popout products. Hybridization of both the *SPT15* and *tbp* probes to the 2.4-kb *Eco*RI band (Fig. 10C, lane 1) demonstrates these recombinants contain sequences from both heteroalleles. A second consequence of the Orientation 1 structure allowed us to identify unambiguously G2 unequal crossovers (Fig. 10B, panel 2) because this class of recombinant leads to triplication of the target gene. *Eco*RI digestion of genomic DNA from these recombinants yielded 3 distinct bands, including a 6.7-kb functional *SPT15* hybrid gene flanked by the two starting mutant alleles (Fig. 10B, panel 2 and 10C, lane 2). *SPT15* function can also be achieved by insertion of the promoter sequences into a copy of *Δ704tbp* or by replacement of the point mutations in *spt15-21* (Fig. 10B, panels 3 and 4). Southern analysis of these classes of

recombinants is shown in Fig. 10C, lanes 3 and 4. Recombinants from homologous control strains containing *sptΔ704* and *spt15-21* in Orientation 1 were isolated and analyzed by similar approaches (see Materials and Methods).

Previous rate experiments (Selva et al., 1995) demonstrated that Orientation 1 homeologous exchanges in *msh2*, *msh3* and *msh2 msh3* backgrounds were increased 12-, 1.2- and 11-fold over wild type. In homologous controls, the values were 7.0-, 1.8- and 2.8-fold, indicating that recombination in Orientation 1 does not provide as much specificity for diverged sequences compared to homologous sequences. Also, *msh3* mutants do not exhibit increased homeologous recombination. Therefore results from recombinants arising from Orientation 1 must be interpreted with caution. However, for the reasons stated in the preceding two paragraphs, it was still informative to see if the results from Orientation 1 and 2 were similar.

Among homologous recombinants from Orientation 1, G2 unequal crossovers occurred most readily in a wild type background, followed by replacement of the point mutation, promoter insertions and popouts (Table 8). The recovery of popouts was much lower than Orientation 2. This result was expected due to the requirement in Orientation 1 that intrachromosomal crossover or SSA is followed by switching of the repair tract or that gene conversion of the promoter deletion must accompany crossover or SSA to produce a functional recombinant. The reduced size of the 3′ homology region (Fig. 10) may also affect popout formation. Additionally, in Orientation 2 the yield of popouts includes G2 unequal crossovers, which are categorized

Table 8

Distribution of Orientation 1 Recombination Products

			Rate x 10^8 (events/cell division)[b]				
	Strain	Genotype	Popout[c]	G2 Unequal Crossover[d]	Promoter Insertion[d]	Point Mutation Replacement[d]	Other[d, e]
Homologous	BL144	WT [a]	13	410	180	300	< 9
	BL146	*msh2*	1400 (113)	1100 (2.6)	430 (2.4)	3200 (11)	< 62
	BL147	*msh3*	19 (1.5)	440 (1.1)	310 (1.7)	830 (2.8)	< 1.6
	BL174	*msh2 msh3*	230 (18)	230 (0.6)	280 (1.6)	1900 (6.3)	< 26
Homeologous	BL105	WT [a]	1.1	0.8	2.2	0.3	0.4
	BL146	*msh2*	19 (17)	8.9 (11)	10 (4.5)	21 (61)	1.4
	BL147	*msh3*	0.1 (0.1)	0.7 (0.9)	3.4 (1.5)	1.5 (4.3)	0.1
	BL174	*msh2 msh3*	11 (10)	8.4 (11)	16 (7.1)	19 (54)	0.8

[a] The overall rate of recombination was 9.0 x 10^{-6} (homologous) and 5 x 10^{-8} (homeologous) events/cell division (Selva *et al.* 1995).

[b] Numbers in parentheses represent the fold increase over wild type.

[c] Calculated from 41 to 57 independent Lys^+ Ura/Trp^- cultures, as described in Materials and Methods.

[d] Calculated from 36 to 47 independent Lys^+ Ura/Trp^+ recombinants, as described in Materials and Methods.

[e] In some cases no products of this class were recovered. Numbers accompanied by a less than symbol indicate a lower detection limit of 1%.

separately in Orientation 1. Table 8 shows that all homologous products in the wild type background could be accounted for by the predicted classes. In the *msh2* mutant, the 7-fold increase in the overall rate of homologous recombination (Selva et al., 1995) can be primarily attributed to increases in the rates of popout and point mutation replacement. Interestingly, the *msh2 msh3* double mutant shows a similar trend to elevate the rates of popout and point mutation replacement without a large increase in the overall rate (2.6-fold; Selva et al., 1995). These results indicate that the single nucleotide mismatch caused by the *spt15-21* point mutation may provide an obstacle to Orientation 1 recombination in the presence of *MSH2*, consistent with the proposal of Alani *et al.* (Alani et al., 1994). In contrast, homologous recombination in the *msh3* strain showed little deviation from the wild type in Orientation 1 (Table 8).

Sequence divergence is a significant barrier to the recovery of all classes of recombinants in the Orientation 1 wild type strain. The rates of homeologous popouts and promoter insertions were 12- and 80-fold lower than homologous events (Table 8). Considerably larger decreases in the rates of homeologous G2 unequal crossovers and point mutation replacement were observed (510- and 1000-fold, respectively). All possible classes of recombinants are observed and greater than 90% of those products can be categorized as predicted, consistent with the hypothesis that homologous and homeologous recombination proceed by similar pathways. Thus the results obtained in Orientation 1 are generally consistent with those of Orientation 2. However, the effects of homeology on specific classes of recombination in Orientation 1 vary considerably from the overall 180-fold rate decrease (Selva et al., 1995). One possible explanation for

this result is that the rates of homeologous recombination events in wild type Orientation 1 strains are at the lower limits of detection for this system. Thus the variations might be due to the inherent experimental error in measuring low rates. Alternatively, homeology in Orientation 1 might influence the outcome of some recombination events. For example, the homeologous region could have a disproportionately large negative effect on point mutation replacement and G2 unequal crossovers. We cannot distinguish between these possibilities at this time.

Elevated rates for all classes of homeologous recombinants were observed in *msh2* and *msh2 msh3* backgrounds (Table 8). Rate increases in these strains ranged from 4.5 to 61 fold and indicated that all types of events contributed to the overall rate increases of 12- and 11-fold (Selva et al., 1995). These data are consistent with Orientation 2 results, supporting the conclusion that *MSH2* is a barrier to all homeologous recombination events. Several differences in the spectrum of products were observed in Orientation 1 in *msh2* and *msh2 msh3* backgrounds. Both *msh2* and *msh2 msh3* strains display increases in the rates of point mutation replacement relative to wild type that are higher than the overall fold increase (61- and 54-fold vs. 12- and 11-fold, respectively). Promoter insertion events in these strains were elevated to a lesser extent (4.5- and 7.1-fold). This effect was also noted in Orientation 2 and is considered more thoroughly in the Discussion.

Although *msh3* did not stimulate the overall rate of homeologous recombination, the recovery of popouts was inhibited in this strain (Table 8).

This result suggests that *MSH3* might contribute to some events in a positive manner, such as SSA (Saparbaev et al., 1996), while still having anti-recombinational effects on homeologous DNA substrates. If the magnitude of the two effects are approximately equal, it would explain the observation of no net change in the overall recombination rate. Opposing functions of *MSH3* are supported by the decreased recovery of popouts (0.1-fold relative to wild type) and the modest increase in point mutation replacements (4.3-fold) observed in Table 8. The same reasoning explains why the recovery of homologous popouts in the *msh2 msh3* double mutant is reduced relative to the *msh2* single mutant (18-fold versus 113-fold).

In summary, results from Orientation 1 are generally in agreement with those of Orientation 2. The great majority (90-100%) of recombinants can be attributed to crossover, SSA or gene conversions, suggesting that homologous and homeologous exchanges occur by the same (or similar) mechanisms. Sequence divergence was a significant block in production of all types of recombinants but this block could be partially overcome in *msh2* mutants. These observations further support the idea that mismatch repair influences numerous kinds of recombination events.

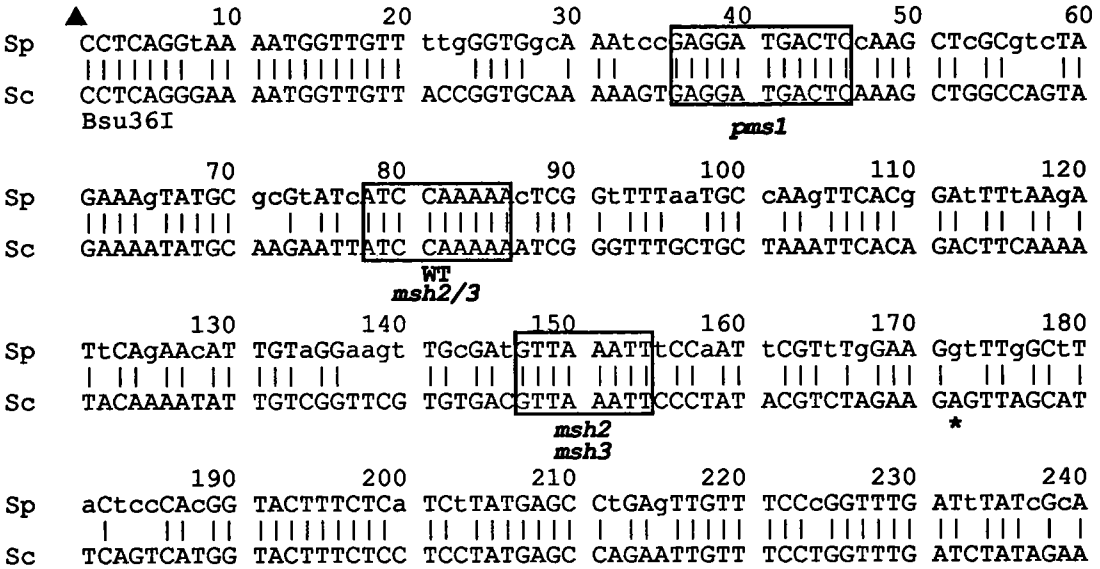
Sequence analysis of selected recombinant products

Among those products that could be categorized by Southern analysis, we sequenced *SPT15* from two classes of recombinants from wild type and mismatch repair mutants. The first class consisted of popouts in Orientation 1

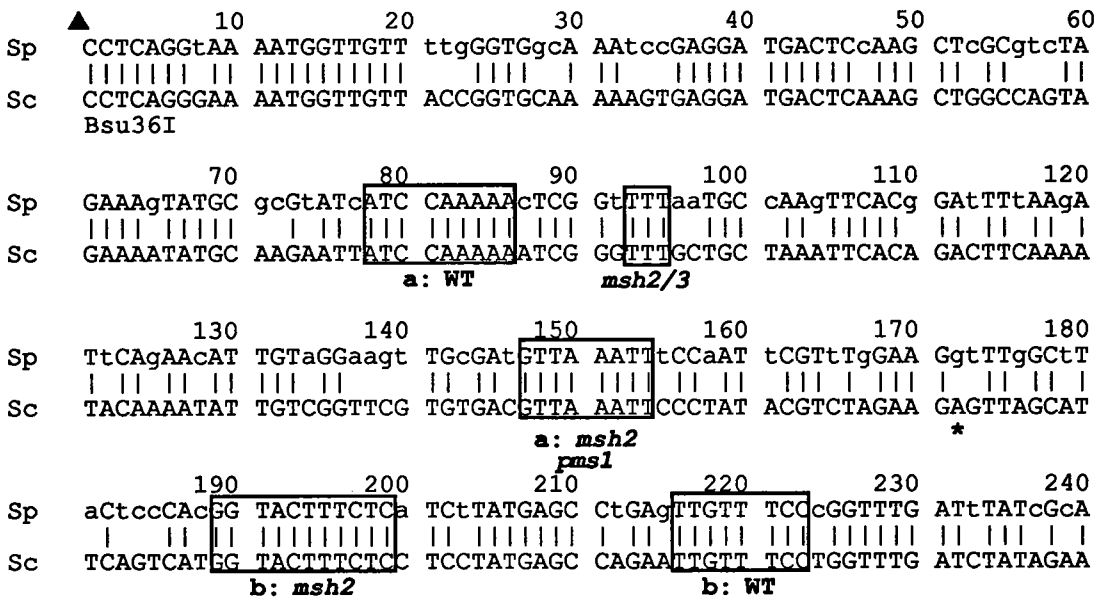
because formation of these recombinants requires either intrachromosomal crossover plus gene conversion or SSA plus gene conversion. Therefore this class might be expected to yield some unusual recombinants. For example, conversion and crossover might occur in two discrete exchanges, which could yield alternating patches of *S. cerevisiae* and *S. pombe* DNA sequences. However, as shown in Figure 11A, we found no evidence of alternating patches. In each of 5 cases a single crossover point was identified in a stretch of 8 to 11 nucleotides of identity, suggesting conversion and crossover occur concurrently. Although *msh3* profoundly reduced the recovery of popouts in Orientation 1, the single product from an *msh3* strain examined was normal by sequencing. In fact, the crossover end point maps to the identical position as the recombinant from an *msh2* background. The second class of products examined were gene conversion events at the point mutation in Orientation 2 (Fig. 11B) because we wished to compare the length of conversion tracts in wild type and mismatch repair mutants. Analysis of 4 recombinants showed that end points occur at small (3-11 nt) blocks of homology within the homeologous region. Wild type and *msh2* Lys$^+$ recombinants showed conversion tracts of as few as 146 and 53 nt, respectively, that span the position of the *spt15-21* allele. For *pms1* and *msh2 msh3* strains, one endpoint was identified in the homeologous region. The other end point presumably occurred in the 3′ flanking region of identity. Results with the *msh2 msh3* sample also showed an endpoint that occurred in a region with only 3 nucleotides of identity. Our preliminary analysis of these two classes of recombinants indicates that genetic exchanges between divergent nucleotide sequences occurred in continuous stretches, transfer endpoints were found in patches of sequence identity and mismatch correction had no obvious effect on

Figure 11. Identification of crossover end points by sequence analysis of functional *SPT15* hybrid genes. Sequence analysis was done with PCR products amplified directly from genomic DNA isolated from Lys^+ recombinant products. (A) Orientation 1 popouts from each strain wild type (WT) *msh2*, *msh3* and *msh2 msh3* (*msh2/3*). Sequences from *S. pombe TBP* and *S. cerevisiae spt15-21* are designated with Sp and Sc, respectively. Vertical bars show nucleotide identity between the two sequences and small letters in Sp indicate nucleotide differences. All recombination products initiate as Sc DNA sequence and switch to Sp after crossover or conversion. The inverted filled triangle represents the position of the 704-bp *tbp* deletion and the asterisk shows the position of the *spt15-21* G-->A point mutation. Boxed sequence identify the crossover end point, which are regions of sequence homology between heteroalleles and cannot be further pinpointed. The mismatch correction genotype from which the DNA was isolated are indicated below the boxed regions. (B) Orientation 2 conversion products that corrected the point mutation from wild type (WT), *pms1*, *msh2* and *msh2 msh3* (*msh2/3*)strains. For two samples, WT and *msh2*, the start and finish of the conversion tracks were present in the 330-bp homeologous region. These are identified by a: (start) and b: (finish).

A.


10 20 30 40 50 60
Sp CCTCAGGtAA AATGGTTGTT ttgGGTGgcA AAtccGAGGA TGACTCcAAG CTcGCgtcTA
Sc CCTCAGGGAA AATGGTTGTT ACCGGTGCAA AAAGTGAGGA TGACTCAAAG CTGGCCAGTA
Bsu36I
pms1
70 80 90 100 110 120
Sp GAAAgTATGC gcGtATcATC CAAAAAcTCG GtTTTaaTGC cAAgTTCACg GAtTTtAAgA
Sc GAAAATATGC AAGAATTATC CAAAAAATCG GGTTTGCTGC TAAATTCACA GACTTCAAAA
WT
msh2/3
130 140 150 160 170 180
Sp TtCAgAAcAT TGTaGGaagt TGcGAtGTTA AATTtCCaAT tCGTtTgGAA GgtTTgGCtT
Sc TACAAAATAT TGTCGGTTCG TGTGACGTTA AATTCCCTAT ACGTCTAGAA GAGTTAGCAT
msh2
msh3
190 200 210 220 230 240
Sp aCtccCAcGG TACTTTCTCa TCtTATGAGC CtGAgTTGTT TCCcGGTTTG ATtTATcGcA
Sc TCAGTCATGG TACTTTCTCC TCCTATGAGC CAGAATTGTT TCCTGGTTTG ATCTATAGAA

B.


10 20 30 40 50 60
Sp CCTCAGGtAA AATGGTTGTT ttgGGTGgcA AAtccGAGGA TGACTCcAAG CTcGCgtcTA
Sc CCTCAGGGAA AATGGTTGTT ACCGGTGCAA AAAGTGAGGA TGACTCAAAG CTGGCCAGTA
Bsu36I
70 80 90 100 110 120
Sp GAAAgTATGC gcGtATcATC CAAAAAcTCG GtTTTaaTGC cAAgTTCACg GAtTTtAAgA
Sc GAAAATATGC AAGAATTATC CAAAAAATCG GGTTTGCTGC TAAATTCACA GACTTCAAAA
a: WT
msh2/3
130 140 150 160 170 180
Sp TtCAgAAcAT TGTaGGaagt TGcGAtGTTA AATTtCCaAT tCGTtTgGAA GgtTTgGCtT
Sc TACAAAATAT TGTCGGTTCG TGTGACGTTA AATTCCCTAT ACGTCTAGAA GAGTTAGCAT
a: msh2
pms1
190 200 210 220 230 240
Sp aCtccCAcGG TACTTTCTCa TCtTATGAGC CtGAgTTGTT TCCcGGTTTG ATtTATcGcA
Sc TCAGTCATGG TACTTTCTCC TCCTATGAGC CAGAATTGTT TCCTGGTTTG ATCTATAGAA
b: msh2
b: WT

the length of conversion tracts. No alterations from the expected sequences were observed, indicating that transfer occurred accurately (Harris et al., 1993; Mezard and Nicolas, 1994; Mezard et al., 1992; Priebe et al., 1994).

Structural analysis of recombinants in *pms1* strains

We previously found (Selva et al., 1995) that mutations in *PMS1* did not substantially change the overall rates of homeologous or homologous recombination in Orientation 2 (3.6- and 3.2-fold relative to wild type) or homeologous events in Orientation 1 (0.5-fold). A 10-fold increase was detected for the Orientation 1 homologous exchange rate. Here we consider whether or not different classes of recombination are affected in *pms1* strains by examination of individual exchange rates. Table 9 shows recombination rates for all classes of Orientation 2 and Orientation 1 homologous and homeologous recombinants from *pms1* strains. In parentheses are the fold changes relative to wild type rates that appear in Tables 7 and 8. Homologous events in Orientation 2 and homeologous events in Orientation 1 exhibited small rate changes in all categories of recombinants that were similar in magnitude to the overall rate changes. Thus there is no evidence in these cases for preferential effects of *PMS1*. In the Orientation 2 homeologous strain, point mutation replacements were increased preferentially over promoter insertions. This distribution change was similar to what was observed for *msh2*, *msh3* and *msh2 msh3* strains (Table 7) and is considered more thoroughly in the Discussion. The overall Orientation 1 homologous rate increase in the *pms1* background was primarily due to a 52-fold elevation in the popout rate (Table 9). Again this result is similar to

Table 9

Distribution of Recombinants from *pms1* Strains

		Rate x 10^8 (events/cell division)[a]				
	Strain	Popout[b]	G2 Unequal Crossover[c]	Promoter Insertion[c]	Point Mutation Replacement[c]	Other[c, d]
			Orientation 2			
Homologous	BL153	19000 (3.0)	-	1200 (3.2)	5200 (3.7)	150
Homeologous	BL119	91 (2.6)	-	2.6 (0.4)	54 (6.8)	42
			Orientation 1			
Homologous	BL145	670 (52)	3900 (10)	2000 (11)	2200 (7.3)	< 87
Homeologous	BL108	0.4 (0.4)	0.4 (0.5)	1.0 (0.5)	0.2 (0.6)	0.2

[a] Wild type recombination rates are reported in Tables 1 and 2. Numbers in parentheses represent the fold increase over wild type.

[b] Calculated from 33 to 60 independent Lys^+ Ura/Trp^- cultures, as described in Materials and Methods.

[c] Calculated from 38 to 48 independent Lys^+ Ura/Trp^+ recombinants, as described in Materials and Methods.

[d] In some cases no products of this class were recovered. Numbers accompanied by a less than symbol indicate a lower detection limit of 1%.

phenotypes observed for *msh2* in Orientation 1 where homologous popouts were increased 113-fold (Table 8).

The *pms1* mutation resulted in the largest number of products that could not be distinguished by Southern, categorized as Other. The nature of these recombinants were further analyzed in *pms1* strains (16 isolates from Orientation 2 and 9 isolates from Orientation 1) and the wild type (6 isolates from Orientation 1). These products may have arisen by a number of alternative events, including extragenic or intragenic suppressors of the *spt15-21* point mutation, reversion of the *spt15-21* point mutation or by an aberrant recombination event to yield an unanticipated change that might restore *SPT15* activity. Alternatively, gene conversion events might have produced very short conversion tracts that escape detection in our Southern analysis. Conversion tracts as short as 18 base pairs were observed in homeologous transfers between *PMA* genes (Harris et al., 1993).

Spontaneous extragenic suppressors of *spt15-21* have been identified in only one gene, *SPT3* (Eisenmann et al., 1992). We tested for the acquisition of an *spt3* extragenic suppressor by crossing the Lys^+ Other products from wild type and *pms1* backgrounds with a strain bearing *spt3-Δ202* (FY294). If the lysine prototrophy in our unidentified products was caused by an *spt3* suppressor mutation, diploids from this cross would be *spt3/spt3* and hence His^+ and Lys^- in this genetic background. By this test, extragenic suppressors in *SPT3* accounted for only a minority of Other recombinants (two of 16 Orientation 2 *pms1*, two of nine Orientation 1 *pms1*/ and one of six Orientation 1 wild type recombinant

products). Thus the majority of Other recombinants were still unaccounted for. Southern analysis designed to identify intragenic suppressors or gross chromosomal rearrangements were negative. Similarly, DNA sequencing of six unexplained Orientation 2 *pms1* recombinants showed that neither point mutation reversion nor small conversion tracts accounted for the lysine prototrophic phenotype. Thus, the mechanism that produced the Lys^+ phenotype for most of the Other class of recombinants could not be identified. However, this category accounted for less than 5% of recombinants from all other strains tested.

RAD52 effects on homologous and homeologous recombination

As a further test of the hypothesis that homologous and homeologous recombination occur by the same or similar mechanism, a preliminary experiment was performed to examine the consequence of a *rad52* mutation on the rate of genetic exchanges (Table 10). *rad52* mutants are defective in meiotic and mitotic homologous genetic exchanges (reviewed in Petes et al., 1991). Previous studies that have examined the effect of *rad52* on homologous direct repeat recombination in mitotic cells have shown that genetic exchanges are reduced 3-to 18-fold with popouts remaining as the primary recombinant product (Jackson and Fink, 1981; Klein, 1988; Saparbaev et al., 1996; Thomas and Rothstein, 1989). Here the effect of a disruption in *RAD52* was examined to determine if this mutation exerts similar effects on homeologous genetic exchanges. Results in Table 10 should be reviewed with caution, since these data were obtained from a single experiment.

Table 10

Effect of a *RAD52* on Homologous and Homeologous Recombination

	Strain	Genotype	Rate x 10^8 (events/cell division)[a]	Fold Decrease from WT level	Popout[b]
			Orientation 2		
Homologous	BL152	WT	2780	1.0	65
	BL183	*rad52*	730	3.8	100
Homeologous	BL117	WT	16	1.0	87
	BL180	*rad52*	2.5	6.5	26
			Orientation 1		
Homologous	BL144	WT	848	1.0	2.5
	BL181	*rad52*	6.6	128	0
Homeologous	BL105	WT	14	1.0	23
	BL178	*rad52*	10	1.4	0

[a] Recombination rates were calculated as the median frequency of lysine prototrophs by the method of Lea and Coulson (Lea and Coulson 1949). Rates shown were from one experiment using 7 or 8 independent cultures.

[b] Marker loss was calculated as an average of the proportion of cells that have lost the intervening marker from independent cultures.

Consistent with other studies that examined the effect of *rad52* on direct repeat recombination (Jackson and Fink, 1981; Klein, 1988; Thomas and Rothstein, 1989) the rate of Orientation 2 homologous recombination was reduced less than 4-fold in *rad52* stains relative to wild type (BL183 compared to BL152). Similarly, the rate of Orientation 2 homeologous recombination in the absence of *RAD52* (BL180) was reduced 6.5-fold from the wild type rate. However, the types of recombinants recovered from homologous and homeologous *spt15* duplications in *rad52* strains, BL183 and BL180, respectively, were quite different. Most products recovered from *rad52* strains that harbored the Orientation 2 homologous duplications were popouts (100% vs. 65% in *RAD52* strain). In contrast, popouts accounted for only 26% of products from *rad52* homeologous recombinants (BL180), as compared to 87% in the *RAD52* strain, BL117. The implication of this difference will be considered in the discussion.

Mutations in *RAD52* caused a 128-fold decrease in the Orientation 1 homologous recombination rate relative to wild type (BL181 compared to BL144) to near background levels. This result suggests genetic exchanges in Orientation 1 are much more dependent on *RAD52* than in Orientation 2. The complete absence of popout products in BL181 is consistent with our prediction that the recovery of Orientation 1 popouts requires a gene conversion event, since these events are *RAD52* dependent (Jackson and Fink, 1981; Klein, 1988). The effect of *rad52* in Orientation 1 homeologous recombination (BL178) was difficult to interpret, since the wild type rate is at the lower limit of detection for this assay system.

CHAPTER V

ISOLATION OF HYPER-HOMEOLOGOUS RECOMBINATION MUTANTS

Summary

The results in the previous two chapters demonstrate that some genes involved in mismatch repair are required to maintain the fidelity of genetic exchanges since homeologous genetic exchanges were increased in their absence. In this chapter, the hyper-homeologous recombination phenotype of mismatch repair mutations will be utilized to develop a screen to isolate new mutants and/or new alleles of known genes that act as a barrier to homeologous recombination and thus are likely to play a role in yeast mismatch repair. Initially, the *spt15* homeologous duplication was tested to demonstrate the feasibility of using this system in a screen to isolate hyper-homeologous recombination mutants. However, due to the genetic inflexibility of the *spt15* marker in subsequent characterization of the mutants, a second generation homeologous duplication in *ura3* was subsequently developed. The *ura3* homeologous duplication was tested to determine if its recombination behavior was similar to that observed for *spt15* homeologous duplications and therefore would be useful in the identification of hyper-homeologous recombination mutants.

Mutagenesis and selection of hyper-homeologous recombination mutants with *spt15* duplication

These experiments were initiated in order to determine if a homeologous duplication system would be useful to identify mutations that produced a hyper-homeologous recombination phenotype. The ultimate goal this work was to develop a relatively simple system to identify mutations in genes involved in DNA mismatch correction. The strain chosen for the initial mutagenesis and screening, BL206, harbors an Orientation 2A *spt15* homeologous duplication for identification of hyper-homeologous recombination mutants and an *ade8* deletion for subsequent characterization of the mutants. Orientation 2A was selected because it offers several advantages. Orientation 1 is not ideal because these homeologous duplications yield a low signal to noise ratio and as a result produce too many false positives for screening purposes. In addition, some mismatch repair mutants do not elevate recombination rates in Orientation 1 (Table 5). These problems are avoided in both Orientation 2 and 2A (Tables 3 and 4). Orientation 2A offers additional advantages for screening purposes relative to Orientation 2. The Orientation 2A construct supports both gene conversions and crossovers, which were shown to be elevated in the absence of *MSH2* and *MSH3* (Tables 6 and 7). Furthermore, *msh2* and *msh3* strains favor gene conversions that replace the *spt15-21* point mutation (Table 6) suggesting mismatch repair proteins might interact more efficiently with multiply mismatched substrates. Since Orientation 2A lacks 5' flanking sequence, homeologous exchanges that might initiate in the 5′ flanking regions of sequence identity cannot occur. Thus, use of the Orientation 2A duplication also avoids

the possibility of isolating mutations that are specifically involved in recognition and repair of large loops.

BL206 was mutagenized by treating cells with EMS and twenty individual pools were established to allow for the recovery of independent mutants. A screening protocol of mutagenized BL206 was chosen based on the ability to utilize several rounds of screening for the homeologous recombination phenotype (to eliminate false positives) and the relative ease of use. In contrast, direct selection of cells that had recombined the homeologous duplication would leave no means to re-evaluate this phenotype and hence was less useful. The screening protocol takes advantage of the ability to identify both recombined and unrecombined cells present in a colony or patch. Briefly, mutagenized cells were grown on non-selective plates to allow recombination. Colonies containing recombinants were identified by papillation on SC-Lys. Clonal cells that had not recombined were isolated by replica plating to SC-His. Potential hyper-homeologous mutants from the SC-His plate could then be screened again by repeating the process with larger patches of cells. The next challenge was to devise a simple protocol to screen large numbers of colonies following mutagenesis. A large number of cells from a given pool were plated on YPD followed by replica plating of colonies to SC-Lys and SC-His. The hyper-homeologous recombination phenotype was evaluated by the number of papillae that formed for each colony on SC-Lys. A criteria of one or more SC-Lys papillae/colony was established based on pilot studies using *msh2* disruptions and wild type strains. Typically *msh2* yielded one or more papillae/SC-Lys replica colony, while the wild type rarely yielded any papillae. Tables 10 show

Table 11

Summary of BL206 Mutagenesis and Screening

Pool Number	Total colonies screened	Primary Homeologous hyper-rec.[a]	Secondary Homeologous hyper-rec.[a]	Tertiary Homeologous hyper-rec.[a]	Tertiary Homeologous hyper-rec. & mutator[b]
1	6000	281	49	16	4
2	7500	522	109	23	5
3	3500	179	57	16	0
Totals	17000	982	215	55	9

[a] The homeologous recombination phenotype was identified by papillation on SC-Lys as described in Materials and Methods.

[b] The mutator phenotype was determined by papillation of an isolate on SC-Arginine + Canavinine.

the initial round of screening BL206 mutagenized cells yielded a high percentage of putative positives (982 candidates from 17000 total colonies). Each cell was also replica plated to SC-His to maintain an unrecombined stock of an isolate for subsequent and more stringent rounds of screening.

False positives from the initial screen were eliminated by repeating the lysine papillation test through two additional rounds on progressively larger populations of the isolate. The secondary screen was performed by patching cells (~2 x 10 mm) from an SC-His master plate to YPD then replica plating to SC-Lys and SC-His. Two or more SC-Lys papillae was established as the criteria for passage to a third and final round of screening. This level of papillation again relied upon wild type and *msh2* strains as a standard. The second round of screening eliminated 70 to 80% of the cells initially identified as positives (Table 11). The YPD patch size in the tertiary screen was approximately 10 x 10 mm. Isolates scored as positives yielded 5 or more papillae on SC-Lys. The final results from screening three of the pools through three rounds of lysine papillation showed that 0.32% of total cells screened (approximately 4 to 9% of initial positives) yielded a hyper-homeologous recombination phenotype. The mutator phenotype of the isolates, based on canavanine resistance tests, was determined as means of preliminary characterization (Table 11). Only a fraction of hyper-homeologous recombination isolates identified in the tertiary screen (0-25%) were also mutators. This result is consistent with phenotypes of mismatch repair mutants known to elevate homeologous recombination rates. For example, *MSH2* deficient strains are strong mutators (Reenan and Kolodner, 1992) whereas strains lacking *MSH3* are not (New et al., 1993).

The preceding experiments clearly demonstrated the feasibility of using a divergent direct repeat to identify hyper-homeologous recombination mutants. However, it became clear at this point that further characterization of these mutants in BL206 would have proven difficult, due in part to problems associated with genetic manipulation of *spt15-21* mutant strains, as well as other limitations of the strain. For example, dominance of a mutation could not be easily established because the *LYS2* δ–element promoter insertion, which allows for the His/Lys selection, places this gene under mating type control. *LYS2* transcription is turned off in diploids regardless of the Spt15 status (personal communication Fred Winston). It would also be difficult to establish complementation groups of BL206 mutants as well as conduct other genetic characterization, since dipliods that are heterozygous for *spt15-21* do not readily sporulate (Eisenmann et al., 1989). Strain BL206 also does not provide a way to evaluate easily the homologous recombination phenotype of these mutants. It was important to eliminate as early as possible mutants that elevate both homologous and homeologous recombination. Evaluation of this phenotype in BL206 would have to be performed by a back cross to a strain that harbored a homologous duplication. Given the difficulty in sporulating *spt15-21* strains, an Spt^+ form of an isolate (duplication recombined) would have to be crossed to a strain that harbored a homologous duplication. Haploids that had the initial mutation, and a homologous duplication, would have to be identified by following appropriate markers one of which must be mutator a phenotype since the ability to access the homeologous recombination phenotype will have been lost. As a result, only a fraction of hyper-homeologous recombination mutants could be evaluated further. The Spt^+ selection also poses problems in the initial

screening steps. Lysine auxotrophy of *spt15-21* is somewhat leaky, and if too many cells are transferred to the SC-Lys during replica plating, papillation of the colony is difficult to evaluate. For these reasons, a new starter strain was developed to allow for the efficient selection and characterization of hyper-homeologous recombination mutants.

Testing and development of *URA3* as a new homeologous gene

The purpose of these experiments was to identify a new gene which could be used in a homeologous recombination assay in a manner similar to the well-characterized *spt15* homeologous duplication. This new gene requires defined, spatially separated, inactivating mutations in which direct repeat recombination would be the primary mechanism employed to restore function. The most important feature of such a gene is the ability to select independently for the unrecombined, mutant duplication for the recombined, functional gene. The gene chosen for this purpose was *URA3*. Growth of Ura$^-$ strains that harbor a homeologous *ura3* duplication on 5-Flouroorotic acid (5-FOA) maintains the unrecombined duplication. Recombination to yield *URA3* can be identified on SC-Ura. However, the feasibility of using *URA3* in a direct repeat homeologous duplication also depended upon the identification of a functional homeologous variant to provide sequence divergence.

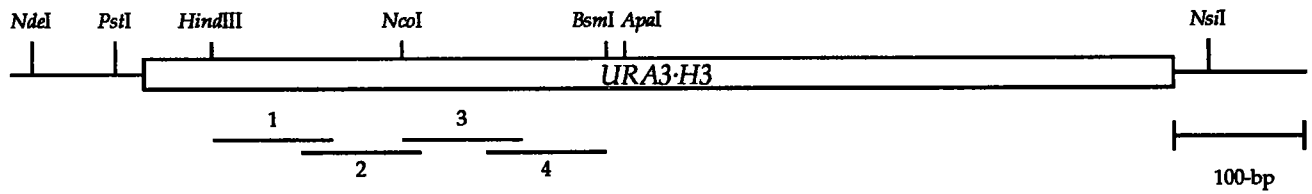
The approach taken to obtain divergent *URA3* was to reconstruct part of the gene synthetically using standard molecular biology techniques. Most of the restriction sites necessary to replace the wild type *URA3* sequence with a

homeologous region constructed from oligonucleotides (described below) and to generate inactivating mutations were present appropriately spaced in the 5′ end of *URA3*. However, an additional restriction site was required for each of these purposes. Close inspection of the *URA3* sequence showed that a *Hind*III site could be engineered at position 56 by a single A --> T nucleotide change that did not alter the amino acid sequence. This mutation was created by PCR and a map of modified *URA3*, *URA3·H3*, is shown in Figure 13A. The next step was to identify restriction sites that could be used to easily create spatially separate inactivating mutations in *URA3·H3*. A deletion from *Pst*I to *Hind*III was chosen for the 5′ deletion and restriction site ablation of *Nco*I to yield a 4-bp insertion was selected for the 3′ mutation. *ADE8* marked centromeric plasmids pYCS16, pYCS17 and pYCS18 containing *URA3·H3*, *ura3ΔNco*I and *ura3ΔPst*I/*Hind*III (*ura3ΔP/H*), respectively were prepared to confirm that these constructs yielded the predicted Ura phenotype. After transformation of these plasmids into BL205 and selection for Ade$^+$ transformants, the phenotype of transformants was confirmed by replica plating onto SC-Ura. Indeed, pYCS16 transformants were Ura$^+$ suggesting the A --> T point mutation did not alter *URA3* function, while pYCS17 and pYCS18 yielded a Ura$^-$ phenotype, confirming the *Pst*I to *Hind*III deletion and *Nco*I insertion inactivate *URA3*.

The *URA3* homeologous sequence was constructed from four oligonucleotides, oHomeo1 to 4, that spanned the region from *Hind*III to *Bsm*I and had specific nucleotide changes to create nucleotide divergence without alteration of the amino acid sequence. The alignment of oHomeo1 to 4 is shown schematically in Figure 12A and the nucleotide sequence is displayed in Figure

Figure 12. Schematic map of *URA3·H3* and the nucleotide sequence of oligonucleotides that were used to construct homeologous *URA3*. (A) The *URA3·H3* map is drawn to scale. The open box represents the coding region and horizontal lines depict 5′ and 3′ non-coding regions. Relevant restriction sites are shown. Of particular importance are *Hind*III, *Nco*I and *Bsm*I, which were necessary for cloning the homeologous region. The horizontal lines below *URA3·H3* marked 1 to 4 represent homeologous oligonucleotides, oHomeo1 to 4 respectively. The alignment of oHomeo1 to 4 correspond to their relative position within the *URA3·H3* sequence. (B) Nucleotide sequence of oHomeo1 to 4. The location of important restriction sites *Hind*III, *Nco*I and *Bsm*I are indicated. oHomeo1 and 3 are listed 5' to 3', while oHomeo2 and 4 are listed 3' to 5' so that the 12-bp complementary region between oHomeo1 and 2 and oHomeo3 and 4 can be easily identified (boxed). Degeneracy of the oligonucleotides are indicated by bolded letters and were assigned according to IUPAC nomenclature (B = GCT, D = AGT, H = ACT, K = GT, N = AGCT, R = AG, V = AGC and W = AT).

A.



B.

oHomeo1

5'-G CGC AAG CTT TTC AAC ATW ATG CAT GAA AAA CAA ACB AAT TTA TGC GCV TCB TTA GAC GTV CGT ACD ACD AAA GAA TTG CTT GAA TT -3'

*Hind*III

oHomeo2

3'- T AAC GAA CTT AAC CAB CTT CGV GAN CCA GGH TTC TAK ACA AAC GAV TTT TGV GTA CAD CTG TAW AAT TGB CTG AAG AGG TAC CCG CG-5'

*Nco*I

oHomeo3

5'-GCG CCC ATG GAA GGC ACB GTV AAA CCH TTR AAA GCB TTG TCD GCC AAA TAT AAC TTC TTG CTD TTT GAA GAT AGA AAG TTC GCT GAT AT -3'

*Nco*I

oHomeo4

3'- C AAG CGA CTA TAK CCA TTG TGV CAH TTC GAN GTC ATA AGB CGD CCA CAV ATA GCN TAR CGV CTT ACC CGV CTA TAK TGC TTA CGT GCG C-5'

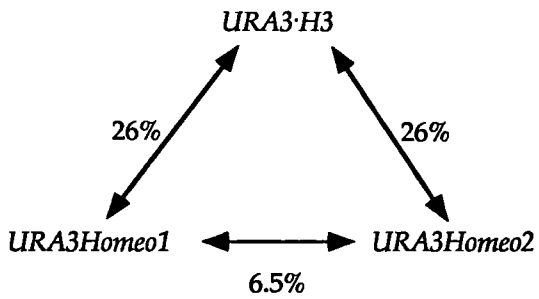
*Bsm*I

12B. Wherever possible, nucleotides were randomized (Fig. 12B, shown in bold). Thus oHomeo1 to 4 represented a library of potentially functional *URA3* sequences. Two pairs of oligonucleotides, oHomeo1 and 2, and oHomeo3 and 4, had 12-bp of complementary sequence to allow for annealing of the oligonucleotides for subsequent DNA polymerase extension reactions to create double stranded molecules. Each oligonucleotide pair possessed 5′ and 3′ ends with restriction sites that correspond to sites in *URA3·H3* and thus could be easily cloned to replace the wild type *URA3·H3* sequence.

A library of homeologous *URA3* genes were prepared and used to transform yeast, BL124. Transformants were selected on SC-Ura, which was a critical step for the isolation of homeologous *URA3* genes, since it demanded that all of the previous cloning steps yielded a functional gene. The plasmids from two BL124 transformants were rescued from yeast and sequenced. These genes will be referred to as *URA3Homeo1* and *URA3Homeo2*. Figure 13A shows that the overall extent of divergence between *URA3Homeo1* and *URA3·H3*, and *URA3Homeo2* and *URA3·H3* was determined to be 26%. Sequence comparison of *URA3Homeo1* with *URA3·H3* is shown in Figure 13B. The homeologous region spans 306 nucleotides between *Hind*III and *Bsm*I and has a maximum of 3 consecutive mismatches and 8 consecutive matches with the wild type *URA3·H3* sequence. Furthermore, introduction of homeology results in the creation of a *Sal*I site common to both *URA3Homeo1* and *URA3Homeo2* and a *URA3Homeo1* unique *Bgl*II site. Comparison of *URA3·H3* with *URA3Homeo2* yielded similar results (Fig. 13C).

Figure 13. Sequence comparison of *URA3·H3* with homeologous *URA3* genes. (A) Shows the overall percentage of divergence between *URA3Homeo1* and *URA3Homeo2* with *URA3·H3* and between the two homeologous *URA3* genes within the 306-bp region from *Hind*III to *Bsm*I. (B) Sequence alignment of *URA3·H3* (upper) with *URA3Homeo1* (lower). Vertical lines represent matches and lower case letters in the *URA3Homeo1* sequence represent mismatches. The location of common restriction sites *Hind*III, *Nco*I and *Bsm*I are shown, as is the *Sal*I site common to homeologous *URA3* genes constructed with oHomeo1 to 4 and a *Bgl*II site unique to *URA3Homeo1*. (C) Sequence alignment of *URA3·H3*(upper) with *URA3Homeo2* (lower). The location of common restriction sites are shown in addition to an *Eag*I site unique to *URA3Homeo2*. Designations of matches and mismatches are the same as in B. (D) Sequence alignment of *URA3Homeo1* (upper) with *URA3Homeo2* (lower). Designations of matches and mismatches are the same as in B.

A.



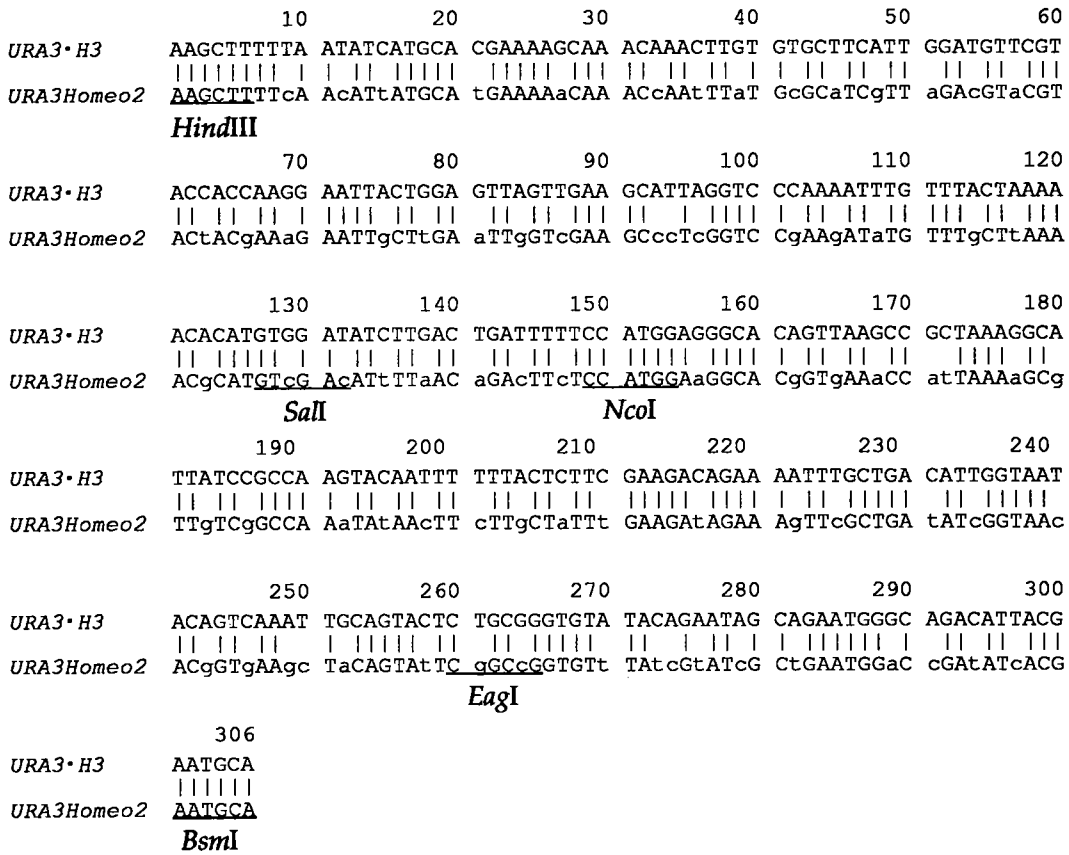
B.

```
                10         20         30         40         50         60
URA3·H3         AAGCTTTTTA ATATCATGCA CGAAAAGCAA ACAAACTTGT GTGCTTCATT GGATGTTCGT
                |||||||| | | || |||||  |||||  ||| || || || | | || || ||  || || |||
URA3Homeo1      AAGCTTTTcA AcATtATGCA tGAAAAaCAA ACcAAtTTaT GcGCaTCcTT aGAcGTaCGT
                HindIII
                70         80         90         100        110        120
URA3·H3         ACCACCAAGG AATTACTGGA GTTAGTTGAA GCATTAGGTC CCAAAATTTG TTTACTAAAA
                || || || | |||| || ||  || || ||| ||  | |||| | || || ||  ||| || |||
URA3Homeo1      ACgACaAAaG AATTgCTtGA aTTgGTgGAA GCgcTgGGTC CtAAgATcTG TTTgCTgAAA
                                                                BglII
                130        140        150        160        170        180
URA3·H3         ACACATGTGG ATATCTTGAC TGATTTTTCC ATGGAGGGCA CAGTTAAGCC GCTAAAGGCA
                || ||||| | | || || ||  || || ||| ||||| |||| | || || ||   |||| ||
URA3Homeo1      ACgCATGTcG AcATaTTaAC aGAcTTcTCC ATGGAaGGCA CgGTaAAaCC atTAAAaGCg
                      SalI                      NcoI
                190        200        210        220        230        240
URA3·H3         TTATCCGCCA AGTACAATTT TTTACTCTTC GAAGACAGAA AATTTGCTGA CATTGGTAAT
                || || |||| | || || ||  || || ||  ||||| |||| | || |||||  || |||||
URA3Homeo1      TTgTCgGCCA AaTAtAAcTT cTTgCTgTTt GAAGAtAGAA AgTTcGCTGA tATcGGTAAc

                250        260        270        280        290        300
URA3·H3         ACAGTCAAAT TGCAGTACTC TGCGGGTGTA TACAGAATAG CAGAATGGGC AGACATTACG
                || || ||   | ||||| ||  || |||||  ||  | || | | ||||||||  || || |||
URA3Homeo1      ACtGTgAAgc TcCAGTAtTC cGCtGGTGTc TAtcGcATtG CtGAATGGGC gGAtATcACG

                306
URA3·H3         AATGCA
                ||||||
URA3Homeo1      AATGCA
                BsmI
```

C.


10 20 30 40 50 60
URA3·H3 AAGCTTTTTA ATATCATGCA CGAAAAGCAA ACAAACTTGT GTGCTTCATT GGATGTTCGT
URA3Homeo2 AAGCTTTTcA AcATtATGCA tGAAAAaCAA ACcAAtTTaT GcGCaTCgTT aGAcGTaCGT
HindIII
70 80 90 100 110 120
URA3·H3 ACCACCAAGG AATTACTGGA GTTAGTTGAA GCATTAGGTC CCAAAATTTG TTTACTAAAA
URA3Homeo2 ACtACgAAaG AATTgCTtGA aTTgGTcGAA GCccTcGGTC CgAAgATaTG TTTgCTtAAA
130 140 150 160 170 180
URA3·H3 ACACATGTGG ATATCTTGAC TGATTTTTCC ATGGAGGGCA CAGTTAAGCC GCTAAAGGCA
URA3Homeo2 ACgCATGTcG AcATtTTaAC aGAcTTcTCC ATGGAaGGCA CgGTgAAaCC atTAAAaGCg
SalI NcoI
190 200 210 220 230 240
URA3·H3 TTATCCGCCA AGTACAATTT TTTACTCTTC GAAGACAGAA AATTTGCTGA CATTGGTAAT
URA3Homeo2 TTgTCgGCCA AaTAtAAcTT cTTgCTaTTt GAAGAtAGAA AgTTcGCTGA tATcGGTAAc
250 260 270 280 290 300
URA3·H3 ACAGTCAAAT TGCAGTACTC TGCGGGTGTA TACAGAATAG CAGAATGGGC AGACATTACG
URA3Homeo2 ACgGTgAAgc TaCAGTAtTC gGCcGGTGTt TAtcGtATcG CtGAATGGaC cGAtATcACG
EagI
306
URA3·H3 AATGCA
URA3Homeo2 AATGCA
BsmI

D.

```
                    10         20         30         40         50         60
URA3Homeo1  AAGCTTTTCA ACATTATGCA TGAAAAACAA ACCAATTTAT GCGCATCCTT AGACGTACGT
            ||||||||||| |||||||||| |||||||||| |||||||||| ||||||| || ||||||||||
URA3Homeo2  AAGCTTTTCA ACATTATGCA TGAAAAACAA ACCAATTTAT GCGCATCgTT AGACGTACGT
            HindIII

                    70         80         90         100        110        120
URA3Homeo1  ACGACAAAAG AATTGCTTGA ATTGGTGGAA GCGCTGGGTC CTAAGATCTG TTTGCTGAAA
            || || |||| |||||||||| |||||| ||| || || |||| | ||||| || |||||| |||
URA3Homeo2  ACtACgAAAG AATTGCTTGA ATTGGTcGAA GCcCTcGGTC CgAAGATaTG TTTGCTtAAA

                    130        140        150        160        170        180
URA3Homeo1  ACGCATGTCG ACATATTAAC AGACTTCTCC ATGGAAGGCA CGGTAAAACC ATTAAAAGCG
            |||||||||| |||| ||||| |||||||||| |||||||||| |||| ||||| ||||||||||
URA3Homeo2  ACGCATGTCG ACATtTTAAC AGACTTCTCC ATGGAAGGCA CGGTgAAACC ATTAAAAGCG
                SalI                        NcoI

                    190        200        210        220        230        240
URA3Homeo1  TTGTCGGCCA AATATAACTT CTTGCTGTTT GAAGATAGAA AGTTCGCTGA TATCGGTAAC
            |||||||||| |||||||||| |||||| ||| |||||||||| |||||||||| ||||||||||
URA3Homeo2  TTGTCGGCCA AATATAACTT CTTGCTaTTT GAAGATAGAA AGTTCGCTGA TATCGGTAAC

                    250        260        270        280        290        300
URA3Homeo1  ACTGTGAAGC TCCAGTATTC CGCTGGTGTC TATCGCATTG CTGAATGGGC GGATATCACG
            || ||||||| | |||||||| || ||||| ||||| || | |||||||| | |||||||||
URA3Homeo2  ACgGTGAAGC TaCAGTATTC gGCcGGTGTt TATCGtATcG CTGAATGGaC cGATATCACG
                                    EagI

                    306
URA3Homeo1  AATGCA
            ||||||
URA3Homeo2  AATGCA
            BsmI
```

There also exists an opportunity for a maximum of 12% sequence divergence between homeologous isolates, since homeologous *URA3* genes were derived from a library. Figure 13A shows that *URA3Homeo1* and *URA3Homeo2* were found to diverge by 6.5%. Sequence alignment of *URA3Homeo1* and *URA3Homeo2* in Figure 13D shows that these genes differ within the 306-bp homeologous region by 20 single nucleotides that are separated by as many as 46 consecutive matched nucleotides and that *URA3Homeo2* contains a unique *Eag*I site. A final test of *URA3Homeo1* and *URA3Homeo2* function was to compare transformation efficiency of these genes with wild type *URA3*. Transformation of BL124 with an equal amount of centromeric plasmids harbored *URA3Homeo1*, *URA3Homeo2* or *URA3* all yielded approximately the same number of Ura$^+$ colonies that grew at the same rate. *URA3Homeo1* and *URA3Homeo2* are functionally equivalent to *URA3*.

Development of starter stains for mutagenesis and screening for hyper-homeologous recombination mutants

Efficient isolation and characterization of hyper-homeologous recombination mutants required the development of two strains. One strain is necessary for mutagenesis and selection of hyper-homeologous recombination mutants and a second isogenic tester strain to facilitate characterization of the mutants. The genotype of the mutagenesis strain included the presence of independent homeologous and homologous duplications, as well as a unique nutritional marker for crossing to the tester strain. Important genetic properties of the tester strain were a homeologous duplication, a unique marker for crossing

to the mutagenesis strain and cycloheximide resistance for random spore analysis. Acquisition of the mutagenesis and tester strains, required many steps which are described next.

The ability to analyze homeologous and homologous recombination in the same strain allows for the early identification of those mutations that specifically increase homeologous recombination and, as a result, reduce the number of mutants that must be characterized in subsequent steps. Mutations that elevate both homologous and homeologous recombination are thereby easily eliminated. The presence of a homeologous duplication in the tester strain should enable simple evaluation of dominance in the diploid and guarantees that spores recovered from the diploid will possess the duplication necessary for future complementation analysis. Significant genetic manipulation had to be performed on BL205, a derivative of FW1259, so the *ura3* homeologous duplication could be present in a strain in which *spt15* homologous recombination could also monitored. Similar manipulations had to be performed on a cycloheximide resistant derivative of FY567, BL207, to obtain an isogenic tester strain. Both BL205 and BL207 contain *ura3-52*, a Ty insertion in *URA3*. The homeologous recombination assay relies on the presence of two spatially separated defined mutations, thus *ura3-52* had to be replaced. A defined 73-bp chromosomal deletion in *URA3* from *Pst*I to *Hind*III (Figure 12A) was constructed in two steps. First, *ura3-52* was replaced with *URA3* by homologous recombination. Next, the 73-bp *Pst*I to *Hind*III deletion was introduced into the chromosome by the two step method yielding BL210, the *Mat*α FW1259 derivative and BL211, the *Mata*

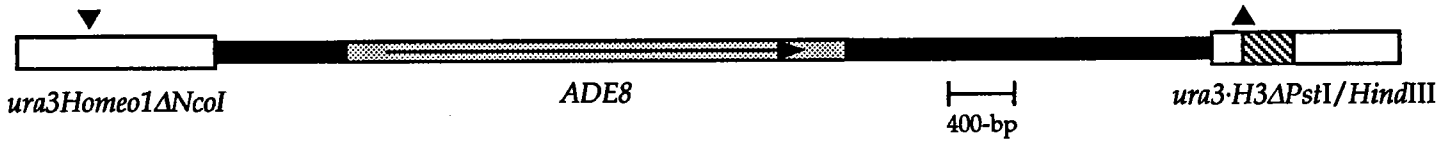
FY567 derivative. Both stains were now competent for introduction of the direct repeat duplication.

The final step in development of the mutagenesis and tester strains was the introduction of the duplications. First, the Orientation 2A *spt15* homologous duplication was introduced into the mutagenesis strain. A schematic diagram of this duplication with the complete 5′ deletion and the location of the *spt15-21* point mutation is shown in the lower panel of Figure 14. It was not necessary to introduce a homologous duplication into the tester strain because once this phenotype is known it does not need to be re-established. In fact, a Lys^+/Spt^+ derivative of the mutant strain that has recombined the homologous duplication will be utilized in subsequent characterization steps, thereby avoiding the problems involved in working an *spt15-21* strain. Mutagenesis and tester strains are currently in the process of being constructed by chromosomal integration of pYIS17, an integration plasmid that harbors *URA3Homeo1* inactivated by *Nco*I ablation. Integration of pYIS17 places the *ura3* homeologous duplication onto the left arm of chromosome V, the arm opposite to the chromosome V *spt15* homologous duplication. The predicted chromosomal structure of the *ura3* homeologous duplication is illustrated in Figure 14, upper panel.

The *ura3* homeologous duplication was modeled after the *spt15* Orientation 2A structure. The divergent region of the *ura3* duplication is 306-bp (Fig. 14B) which is similar to the 330-bp *spt15* homeologous region (Fig. 4A). The *Nco*I insertion mutation resides in the middle of the homeologous region, as does the *spt15-21* point mutation. This placement of the mutation is important so that

Figure 14. Chromosomal structure of the *ura3* homeologous and *spt15* homologous direct repeat duplications. Regions of homology are shown as open boxes and only the homology shared between duplicated genes is shown. The homeologous region in the *ura3* duplication is shown as a hatched box. Intervening plasmid sequence is shown in black and plasmid markers are stippled. The *ura3-H3 Pst*I/*Hind*III deletion and the *spt15* Δ5′ deletion are shown as triangles. The inverted triangle represents the *Nco*I insertion mutation in *ura3Homeo1* and the black dot in *spt15-21* represents the G --> A point mutation.

ura3 Homeologous Duplication



spt15 Homologous Duplication



the primary mechanism to recover function is by recombination that must pass through the region of homeology. The distances separating the *ura3* and *spt15* direct repeats is similar, about 7-kb, as are the orientation of the plasmid markers (Fig. 14). The 3' *Nco*I insertion mutation is found upstream in the duplication, like *spt15-21*, and the 73-bp *Pst*I/*Hind*III promoter and 5' coding deletion are downstream, like *Δ5'spt15*. There are, however, some differences between the *ura3* and *spt15* duplications. The 3' flanking sequence in the *spt15* duplication is approximately 1.5-kb, but in the *ura3* duplication it is only 583-bp. The *ura3* duplication has 139-bp of 5' flanking sequence necessary for proper orientation of homeologous *URA3* genes upon integration which is separated from the homeologous region by a deletion of only 75-bp, while the 5' flanking sequence is completely absent from the Orientation 2A duplications.

CHAPTER VI
DISCUSSION

Mismatch correction acts as a barrier to homeologous recombination in *Saccharomyces cerevisiae*

The mitotic recombination assay described in Chapter 3 was designed to assess the role of DNA mismatch correction in recombination fidelity. I focused on quantitative differences in the rates of recombination between homeologous and homologous sequences. In strains wild type for mismatch repair there was a 150-180 fold decrease in the recombination rate between homeologous sequences relative to homologous controls. Other laboratories (Alani et al., 1994; Harris et al., 1993; Mezard et al., 1992; Resnick et al., 1992) have noted similar decreases in assays of mitotic recombination. Some (Borts and Haber, 1987) but not all (Malone et al., 1994; Symington and Petes, 1988) meiotic assays have also shown decreased recombination between genes bearing multiple sequence heterozygosities. This propensity to limit recombination between diverged sequences is consistent with the idea that mispaired recombination intermediates are somehow formed at reduced rates or are inhibited from undergoing resolution to form crossover or gene conversion products.

My results indicate that the mismatch repair genes *MSH2* and, in some cases, *MSH3* play active roles in recombination fidelity. Inactivation of these genes leads to partial restoration of the recombination rates observed with homologous sequences. In one case (Orientation 2), the *msh2 msh3* double

mutant exhibited a rate of homeologous recombination that was 30% the homologous rate in a wild type background. This finding is consistent with the idea that the barrier to homeologous recombination is substantially alleviated in the *msh2 msh3* double mutant. My results also indicate that the sequence similarity of *MSH2* and *MSH3* to the bacterial *mutS* is paralleled by a functional similarity at the level of controlling recombination fidelity. Bacterial *mutS* strains show a large enhancement in the rate of homeologous recombination, but this increased rate is less than 10% of the recombination rate between identically matched sequences (Rayssiguier et al., 1989). Recent *in vitro* experiments (Worth et al., 1994) demonstrated that MutS abolishes RecA-catalyzed strand transfer between homeologous DNA molecules but that MutS does not affect homologous strand transfer reactions. The role of MutS along with MutL is to block branch migration of the mispaired heteroduplex that results from pairing of homeologous strands. My evidence suggests that the product of *MSH2* plays a similar role in *S. cerevisiae*, consistent with the prediction of Alani et al. (Alani et al., 1994). In the case of Orientation 2 and 2A, the data supports a similar role for the *MSH3* gene product. If one assumes that other *mutS* homologs also confer a recombination fidelity activity, then an unexpected phenotype of yeast *MSH1* mutants can be explained. *MSH1* was isolated in the same PCR-based homology search that yielded *MSH2* (Reenan and Kolodner, 1992). Disruption of *MSH1* led to a petite phenotype that was rapidly established (Reenan and Kolodner, 1992). Large-scale rearrangements of mitochondrial DNA were observed in *msh1* strains, indicating that *MSH1* plays a role in repair or stability of mitochondrial DNA (Reenan and Kolodner, 1992). In light of my results, I suggest that one function of *MSH1* is to prevent homeologous recombination in yeast

mitochondrial DNA, presumably between imperfectly repeated sequences. In *msh1* strains homeologous recombination would occur unimpeded and could rapidly result in loss of mitochondrial function.

The rate data in Orientation 2 indicates that single mutations in *msh2* or *msh3* elevate the rate of homeologous recombination 17- or 9.6-fold , respectively. The *msh2 msh3* double mutant exhibits a rate enhancement of 43-fold, implying that Msh2 and Msh3 might act independently in the process of recombination fidelity. Similar results were also obtained for Orientation 2A. I interpret this data according to the analysis of Morrison et al. (Morrison et al., 1993) who developed models for possible relationships between DNA replication error correction systems. My data are consistent with the model that Msh2 and Msh3 act in parallel, non-competing pathways. Alternatively my data also fits a second prediction of competitive pathways acting on a common intermediate, in which case either Msh2 or Msh3 may partially compensate for defects in one another. I cannot at present distinguish whether the rate observed in the *msh2 msh3* double mutant resulted from parallel non-competing versus competitive pathway models or perhaps a combination of both. However in either case it appears that Msh2 and Msh3 act to a greater or lesser degree independently.

Recently, it has been has shown that Msh2 dimerizes with Msh3 or Msh6 to form specific mismatch recognition complexes (Marsischky et al., 1996). This study demonstrated that the Msh2/Msh6 heterodimers recognize single base pair mismatches and 1 base insertion mutations, while the Msh2/Msh3 heterodimer primarily handles small insertion mutations (Marsischky et al.,

1996). This study only addressed the ability of the Msh heterodimers to deal with small insertion mutation unlike those that might be encountered in an Spt15 heteroduplex which has as many as 5 consecutive base mismatches. Based on my results, I propose that Msh3 might interact with a different Msh partner to form a complex that recognize larger base mispair aberrations. According to this hypothesis Msh2/Msh6 heterodimers would detect single base mismatches in the Spt15 heteroduplex and Msh3/MshX heterodimers would handle larger stretches of mismatched bases. Competition between these pathways might arise if there were overlap between the substrate specificity of Msh2/Msh6 and Msh3/MshX heterodimers or between Msh2/Msh3 verses Msh3/MshX dimer formation. Otherwise the action of these two pathways would be independent regarding mismatch recognition.

The marker loss data provides some clues as to which recombinant products are formed in the various genetic backgrounds. This point is of particular interest in addressing the question of whether the products from hyper-recombinant strains (*msh2* strains, for example) are due to increased formation of all possible products or whether specific recombination events are enhanced in different mutant backgrounds. In Orientation 2 and 2A, the majority of recombinants have lost the intervening marker (Table 4), with values ranging from 37-85%. Marker loss is expected to result from either intrachromosomal crossover (popout) event, single strand annealing or G2 unequal crossover (Fig. 5B). In contrast, gene conversion or post-mitotic segregation events result in retention of the marker. Thus in most cases the total of popout, SSA and sister chromatid exchange forms the majority of events. In

Orientation 2 strains bearing a homeologous duplication (Table 4, top), the wild type background produced 70% marker loss events whereas the mismatch repair mutants yielded 50-58% marker loss. I feel that the decreased values in the mutant backgrounds are not significant although detailed statistical analysis has not been performed. Marker loss from Orientation 2A accounted for 85% of recombinants in the wild type (Table 5), a slightly higher percentage than Orientation 2 (Table 4, 70%). Perhaps the increase in Orientation 2A popouts is compensation for the loss a pathway to restore the *Δ5'tbp* promoter to yield a similar overall recombination rate in the wild type (Table 4, 5.3×10^{-7} verses Table 5, 8.5×10^{-7}). These results imply that the acceleration in rate of homeologous recombination in Orientation 2 from *msh2*, *msh3* and *msh2 msh3* strains result from increased levels of all events (Fig. 5B) although I cannot distinguish between popouts, SSA and sister chromatid exchange in the Orientation 2 arrangement of homeologous sequences.

The rate results in Orientation 1 showed several similarities to Orientation 2, including the 180-fold decrease in homeologous versus homologous recombination, the 12-fold increase in rate in an *msh2* strain and the lack of effect of a *pms1* mutation. One major difference between the orientations was that the absolute recombination rates were reduced in Orientation 1 compared to Orientation 2. For example, the wild type strains in Orientation 1 yielded approximately 10-fold lower rates than their Orientation 2 counterparts (Tables 3 and 5). Part of this difference can be accounted for by the ability of Orientation 2 structures to undergo deletion events without the need for repair tract switching or associated gene conversion (compare Figure 5B, Panel 1 with Figure 7B, Panel

1). The remainder of the difference must be due to other factors that are currently less clear. I note that Orientation 2 contains an extra 1-kb of 3' flanking sequence that was necessary for purposes of integration. It is possible that the increased size of homology or specific sequences in this region stimulates overall recombination. Alternatively, one can invoke position effects to explain the differences between the orientations. For example, chromatin structure may differ in the two cases and hence affect the absolute rates of recombination. However, as noted earlier, relative changes in rates within the all three data sets largely parallel one another. Thus my basic conclusions do not appear to be significantly affected by the difference in absolute rates.

The rate results in Orientation 1 show that an *msh2* strain exhibits a 12-fold increase in the rate of recombination, consistent with the notion that Msh2 plays a role in limiting recombination in this arrangement of sequences. However the *msh3* strain was not elevated for homeologous recombination (1.2-fold) nor was the *msh2 msh3* double mutant (11-fold) significantly altered from the *msh2* single mutant. Thus Msh3 does not appear to block recombination of homeologous sequences in Orientation 1. There are several possible explanations for this result. For example, perhaps Msh3 acts to *aid* certain events in Orientation 1 while *blocking* formation of products from other events. As an example, it is possible that Msh3 might stimulate single-strand annealing between homeologous sequences by activating nucleases necessary for SSA (Saparbaev et al., 1996). Msh3 might block other types of recombination events under these conditions. If these two effects were of similar magnitude, then loss of Msh3 function would result in no net gain of recombinants but might alter the

spectrum of recombinants that is observed. Although we have not yet addressed this possibility directly, analysis of marker loss data (see below) does lend some support to the idea. Alternative explanations for the lack of an *msh3* effect on Orientation 1 rates include position effects or the lack of the 1-kb 3' flanking region. We are attempting to address the *MSH3* situation more directly. However the observation that *msh3* mutants affect Orientation 2 provides positive evidence of a role for Msh3 in recombination fidelity.

In Orientation 1, marker loss among the recombinants is predicted to result from a variety of low probability events. These include: 1) crossovers that initiate upstream or down stream of the homeology region with switching of the repair tract between the promoter deletion and the point mutation; 2) SSA events with repair occurring on opposite strands upstream and downstream of the homeology region that meet between the two both *spt* mutations; 3) Gene conversion of the promoter deletion followed by SSA or intrachromosomal crossovers (Figure 7B, panel 1). All other events result in retention of the marker. Among the strains harboring homeologous duplications (Table 6, top), the wild type level of marker loss (22%) shows relatively small changes, either up or down, in *pms1*, *msh2* and *msh2 msh3* backgrounds. It is difficult to know if these small changes are of significance. One change that does stand out is the strong reduction (to 2%) in the *msh3* background. This reduction suggests the possibility that SSA or intrachromosomal crossovers with gene conversion may be dependent on *MSH3* function, a hypothesis that is currently being tested. Clearly there is more to be learned about *MSH3*.

Strains bearing a *pms1* mutation did not lead to excess recombinants between homeologous sequences compared to homologous control strains, an observation that has been made by other investigators (Bailis and Rothstein, 1990; Resnick et al., 1992). This result was initially disturbing in light of the similarities between *PMS1* and bacterial *mutL* (Kramer et al., 1989; Williamson et al., 1985). One would predict that since *mutL* strains are hyper-recombinant for homeologous recombination (Rayssiguier et al., 1989) and since MutL enhances the effects of MutS in blocking branch migration, the expectation is that *PMS1* might act similarly in yeast. The fact that *pms1* strains do not exhibit this particular phenotype might be explained by the discovery of two additional yeast *mutL* homologs, *MLH1* and *MLH2* (Prolla et al., 1994). It is possible that *MLH1* or *MLH2* encodes a protein that provides recombination fidelity activity or that some combination of *PMS1*, *MLH1* and *MLH2* provide overlapping function. This point needs to be investigated further before solid conclusions can be drawn.

The results described in Chapter 3 indicate that the mismatch repair genes *MSH2* and in some cases *MSH3* are involved in controlling recombination fidelity in *S. cerevisiae*. To my knowledge, this is the first direct demonstration of such a role for mismatch repair in a eukaryotic system. These observations have subsequently been confirmed using homeologous inverted repeats (Datta et al., 1996). The results of Alani et al (Alani et al., 1994) indicated that Msh2 might function in this manner, at least during meiotic recombination. My results support and extend this finding. However many questions remain to be answered. Important future directions for this research should address three

major questions. First, what other genes are involved in control of recombination fidelity? One prediction is that a *mutL* homolog or homologs are necessary for this function. The data presented here indicate that *PMS1* alone does not provide this function. Second, which events are enhanced in mismatch repair mutants? The molecular analysis of the recombinant products presented in Chapter 4 is designed to elucidate some of the mechanistic details of the reaction. Third, does Msh3 play another role in homeologous recombination besides acting in an inhibitory manner?

Homologous and homeologous recombinants in wild type and mismatch repair deficient *Saccharomyces cerevisiae*

The study presented in Chapter 4 was designed to examine the effects of homeology and mismatch correction on genetic transfers. To achieve these ends I evaluated recombination between direct duplications of homologous and homeologous substrates in wild type and mismatch correction deficient backgrounds. My results are consistent with the hypothesis that sequence divergence is a barrier to all types of recombination events. *MSH2* and in some cases *MSH3* interfered with homeologous exchanges, since all classes of recombination events proceed at a higher rate in their absence. Thus these mismatch correction proteins act to maintain accuracy of genetic exchanges, presumably by interacting with mispaired recombination intermediates.

The simplest model for homeologous recombination assumes that it occurs by the same or similar mechanisms as homologous exchanges. Several

lines of evidence are consistent with this notion. First, my results show that there is a close resemblance in the distribution of products arising from homologous and homeologous *spt15* duplications. In Orientation 2 this correlation was particularly clear. Orientation 1 yielded similar results, although some exceptions were observed. Second, homeology between duplicated *spt15* decreased the rate of each class of product in both Orientation 1 and Orientation 2. Thus the recombination barrier due to sequence divergence was distributed among the possible classes of recombinants. Third, the majority of products, in most cases greater than 90%, could be accounted for as either crossovers or gene conversions. Homeology might be predicted to generate some unusual recombination products, similar to those observed for meiotic exchanges between substrates that differ by 7 heterologies in a 9 kb stretch (Borts and Haber, 1987; Borts et al., 1990). However, only homeologous exchanges from the wild type in Orientation 1 and *pms1* in both orientations produced a substantial number of unexpected products and even these were a minority (10-22%) of the total. Fourth, sequence analysis of a limited number of homeologous recombinants suggests that, like homologous recombination (Liskay and Stachelek, 1986; Petes et al., 1991), information in homeologous exchanges is usually transferred in continuous blocks. My results are generally consistent with previous studies that utilized homeologous sequences located on different chromosomes (Bailis and Rothstein, 1990; Harris et al., 1993; Matic et al., 1994) or on a plasmid and a chromosome (Goguel et al., 1992; Mezard et al., 1992; Priebe et al., 1994). Taken together my results support the hypothesis that the pathway of homologous and homeologous recombination is comparable. The formal possibility exists that the actual mechanism of homologous and homeologous genetic transfer might be

different, but result in a similar outcome. My results do not exclude this possibility.

The products and distribution of recombinants recovered in this study are also generally consistent with other studies that examined homologous exchanges. The major recombination products recovered from homologous direct repeats include popouts, gene conversions and G2 unequal crossovers (Jackson and Fink, 1981; Klein, 1988; Thomas and Rothstein, 1989). The distribution of these events varies with the experimental system used. Klein (Klein, 1988) observed 50-53% gene conversion and 44-47% popouts in yeast constructs at *LEU2* and *HIS3* that are analogous to my Orientation 2. Thomas and Rothstein (Thomas and Rothstein, 1989) observed about 70% popouts and 30% gene conversions of a *GAL10* duplication, while Jackson and Fink (Jackson and Fink, 1981) found that gene conversion unassociated with crossovers was the major event (88%) in yeast *HIS4* duplications. In my system, popouts are the primary products obtained from the wild type strain in Orientation 2 (78%), while gene conversions comprise the majority of Orientation 1 products (53%). This variability in product distributions is likely due to differences in the experimental systems, such as target size, the alleles used and the relative orientation of the markers. Additional factors that might affect the outcome of recombination are the site of initiation relative to the marker, the distance separating the markers and other metabolic events in the vicinity like transcription. For example, the level of transcriptional activity at the *GAL10* locus has been shown to influence the outcome of direct repeat recombination (Thomas and Rothstein, 1989).

Results of this study also demonstrated that *MSH2* and *MSH3* control the fidelity of recombination in all types of exchanges. If mismatch repair controlled only a subset of recombination pathways, then I might expect one or a few product types to predominate in mismatch repair mutants. The results from Orientation 2 clearly indicate that all categories of products are produced at higher rates in *msh2* and *msh3* mutants. Moreover, the rate of formation for each class of recombinant is enhanced to about the same level as the overall increase in recombination rate. Similar results were observed for *msh2* mutants in Orientation 1, although the quantitative correlations were not quite as strong. Thus to a first approximation, these findings suggest that the mismatch repair proteins Msh2 and Msh3 provide an extra level of control over recombination by inhibiting the outcome of all types of homeologous exchanges.

Variance in product distribution from the first level approximation provides clues to the inhibitory nature of the mismatch repair proteins Msh2 and Msh3. Both proteins are homologs of bacterial MutS and hence might act to inhibit branch migration by interaction with mispaired bases formed during recombination (Alani et al., 1994; Worth et al., 1994). My results indicate that Msh2 and Msh3 interact more strongly with mispairs at or near the point mutation than with mispairs at or near the promoter deletion. In *msh2*, *msh3* or *msh2 msh3* backgrounds, I consistently observe a greater fold increase in replacement of the point mutation than promoter insertions. There is little (Orientation 1) or no (Orientation 2) such bias in homologous controls. These results suggest that Msh2 and Msh3 interact more effectively with the multiply mismatched intermediate presumed to surround the *spt15-21* allele than with the

large loop at the deletion. This interpretation is consistent with the mitotic function of *MSH2* and *MSH3* in recognition of single base mismatches and small loops (Marsischky et al., 1996; Miret et al., 1993). There is some indication in my data that Pms1 may also influence these interactions. In Orientation 2, there is a homeology-dependent bias in the *pms1* background, similar to *msh2* and *msh3* strains, towards elevated extents of point mutant replacements relative to promoter insertions (Table 4). The lack of a *pms1* effect on the overall rate of homeologous recombination might be attributable to the relatively high degree of homeology in my system. For example, the extent of sequence divergence might trigger a strong block by Msh2 and Msh3 which could conceal the role of Pms1. This leads to the prediction that Pms1 should inhibit crossovers at low but not high levels of sequence divergence. This has been recently demonstrated by Jinks-Robertson and colleagues who showed that *pms1* mutations led to elevated homeologous recombination when substrates diverged by 9% but not by 23% (Datta et al., 1996). However, additional experimentation will be required to define better the role of *PMS1*.

The site of initiation of strand exchange is another feature that may affect recombination fidelity. In my experiments, flanking regions of perfect homology may serve as initiation sites for strand exchange and hence mispairs would be created upon branch migration across the heteroalleles and into the divergent region. In principle, this process could be distinct from initiation within homeologous sequences because in the absence of flanking homology, mispairs would be formed upon strand annealing and hence no branch migration is required to generate mismatches. If mismatch repair controls recombination

fidelity through effects on branch migration (Alani et al., 1994; Worth et al., 1994), then this issue becomes of particular significance. Resnick and colleagues (Priebe et al., 1994) have suggested an alternative viewpoint in which homeology primarily influences recombination-dependent DNA synthesis rather than branch migration. To my knowledge, no experimental system has yet directly tested how the presence or absence of homologous flanking DNA affects homeologous recombination. In a study that impinges on this point, Waldman and Liskay (Waldman and Liskay, 1988) showed that placement of two mismatches within a 232 base pair region of homology reduced recombination at a nearby marker by 20-fold in mouse cells. However it was not possible to distinguish unambiguously the effects of divergence on early versus late steps in the recombination process, although the authors favored the first possibility. In yeast, crossovers between *spt15* homeologous substrates (23% diverged) that lacked flanking regions of homology were found to occur 2000-fold less frequently than with homologous sequences (Datta et al., 1996). When 0.5 to 1.5 kb of sequence identity flanked the *spt15* homeologous region, the recombination rates were only 150- to 180-fold lower than homologous exchanges (Selva et al., 1995). However these studies are not directly comparable since the first utilized indirect repeats whereas the second utilized direct repeats.

In some mutant backgrounds that do not exhibit elevated rates of homeologous exchanges, differences in product distribution may be ascribable to alternative recombination events. For example, a significant fraction (16-22%) of homeologous recombinants arising in the *pms1* background could not be readily classified as crossovers or gene conversions (Table 4). Some Lys^+ products were

identified as extragenic suppressors in *spt3*, but the majority remain enigmatic. For *msh3* mutants, another explanation may account for the differential effects on recombination in Orientation 1 and 2. According to the simplest hypothesis, Msh3 is expected to act in a negative manner to inhibit homeologous recombination. The results from Orientation 2 support this notion (Selva et al., 1995; also Table 3). However in Orientation 1, *msh3* mutants do not exhibit elevated rates of homeologous exchanges. In addition, occurrence of popouts is markedly decreased for homeologous events (Selva et al., 1995). This led to the hypothesis that an alternative role for Msh3 might exist in stimulating SSA. If the positive and negative effects due to loss of *MSH3* function were of similar magnitudes, the overall recombination rate would appear unchanged. The homeologous results of Table 7 generally support this notion. Recently, the Prakash laboratory (Saparbaev et al., 1996) found that *RAD1*, *RAD10* and *MSH3* functioned in the same pathway to promote reciprocal homologous recombination. With duplications containing deletion alleles of *his3*, they observed 5-10 fold reductions in popout formation in single and combinatorial mutants of the three genes. For popouts from a *his4C pBR313 his4A* duplication, similar to my Orientation 1, there was little effect of mutations in *RAD1*, *RAD10* or *MSH3* in a *RAD52* background; however in a *rad52Δ* strain, 3-5 fold decreases in popouts resulted from loss of *RAD1*, *RAD10* or *MSH3* (Saparbaev et al., 1996). These results are consistent with my hypothesis that *MSH3* has an important function in stimulating SSA for both homologous and homeologous recombination and thus provides an explanation for the behavior of *msh3* mutants in Orientation 1.

The results in Chapter 4 support the conclusion that the mechanism of homologous and homeologous recombination are equivalent. However, it is possible that homeologous and homologous recombination occur by different mechanisms that lead to the same outcome. In order to investigate this question more rigorously a mutation in the recombinational repair gene *RAD52* was introduced into cells that harbored either the Orientation 1 or 2 *spt15* duplication. Previous studies using homologous substrates similar to my Orientation 1 and 2 have shown that *RAD52* mutations reduce the mitotic recombination rate of homologous direct repeats by only 3- to 18-fold (Jackson and Fink, 1981; Klein, 1988; Saparbaev et al., 1996; Thomas and Rothstein, 1989). In most cases, the majority of these recombination products recovered from *rad52* mutants were popouts (Jackson and Fink, 1981; Klein, 1988; Saparbaev et al., 1996), suggesting *RAD52* dependent genetic exchanges of direct repeats chiefly yield gene conversion products. In contrast, homologous inverted repeat recombination was decreased almost 3000-fold in the absence of *RAD52* (Rattray and Symington, 1994). These authors suggested that all conservative recombination events, gene conversions and crossovers alike, required *RAD52*, while popouts recovered from direct repeats in the absence of *RAD52* might be the product of non-conservative events that involve SSA or replication slippage (Rattray and Symington, 1994). This hypothesis is also consistent with the observation that *rad1 rad52* double mutants synergistically decrease direct repeat recombination(Klein, 1988; Saparbaev et al., 1996; Thomas and Rothstein, 1989), since the excision repair genes *RAD1 RAD10* are known to play a role in SSA (Fishman-Lobell et al., 1992; Ivanov and Haber, 1995; Schiestl and Prakash, 1988).

The Orientation 2 homologous recombination results are consistent with these observations (Table 10). The rate of recombination was reduced 3.8-fold and 100% of those products were popouts (Table 10). Consistent with the notion that homologous and homeologous recombination occur by an equivalent mechanism, a similar reduction in the Orientation 2 homeologous recombination was observed in BL180. However, popouts recovered from homeologous substrates only accounted for 26% of the products from the *rad52* strain. This result suggests there may be differences between the mechanism of homologous and homeologous recombination. Homeologous recombination might proceed by an independent mechanism, as previously suggested, or the presence of *RAD52* might drive homeologous recombination toward the homologous exchange pathway, but in its absence some homeologous substrates might be channeled into alternative exchange pathways. The later mechanism could be homeology driven and might involve mismatch correction. Although these hypotheses are highly speculative due to the preliminary nature of the results, they provide some intriguing avenues for future experimentation. These investigations would include examining the effect of mutations in mismatch repair and *RAD1* and *RAD10* on *RAD52* independent homeologous genetic exchanges.

Orientation 1 homologous genetic exchanges demonstrated a much stronger dependence on *RAD52* than Orientation 2. I predicted that all Orientation 1 recombination products required some kind of *bona fide* recombination event such as gene conversions, G2 unequal crossovers or intrachromosomal crossover to yield a functional Spt15$^+$ product. This is best

illustrated by Orientation 1 popout recombinants, which require a gene conversion to accompany intrachromosomal crossover or SSA (Fig. 10B). This result is consistent with the notion that all conservative genetic exchanges require *RAD52*. In contrast, other groups that have examined recombination of direct repeats with constructs similar to my Orientation 1 and 2 have reported slightly larger *rad52* dependent decreases in Orientation 2. Furthermore, *rad52* alone was never found to completely abolish direct repeat recombination, as observed here for Orientation 1 (Jackson and Fink, 1981; Klein, 1988; Saparbaev et al., 1996). The most plausible explanation for these discrepancies is differences between the experimental systems used, but this experiment need to be performed more rigorously to substantiate the results.

Isolation of hyper-homeologous recombination mutants

The results presented in Chapter 5 are not a conclusion of this work but rather develop a foundation for the future of this project. Preliminary screening of EMS mutagenized BL206 that harbored a homeologous *spt15* direct repeat demonstrated the utility of this system to isolate hyper-homeologous recombination mutants. The remainder of this section dealt with the creation of a second generation homeologous duplication in *ura3* as prelude to the development of the ideal starter strains for the isolation and characterization of hyper-homeologous recombination mutants. The ultimate goal of these studies is to identify novel genes or new alleles of known genes that function in yeast mismatch correction. In this way, we might develop a better understanding of the role of mismatch correction in homeologous recombination as well as yield

some insight into the basic mechanistic principles that govern mismatch correction function.

The methodology described for screening cells that harbor a homeologous direct repeat was shown to be a rational approach to evaluate a large number of mutagenized cells for the hyper-homeologous recombination phenotype. Only a small percentage of total BL206 cells screened (0.3%, Table 11) consistently yielded a hyper-homeologous recombination phenotype through three successive rounds of lysine papillation. Although the utility of the screen had been proven it became apparent that further characterization of these mutants would be difficult due to the limitations of BL206 and working with *spt15-21* strains. Therefore, a second homeologous duplication in *ura3* was constructed, which maintained the useful traits of the *spt15* duplication but avoided many of its deficiencies. For example, detection of Ura^+ recombinants should be much tighter than the recovery of lysine prototrophs produced indirectly by recombination of *spt15* heteroalleles and thus should increase the sensitivity of the assay by leading to fewer false positives. The use of the *ura3* homeologous duplication was critical to the development of mutagenesis and tester strains that will allow for more efficient isolation and characterization of hyper-homeologous recombination mutants. These advantages include the ability to evaluate simultaneously the homologous and homeologous recombination phenotype in the mutagenized strain and a mechanism to easily characterize mutants.

Once the new starter strains are completed some tests should be conducted to demonstrate the efficacy of these strains for specific identification of

hyper-homeologous recombination mutants and subsequent characterization of those mutants. The activity of the *spt15* homologous and *ura3* homeologous duplication in the mutagenesis strain, BL213, needs to be tested to determine if this strain will be useful to identify mutations that specifically increase homeologous recombination. Mutations that increase the rate of homeologous recombination, such as *msh2*, should increase recombination of the *ura3* homeologous duplication and thus increase the rate of uracil prototrophy, but not increase homologous recombination to Lys^+. An *MSH2* disruption will be introduced into the mutagenesis strain. Another important feature of the mutagenesis strain will be the ability to identify mutations that increase recombination in general. *HPR1* was identified as a gene that elevates homologous recombination in a screen similar to that described here (Aguilera and Klein, 1990). Mutations in *HPR1* increase the rate of deletions between homologous direct repeats 500- to 1000-fold over that of wild type (Aguilera and Klein, 1990). The efficiency of the *spt15* homologous duplication will be assessed by introduction of a *HPR1* disruption into the starter strain, as an example of hyper-homologous recombination mutations that will be discarded in my screen.

Initially, a simple qualitative comparison of wild type, *msh2* and *hpr1* strains that harbor homologues and homeologous duplications can be performed to determine if these mutations yield the predicted phenotypes. Serial dilutions of the saturated cultures grown non-selectively will be spotted on SC-Ura and SC-Lys. The homeologous and homologous recombination phenotype will be judged by the number of papillae on SC-Ura and SC-Lys in *msh2* and *hpr1*

derivatives relative to wild type. It would be predicted that *msh2* will specifically affect homeologous recombination to increase the number of SC-Ura papillae over wild type, while *hpr1* is predicted to affect both homologous and homeologous exchanges to elevate both SC-Lys and SC-Ura papillation. To a first approximation this test will reveal the utility of BL213 as the starting strain for mutagenesis. Homologous and homeologous rate analysis should also be performed with this strain in order to quantitate the recombination rates in wild type, *msh2* and *hpr1* strains as a basis for comparison to mutant isolates.

Another aspect of the starter strains that remains to be tested is the ability to assay the homeologous recombination phenotype in diploids obtained from crosses of the mutagenesis and tester strains. Evaluation of the homeologous recombination phenotype in diploids will be important for establishing complementation groups and recessive/dominance relationships of a given mutation. Phenotypic complementation includes establishing groups from mutants isolated in the screen and identifying isolates that are the result of mutations in genes that are known to effect the rate of homeologous recombination, such as *MSH2*. The behavior of the homeologous duplication in diploids can be evaluated by a qualitative papillation patch test, described above or a quantitative rate comparison in wild type and homozygous mismatch repair deficient diploids.

The next obvious step for the project is to begin mutagenesis and characterization. Isolation and characterization of hyper-homeologous recombination mutants should employ a methodology similar to that briefly

outlined below. Following treatment of the mutagenesis strain with EMS, mutants that displays a hyper-homeologous recombination phenotype will be identified through three sequential round of papillation on SC-Ura. Next, homologous recombination of the *spt15* duplication in those isolates that persist through the tertiary screen will be evaluated by comparison to wild type unmutagenized cells. Those mutants that show a higher frequency of SC-Lys papillation than the wild type will be eliminated. An Spt15$^+$ (Lys$^+$ with the homologous duplication recombined) derivative of each isolate will be used in all subsequent steps to avoid problems of working with *spt15-21* strains. Characterization of *bona fide* hyper-homeologous recombination mutants will begin by determining their mutator phenotype on canavanine media, since this phenotype is a hallmark for many mismatch repair mutants. The remaining characterization steps involve crossing each isolate to the tester strain. First, the dominance of the hyper-homeologous phenotype will be determined in diploids. Sporulation and tetrad analysis of these diploid will show the segregation pattern of the hyper-homeologous recombination phenotype to determine if a single mutation produced the phenotype (i.e. 2:2 segregation of the hyper-homeologous recombination phenotype). The tetrads should also generate a suitable *MATa* derivative of each isolate to establish complementation groups. Complementation analysis will be performed by back crossing to initial *MAT*α isolates, assuming the phenotype was shown to be produced by a single mutation. The final step for the preliminary characterization of these mutants would be to determine whether an isolate will complement known mutations. My laboratory has host strains that bear mutations in many of the known and suspected mismatch repair genes.

The results presented in this section and other sections of this thesis lead to other potentially fruitful avenues of future experimentation. As previously noted, the methodology utilized to generate the homeologous *URA3* genes resulted in a library of genes that had the potential for 0 to 12% sequence divergence. The nucleotide sequence of *URA3Homeo1* and *URA3Homeo2* were found to differ by 6.5% in the 306-bp region between *Hind*III and *Bsm*I (Figs 10A and D), whereas wild type *URA3·H3* diverged from both homeologous *URA3* genes by 26% (Fig. 13A, B and C). Differences in the nucleotide sequence among wild type and homeologous *URA3* genes raises the possibility of comparing the effect of varying levels of sequence divergence on recombination. This becomes a particularly interesting question in light of the recent work done in the Jinks-Robertson laboratory where it was shown that *pms1* increased the rate of homeologous recombination 11-fold when inverted repeats diverged by 9% (Datta et al., 1996). However, when the level of sequence divergence was higher (23 to 25%) the absence of *PMS1* did not increase the recombination rate of Orientation 1, 2 or 2A direct repeats (Tables 3, 4 and 5) or inverted repeats (Datta et al., 1996). Indeed, it would be interesting to determine if the *pms1* mutation differentially affects the recombination rate of *ura3* duplications that diverged by 6.5 verses 26%. Another factor that might have bearing on the efficiency of homeologous genetic transfers in my system is the presence of homologous flanking regions. In contrast to my results, intermolecular gene conversion between an inactivated chromosomal copy of *his4* and a 14% diverged plasmid copy of the gene was not enhanced in the absence of *MSH2* or *PMS1*, which the authors attributed to a lack of flanking homology to stabilize branch migration (Wu and Marinus, 1994). The requirement for flanking sequence homology can

be directly addressed using either the *spt15* or *ura3* homeologous duplication by changing the length of the identity region and monitoring its effect on the rate of recombination. Clearly, additional structural manipulation of the *spt15* or *ura3* homeologous duplication could be performed to ask even more detailed questions about the mechanisms of homeologous exchanges and the role of mismatch correction in the process.

CHAPTER VII

REFERENCES

Aaltonen, L. A., Peltomaki, P., Leach, F. S., Sistonen, P., Pylkkanen, L., Mecklin, J.-P., Jarvinen, H., Powell, S. M., Jen, J., Hamilton, S. R., Petersen, G. M., Kinzler, K. W., Vogelstein, B., and de la Chapelle, A. (1993). Clues to the pathogenesis of familial colorectal cancer. Science *260*, 812-816.

Aguilera, A., and Klein, H. L. (1990). *HPR1*, a novel yeast gene that prevents intrachromosomal excision recombination, shows carboxy-terminal homology to the *Saccharomyces cerevisiae TOP1* gene. Mol. Cell. Biol. *10*, 1439-1451.

Alani, E., Reenan, R. A., and Kolodner, R. D. (1994). Interaction between mismatch repair and genetic recombination in Saccharomyces cerevisiae. Genetics *137*, 19-39.

Ausubel, F. M., Brent, R., Kingston, R. E., Moore, D. D., Seidman, J. G., Smith, J. A., and Struhl, K. (1994). Current Protocols in Molecular Biology. In Current Protocols, K. Janssen, ed. (Brooklyn: Greene Publishing Associates).

Bailis, A. M., and Rothstein, R. (1990). A defect in mismatch repair in *Saccharomyces cerevisiae* stimulates ectopic recombination between homeologous genes by an excision repair dependent process. Genetics *126*, 535-547.

Baker, S. M., Bronner, C. E., Zhang, L., Plug, A., Robatzek, M., Warren, G., Elliott, E. A., Yu, J., Ashley, T., Arnheim, N., Flavell, R. A., and Liskay, R. M. (1995). Male mice defective in the DNA mismatch repair gene *PMS2* exhibit abnormal chromosome synapsis in meiosis. Cell *82*, 309-319.

Bishop, D. K., Williamson, M. S., Fogel, S., and Kolodner, R. D. (1987). The role of heteroduplex correction in gene conversion in *Saccharomyces cerevisiae*. Nature *328*, 362-364.

Borts, R. H., and Haber, J. E. (1987). Meiotic recombination in yeast: alteration by multiple heterozygosities. Science 237, 1459-1465.

Borts, R. H., Leung, W. Y., Kramer, W., Kramer, B., Williamson, M., Fogel, S., and Haber, J. E. (1990). Mismatch repair-induced meiotic recombination requires the *PMS1* gene product. Genetics *124*, 573-584.

Bronner, C. E., Baker, S., Morrison, P. T., Warren, G., Smith, L. G., Lescoe, M. K., Kane, M., Earabino, C., Lipford, J., Lindblom, A., Tannergard, P., Bollag, R. J., Godwin, A. R., Ward, D. C., Nordenskjold, M., Fishel, R., Kolodner, R., and Liskay, R. M. (1994). Mutation in the DNA mismatch repair gene homologue hMLH1 is associated with hereditary non-polyposis colon cancer. Nature *368*, 258-61.

Cao, L., Alani, E., and Kleckner, N. (1990). A pathway for generation and processing of double-strand breaks during meiotic recombination in *S. cerevisiae*. Cell *61*, 1089-1101.

Chi, N. W., and Kolodner, R. D. (1994). The effect of DNA mismatches on the ATPase activity of MSH1, a protein in yeast mitochondria that recognizes DNA mismatches. J. Biol. Chem. *269*, 29993-7.

Chi, N. W., and Kolodner, R. D. (1994). Purification and characterization of MSH1, a yeast mitochondrial protein that binds to DNA mismatches. J. Biol. Chem. *269*, 29984-92.

Cooper, D. L., Lahue, R. S., and Modrich, P. (1993). Methyl-directed mismatch repair is bidirectional. J. Biol. Chem. *268*, 11823-11829.

DasGupta, C., and Radding, C. M. (1982). Polar branch migration promoted by recA protein: Effect of mismatched base pairs. Proc. Natl. Acad. Sci. USA *79*, 762-766.

Datta, A., Adjiri, A., New, L., Crouse, G. F., and Jinks-Robertson, S. (1996). Mitotic crossovers between diverged sequences are regulated by mismatch repair proteins in *Saccharomyces cerevisiae*. Mol. Cell. Biol. *16*, 1085-1093.

de Wind, N., Dekker, M., Berns, A., Radman, M., and te Riele, H. (1995). Inactivation of the mouse *Msh2* gene results in mismatch repair deficiency,

methylation tolerance, hyperrecombination, and predisposition to cancer. Cell *82*, 321-330.

Detloff, P., Sieber, J., and Petes, T. D. (1991). Repair of specific base pair mismatches formed during meiotic recombination in the yeast *Saccharomyces cerevisiae*. Mol. Cell. Biol. *11*, 737-745.

Drummond, J. T., Li, G.-M., Longley, M. J., and Modrich, P. (1995). Isolation of an hMSH2•p160 heterodimer that restores mismatch repair to tumor cells. Science *268*, 1909-1912.

Eisenmann, D. M., Arndt, K. M., Ricupero, S. L., Rooney, J. W., and Winston, F. (1992). SPT3 interacts with TFIID to allow normal transcription in *Saccharomyces cerevisiae*. Genes Dev. *6*, 1319-1331.

Eisenmann, D. M., Dollard, C., and Winston, F. (1989). SPT15, the gene encoding the yeast TATA binding factor TFIID, is required for normal transcription initiation in vivo. Cell *58*, 1183-1191.

Feinberg, A. P., and Vogelstein, B. (1983). A technique for radiolabeling DNA restriction endonuclease fragments to high specific activity. Analytical Biochemistry *132*, 6-13.

Fikes, J. D., Becker, D. M., Winston, F., and Guarente, L. (1990). Striking conservation of TFIID in *Schizosaccharomyces pombe* and *Saccharomyces cerevisiae.* Nature *346*, 291-294.

Fishel, R., Lescoe, M. K., Rao, M. R., Copeland, N. G., Jenkins, N. A., Garber, J., Kane, M., and Kolodner, R. (1993). The human mutator gene homolog *MSH2* and its association with hereditary nonpolyposis colon cancer. Cell *75*, 1027-38.

Fishman-Lobell, J., Rudin, N., and Haber, J. (1992). Two alternative pathways of double-strand break repair that are kinetically separable and independently modulated. Mol. Cell. Biol. *12*, 1292-1303.

Gietz, D., St. Jean, A., Woods, R. A., and Schiestl, R. H. (1992). Improved method for high efficiency transformation of intact yeast cells. Nucleic Acids Research *20*, 1425.

Goguel, V., Delahodde, A., and Jacq, C. (1992). Connections between RNA splicing and DNA intron mobility in yeast mitochondria: RNA maturase and DNA endonuclease switching experiments. Mol. Cell. Biol. *12*, 696-705.

Goyon, C., and Lichten, M. (1993). Timing of molecular events in meiosis in *Saccharomyces cerevisiae*: stable heteroduplex DNA is formed late in meiotic prophase. Mol. Cell. Biol *13*, 373-382.

Grilley, M., Griffith, J., and Modrich, P. (1993). Bidirectional excision in methyl-directed mismatch repair. J. Biol. Chem. *268*, 11830-11837.

Grilley, M., Welsh, K. M., Su, S.-S., and Modrich, P. (1989). Isolation and characterization of the *Escherichia coli mutL* gene product. J. Biol. Chem. *264*, 1000-1004.

Haber, J. E. (1992). Exploring the pathways of homologous recombination. Curr. Opin. Cell Biol. *4*, 401-412.

Haber, J. E., Ray, B. L., Kolb, J. M., and White, C. I. (1993). Rapid kinetics of mismatch repair of heteroduplex DNA that is formed during recombination in yeast. Proc. Natl. Acad. Sci. USA *90*, 3363-3367.

Hanahan, D. (1983). Studies on transformation of *Escherichia coli* with plasmids. J. Mol. Biol. *166*, 557-580.

Harris, S., Rudnicki, K. S., and Haber, J. E. (1993). Gene conversions and crossing over during homologous and homeologous ectopic recombination in *Saccharomyces cerevisiae*. Genetics *135*, 5-16.

Holliday, R. A. (1964). A mechanism for gene conversion in fungi. Genet. Res. *5*, 282-304.

Hollingsworth, N. M., Ponte, L., and Halsey, C. (1995). *MSH5*, a novel MutS homolog, facilitates meiotic reciprocal recombination between homologs in *Saccharomyces cerevisiae* but not mismatch repair. Genes Dev. *9*, 1728-1739.

Hummerich, H., and Lehrach, H. (1995). Trinucleotide repeat expansion and human disease. Electrophoresis *16*, 1698-1704.

Hunter, N., Chambers, S. R., Louis, E. J., and Borts, R. H. (1996). The mismatch repair system contributes to meiotic sterility in an interspecific yeast hybrid. EMBO J. *15*, 1726-1733.

Ionov, Y., Peinado, M. A., Malkhosyan, S., Shibata, D., and Perucho, M. (1993). Ubiquitous somatic mutations in simple repeated sequences reveal a new mechanism for colonic carcinogenesis. Nature *363*, 558-61.

Ivanov, E. L., and Haber, J. E. (1995). *RAD1* and *RAD10*, but not other excision repair genes, are required for double-strand break-induced recombination in *Saccharomyces cerevisiae*. Mol. Cell. Biol. *15*, 2245-2251.

Iype, L. E., Wood, E. A., Inman, R. B., and Cox, M. M. (1994). RuvA and RuvB protein facilitate the bypass of heterologous DNA insertions during RecA protein-mediated DNA strand exchange. J. Biol. Chem. *269*, 24967-24978.

Jackson, J. A., and Fink, G. R. (1981). Gene conversion between duplicated genetic elements in yeast. Nature *292*, 306-311.

Johnson, R. E., Kovvali, G. K., Prakash, L., and Prakash, S. (1996). Requirement of the yeast *MSH3* and *MSH6* genes for *MSH2*-dependent genomic stability. J. Biol. Chem. *271*, 7285-7288.

Johnson, R. E., Kovvali, G. K., Prakash, L., and Prakash, S. (1995). Requirement of the yeast *RTH1* 5′ to 3′ exonuclease for the stability of simple repetitive DNA. Science *269*, 238-240.

Kang, Y.-S., Kane, J., Kurjan, J., Stadel, J. M., and Tipper, D. J. (1990). Effects of expression of mammalian Gα and hybrid mammalian-yeast Gα proteins on the yeast pheromone response signal transduction pathway. Mol. Cell. Biol. *10*, 2582-2590.

Klein, H. L. (1988). Different types of recombination events are controlled by the *RAD1* and *RAD52* genes of *Saccharomyces cerevisiae*. Genetics *120*, 367-377.

Knight, K. L., and Sauer, R. T. (1988). The mnt repressor of bacteriophage P22: role of C-terminal residues in operator binding and tetramer formation. Biochemistry *27*, 2088-2094.

Kramer, B., Kramer, W., Williamson, M. S., and Fogel, S. (1989). Heteroduplex DNA correction in *Saccharomyces cerevisiae* is mismatch specific and requires functional *PMS* genes. Mol. Cell. Biol. *9*, 4432-4440.

Kramer, W., Kramer, B., Williamson, M. S., and Fogel, S. (1989). Cloning and nucleotide sequence of DNA mismatch repair gene *PMS1* from *Saccharomyces cerevisiae*: homology of PMS1 to prokaryotic MutL and HexB. J. Bacteriol. *171*, 5339-5346.

Krawczak, M., and Cooper, D. N. (1991). Gene deletions causing human genetic disease: mechanisms of mutagenesis and the role of the local DNA sequence environment. Hum. Genet. *86*, 425-441.

Lahue, R. S., Au, K. G., and Modrich, P. (1989). DNA mismatch correction in a defined system. Science *245*, 160-164.

Lea, D. E., and Coulson, C. A. (1948). The distribution of the number of mutants in bacterial populations. J. Genet. *49*, 264-284.

Leach, F. S., Nicolaides, N. C., Papadopoulos, N., Liu, B., Jen, J., Parsons, R., Peltomäki, P., Sistonen, P., Aaltonen, L. A., Nyström-Lahti, M., Guan, X.-Y., Zhang, J., Meltzer, P. S., Yu, J.-W., Kao, F.-T., Chen, D. J., Cerosaletti, K. M., Fournier, R. E. K., Todd, S., Lewis, T., Leach, R. J., Naylor, S. L., Weissenbach, J., Mecklin, J.-P., Järvinen, H., Petersen, G. M., Hamilton, S. R., Green, J., Jass, J., Watson, P., Lynch, H. T., Trent, J. M., de la Chapelle, A., Kinzler, K. W., and Vogelstein, B. (1993). Mutations of a mutS homolog in hereditary nonpolyposis colorectal cancer. Cell *75*, 1215-25.

Lichten, M., Goyon, C., Schultes, N. P., Treco, D., Szostak, J. W., Haber, J. E., and Nicolas, A. (1990). Detection of heteroduplex DNA molecules among the products of *Saccharomyces cerevisiae* meiosis. Proc. Natl. Acad. Sci. USA *87*, 7653-7657.

Lin, F., Sperle, K., and Sternberg, N. (1984). Model for homologous recombination during transfer of DNA into mouse L cells: role for DNA ends in the recombination process. Mol. Cell. Biol. *4*, 1020-1034.

Linton, J. P., Yen, J.-Y. J., Selby, E., Chen, Z., Chinsky, J. M., Liu, K., Kellems, R. E., and Crouse, G. F. (1989). Dual bidirectional promoters at the mouse *DHFR* locus: cloning and characterization of two mRNA classes of the divergently transcribed *Rep-1* gene. Mol. Cell. Biol. *9*, 3058-3072.

Liskay, R. M., and Stachelek, J. L. (1986). Information transfer between duplicated chromosomal sequences in mammalian cells involves contiguous regions of DNA. Proc. Natl. Acad. Sci. USA *83*, 1802-1806.

Liu, K., Niu, L., Linton, J. P., and Crouse, G. F. (1994). Characterization of the mouse *Rep*-3 gene: sequence similarities to bacterial and yeast mismatch-repair proteins. Gene *147*, 169-77.

Malone, R. E., Kim, S., Bullard, S. A., Lundquist, S., Hutchings-Crow, L., Cramton, S., Lutfiyya, L., and Lee, J. (1994). Analysis of a recombination hotspot

for gene conversion occurring at the *HIS2* gene of *Saccharomyces cerevisiae*. Genetics *137*, 5-18.

Markowitz, S., Wang, J., Myeroff, L., Parsons, R., Sun, L., Lutterbaugh, J., Fan, R. S., Zborowska, E., Kinzler, K. W., Vogelstein, B., Brattain, M., and Willson, J. K. V. (1995). Inactivation of the type II TGF-β receptor in colon cancer cells with microsatellite instability. Science *268*, 1336-1338.

Marsischky, G. T., Filosi, N., Kane, M. F., and Kolodner, R. (1996). Redundancy of *Saccharomyces cerevisiae MSH3* and *MSH6* in *MSH2*-dependent mismatch repair. Genes Dev. *10*, 407-420.

Matic, I., Radman, M., and Rayssiguier, C. (1994). Structure of recombinants from conjugational crosses between *Escherichia coli* donor and mismatch-repair deficient *Salmonella typhimurium* recipients. Genetics *136*, 17-26.

Matic, I., Rayssiguier, C., and Radman, M. (1995). Interspecies gene exchange in bacteria: the role of SOS and mismatch repair systems in evolution of species. Cell *80*, 507-15.

McDonald, J. P., and Rothstein, R. (1994). Unrepaired heteroduplex DNA in *Saccharomyces cerevisiae* is decreased in *RAD1 RAD52*-independent recombination. Genetics *137*, 393-405.

Meselson, M. S., and Radding, C. M. (1975). A general model for genetic recombination. Proc. Natl. Acad. Sci. USA *72*, 358-361.

Meuth, M. (1990). The structure of mutation in mammalian cells. Biochem. Biophys. Acta *1032*, 1-17.

Mezard, C., and Nicolas, A. (1994). Homologous, homeologous, and illegitimate repair of double-strand breaks during transformation of a wild-type strain and a *rad52* mutant strain of *Saccharomyces cerevisiae*. Mol. Cell Biol. *14*, 1278-1292.

Mezard, C., Pompon, D., and Nicolas, A. (1992). Recombination between similar but not identical DNA sequences during yeast transformation occurs within short stretches of identity. Cell *70*, 659-670.

Miret, J. J., Milla, M. G., and Lahue, R. S. (1993). Characterization of a DNA mismatch-binding activity in yeast extracts. J. Biol. Chem. *268*, 3507-13.

Modrich, P., and Lahue, R. S. (1996). Mismatch repair in replication fidelity, genetic recombination and cancer biology. Annu. Rev. Biochem. *65*, 101-133.

Morrison, A., Johnson, A. L., Johnston, L. H., and Sugino, A. (1993). Pathway correcting DNA replication errors in *Saccharomyces cerevisiae*. The EMBO Journal *12*, 1467-1473.

Muller, B., Tsaneva, I. R., and West, S. C. (1993). Branch migration of Holliday junctions promoted by the *Escherichia coli* RuvA and RuvB proteins. I. Comparison of the RuvAB- and RuvB-mediated reactions. J. Biol. Chem. *268*, 17179-17184.

Nag, D. K., and Petes, T. D. (1991). Seven-base-pair inverted repeats in DNA form stable hairpins *in vivo* in *Saccharomyces cerevisiae*. Genetics *129*, 669-673.

Nag, D. K., White, M. A., and Petes, T. D. (1989). Palindromic sequences in heteroduplex DNA inhibit mismatch repair in yeast. Nature *340*, 318-320.

Nevers, P., and Spatz, H. (1975). *Escherichia coli* mutants *uvrD uvrE* deficient in gene conversion of lambda heteroduplexes. Mol. Gen. Genet. *139*, 233-243.

New, L., Liu, K., and Crouse, G. F. (1993). The yeast gene *MSH3* defines a new class of eukaryotic MutS homologues. Mol. Gen. Genet. *239*, 97-108.

Nicolaides, N. C., Papadopoulos, N., Liu, B., Wei, Y.-F., Carter, K. C., Ruben, S. M., Rosen, C. A., Haseltine, W. A., Fleischmann, R. D., Fraser, C. M., Adams, M. D., Venter, J. C., Dunlop, M. G., Hamilton, S. R., Petersen, G. M., de la Chapelle, A., Vogelstein, B., and Kinzler, K. W. (1994). Mutations of two PMS homologs in hereditary nonpolyposis colon cancer. Nature *371*, 75-80.

Olopade, O. I., Jenkins, R. B., Ransom, D. T., Malik, K., Pomykala, H., Nobori, T., Cowan, J. M., Rowley, J. D., and Diaz, M. O. (1992). Molecular analysis of

deletions of the short arm of chromosome 9 in human gliomas. Canc. Res. *52*, 2523-2529.

Palombo, F., Gallinari, P., Iaccarino, I., Lettieri, T., Hughes, M., D'Arrigo, A., Truong, O., Hsuan, J. J., and Jiricny, J. (1995). GTBP, a 160 kDa protein essential for mismatch-binding activity in human cells. Science *268*, 1912-1914.

Papadopoulos, N., Nicolaides, N. C., Wei, Y.-F., Ruben, S. M., Carter, K. C., Rosen, C. A., Haseltine, W. A., Fleischmann, R. D., Fraser, C. M., Adams, M. D., Venter, J. C., Hamilton, S. R., Peterson, G. M., Watson, P., Lynch, H. T., Peltomäki, P., Mecklin, J.-P., de la Chapelle, A., Kinzler, K. W., and Vogelstein, B. (1994). Mutation of a *mutL* homolog in hereditary colon cancer. Science *263*, 1625-1629.

Parker, B. O., and Marinus, M. G. (1992). Repair of DNA heteroduplexes containing small heterologous sequences in *Escherichia coli.* Proc. Natl. Acad. Sci. USA *89*, 1730-1734.

Parsons, R., Li, G. M., Longley, M., Modrich, P., Liu, B., Berk, T., Hamilton, S. R., Kinzler, K. W., and Vogelstein, B. (1995). Mismatch repair deficiency in phenotypically normal human cells. Science *268*, 738-40.

Petes, T. D., Malone, R. E., and Symington, L. S. (1991). Recombination in yeast. In The Molecular and Cellular Biology of the Yeast *Saccharomyces*, J. R. Broach, J.

R. Pringle and E. W. Jones, eds. (Cold Spring Harbor, NY: Cold Spring Harbor Laboratory Press), pp. 407-521.

Petit, M.-A., Dimpfl, J., Radman, M., and Echols, H. (1991). Control of large chromosomal duplications in *Escherichia coli* by the mismatch repair system. Genetics *129*, 327-332.

Poon, D., Schroeder, S., Wang, C. K., Yamamoto, T., Horikoshi, M., Reoder, R. G., and Weil, P. A. (1991). The conserved carboxy-terminal domain of *Saccharomyces cerevisiae* TFIID is sufficient to support normal cell growth. Molecular and Cellular Biology *11*, 4809-4821.

Priebe, S. D., Westmoreland, J., Nilsson-Tillgren, T., and Resnick, M. A. (1994). Induction of recombination between homologous and diverged DNAs by double-strand gaps and breaks and role of mismatch repair. Mol. Cell. Biol. *14*, 4802-4814.

Prolla, T. A., Christie, D. M., and Liskay, R. M. (1994). Dual requirement in yeast DNA mismatch repair for *MLH1* and *PMS1*, two homologs of the bacterial mutL gene. Mol. Cell. Biol. *14*, 407-15.

Prolla, T. A., Pang, Q., Alani, E., Kolodner, R. D., and Liskay, R. M. (1994). MLH1, PMS1, and MSH2 interactions during the initiation of DNA mismatch repair in yeast. Science *265*, 1091-1093.

Pukkila, P. J., Peterson, J., Herman, G., Modrich, P., and Meselson, M. (1983). Effects of high levels of DNA adenine methylation on methyl-directed mismatch repair in *Escherichia coli.* Genetics *104*, 571-582.

Radman, M. (1988). Mismatch repair and genetic recombination. In Genetic Recombination, R. Kucherlapati and G. R. Smith, eds. (Washington, D. C.: American Society for Microbiology), pp. 169-192.

Rattray, A. J., and Symington, L. S. (1994). Use of a chromosomal inverted repeat to demonstrate that the *RAD51* and *RAD52* genes of *Saccharomyces cerevisiae* have different roles in mitotic recombination. Genetics *138*, 587-595.

Rayssiguier, C., Thaler, D. S., and Radman, M. (1989). The barrier to recombination between *Escherichia coli* and *Salmonella typhimurium* is disrupted in mismatch-repair mutants. Nature *342*, 396-401.

Reenan, R. A., and Kolodner, R. D. (1992). Characterization of insertion mutations in the *Saccharomyces cerevisiae MSH1* and *MSH2* genes: evidence for separate mitochondrial and nuclear functions. Genetics *132*, 975-85.

Reenan, R. A., and Kolodner, R. D. (1992). Isolation and characterization of two *Saccharomyces cerevisiae* genes encoding homologs of the bacterial HexA and MutS mismatch repair proteins. Genetics *132*, 963-73.

Resnick, M. A., Zgaga, Z., Hieter, P., Westmoreland, J., Fogel, S., and Nilsson-Tillgren, T. (1992). Recombinational repair of diverged DNAs: a study of homeologous chromosomes and mammalian YACs in yeast. Mol. Gen. Genet. *234*, 65-73.

Reynaud, C.-A., Anquez, V., Dahan, A., and Weill, J.-C. (1985). A single rearrangement event generates most of the chicken immunoglobulin light chain diversity. Cell *40*, 283-291.

Reynaud, C.-A., Dahan, A., Anquez, V., and Weill, J.-C. (1989). Somatic hyperconversion diversifies the single V_H gene of the chicken with a high incidence in the D region. Cell *59*, 171-183.

Risinger, J. I., Umar, A., Barrett, J. C., and Kunkel, T. A. (1995). A *hPMS2* mutant cell line is defective in strand-specific mismatch repair. J. Biol. Chem. *270*, 18183-18186.

Ross-MacDonald, P., and Roeder, G. S. (1994). Mutation of a meiosis-specific MutS homolog decreases crossing over but not mismatch correction. Cell *79*, 1069-80.

Rothstein, R., Helms, C., and Rosenberg, N. (1987). Concerted deletions and inversions are caused by mitotic recombination between delta sequences in *Saccharomyces cerevisiae*. Mol. Cell. Biol. *7*, 1198-1207.

Rothstein, R. J. (1983). One-step gene disruption in yeast. Methods in Enzymology *101*, 202-210.

Sanger, F., Nicklen, S., and Coulson, A. R. (1977). DNA sequencing with chain-terminating inhibitors. Proc. Natl. Acad. Sci. USA *74*, 5463-5467.

Saparbaev, M., Prakash, L., and Prakash, L. (1996). Requirement of mismatch repair genes *MSH2* and *MSH3* in the *RAD1-RAD10* pathway of mitotic recombination in *Saccharomyces cerevisiae*. Genetics *142*, 727-736.

Scherer, S., and Davis, R. W. (1979). Replacement of chromosome segments with altered DNA sequences constructed *in vitro*. Proc. Natl. Acad. Sci. USA *76*, 4951-4955.

Schiestl, R. H., and Gietz, D. (1989). High efficiency transformation of intact yeast cells by single stranded nucleic acids as carrier. Current Genetics *16*, 339-346.

Schiestl, R. H., and Prakash, S. (1988). *RAD1*, an excision repair gene of *Saccharomyces cerevisiae*, is also involved in recombination. Mol. Cell. Biol. *8*, 3619-3626.

Selva, E. M., New, L., Crouse, G. F., and Lahue, R. S. (1995). Mismatch correction acts as a barrier to homeologous recombination in *Saccharomyces cerevisiae*. Genetics *139*, 1175-1188.

Shen, P., and Huang, H. V. (1986). Homologous recombination in *Escherichia coli*: dependence on substrate length and homology. Genetics *112*, 441-457.

Sherman, F., Fink, G., and Lawrence, C. (1979). Methods in Yeast Genetics (NY: Cold Spring Habor).

Sikorski, R. S., and Hieter, P. (1989). A system of shuttle vectors and yeast host strains designed for efficient manipulation of DNA in *Saccharomyces cerevisiae*. Genetics *122*, 19-27.

Strand, M., Earley, M. C., Crouse, G. F., and Petes, T. D. (1995). Mutations in the *MSH3* gene preferentially lead to deletions within tracts of simple repetitive DNA in *Saccharomyces cerevisiae*. Proc. Natl. Acad. Sci. USA *92*, 10418-10421.

Strand, M., Prolla, T. A., Liskay, R. M., and Petes, T. D. (1993). Destabilization of tracts of simple repetitive DNA in yeast by mutations affecting DNA mismatch repair. Nature *365*, 274-276.

Su, S.-S., Lahue, R. S., Au, K. G., and Modrich, P. (1988). Mispair specificity of methyl-directed DNA mismatch correction *in vitro*. J. Biol. Chem. *263*, 6829-6835.

Su, S.-S., and Modrich, P. (1986). *Escherichia coli mutS*-encoded protein binds to mismatched DNA base pairs. Proc. Natl. Acad. Sci. USA *83*, 5057-5061.

Sun, H., Treco, D., Schultes, N. P., and Szostak, J. W. (1989). Double-strand breaks at an initiation site for meiotic gene conversion. Nature *338*, 87-90.

Symington, L. S., and Petes, T. D. (1988). Expansions and contractions of the genetic map relative to the physical map of yeast chromosome III. Mol. Cell. Biol. *8*, 595-604.

Szankasi, P., and Smith, G. R. (1995). A role for exonuclease I from *S. pombe* in mutation avoidance and mismatch correction. Science *267*, 1166-1169.

Szostak, J. W., Orr-Weaver, T. L., Rothstein, R. J., and Stahl, F. W. (1983). The double-strand break repair model for recombination. Cell *33*, 25-35.

Thibodeau, S. N., Bren, G., and Schaid, D. (1993). Microsatellite instability in cancer of the proximal colon. Science *260*, 816-819.

Thomas, B. J., and Rothstein, R. (1989). Elevated recombination rates in transcriptionally active DNA. Cell *56*, 619-630.

Thomas, B. J., and Rothstein, R. (1989). The genetic control of direct-repeat recombination in Saccharomyces: the effect of *rad52* and *rad1* on mitotic recombination at *GAL10*, a transcriptionally regulated gene. Genetics *123*, 725-738.

Thompson, C. B., and Neiman, P. (1987). Somatic diversification of the chicken immunoglobulin light chain gene is limited to the rearranged variable gene segment. Cell *48*, 369-378.

Tiraby, J.-G., and Fox, M. S. (1973). Marker discrimination in transformation and mutation of pneumococcus. Proc. Natl. Acad. Sci. USA *70*, 3541-3545.

Waldman, A. S., and Liskay, R. M. (1988). Dependence of intrachromosomal recombination in mammalian cells on uninterrupted homology. Mol. Cell. Biol. *8*, 5350-5357.

Waldman, A. S., and Liskay, R. M. (1987). Differential effects of base-pair mismatch on intrachromosomal versus extrachromosomal recombination in mouse cells. Proc. Natl. Acad. Sci. USA *84*, 5340-5344.

Wheeler, C. J., Maloney, D., Fogel, S., and Goodenow, R. S. (1990). Microconversion between murine H-2 genes integrated into yeast. Nature *347*, 192-194.

Williamson, M. S., Game, J. C., and Fogel, S. (1985). Meiotic gene conversion mutants in *Saccharomyces cerevisiae*. I. Isolation and characterization of *pms1-1* and *pms1-2*. Genetics *110*, 609-646.

Worth, L., Clark, S., Radman, M., and Modrich, P. (1994). Mismatch repair proteins MutS and MutL inhibit RecA-catalyzed strand transfer between diverged DNAs. Proc. Natl. Acad. Sci. USA *91*, 3238-3241.

Wu, T.-H., and Marinus, M. G. (1994). Dominant negative mutator mutations in the *mutS* gene of *Escherichia coli*. J. Bacteriol. *176*, 5393-5400.